CHAPTER 2

Chemical characterization and cycling of dissolved organic matter

NON-PRINT ITEMS

Abstract

This chapter summarizes advances in our knowledge of dissolved organic matter (DOM) composition, with a particular emphasis on studies completed over the last decade that utilize high field nuclear magnetic resonance, high resolution mass spectrometry, proteomics and related immunochemical assays. Up to 75% of marine dissolved organic matter can now be recovered for analysis using solid phase extraction, ultrafiltration, or electrodialysis/reverse osmosis. Spectral and chemical analyses show carbohydrates, proteins, and structurally complex carboxyl-rich aliphatic matter (CRAM) contribute the majority of characterized material. The chemical composition of DOM has a large impact on its accumulation and residence time in the ocean. Carbohydrates and proteins are cycled much more quickly, have much shorter residence times and lower global inventories than CRAM. Processes that lead to the accumulation of carbohydrates and proteins are highly selective, and only a specific fraction of these biopolymers escape degradation to accumulate as DOM. The origin and fate of CRAM are largely unknown, although recent studies suggest a portion of this material has been subjected to elevated temperatures, either in hydrothermal systems or during biomass burning of terrestrial organic matter before transport to the ocean. Radiocarbon measurements and global surveys of deep sea DOM concentration are providing new insights into the location and timescale of refractory DOM removal processes, significantly enhancing our understanding of CRAM cycling.

Key Words

Dissolved organic matter; composition; cycling; marine; polysaccharides; proteins; humic substances; ultrafiltration; solid phase extraction; microbial cycling; photochemistry

Chapter starts here

2.1 Introduction

Each year, between 15-25 Pg of dissolved organic matter (DOM) are added to seawater by the activity of marine microbes, by atmospheric, fluvial, and groundwater transport of organic matter from the continents, and by the release of organic matter from the benthic boundary layer (Burdige, 2007; Jurado et al., 2008; Bauer and Bianchi, 2011; Hansell, 2012). Most DOM is immediately respired by marine microheterotrophs, oxidized by photochemical processes, or permanently buried in sediments. However, a significant fraction is stored in the water column where it interacts with a variety of

63 biogeochemical cycles over timescales ranging from hours to millennia. Marine DOM
64 stores nitrogen and phosphorus that would otherwise be immediately available to
65 microbes in the upper water column, affects the bioavailability of essential trace metals,
66 attenuates the penetration of UV and visible light in the euphotic zone, and sequesters an
67 amount of carbon approximately equal to atmospheric carbon dioxide. All production,
68 removal, and transformation processes leave an imprint on the composition of DOM, and
69 it is the potential that DOM composition can help to understand the sources and sinks of
70 DOM, and how it is cycled in the water column, as well as the interest in describing one
71 of the largest reservoirs of organic matter on Earth, that drives much of the current
72 research on DOM composition.
73 Composition refers to the broad suite of molecular characteristics that define
74 DOM, and includes levels of detail that range from simple elemental ratios of carbon,
75 nitrogen, and phosphorus, to stable and radio-isotopic content, to the stereochemistry of
76 amino acids. How DOM is characterized, the extent to which the composition is known,
77 therefore changes with the characteristics of interest. Global surveys of dissolved organic
78 carbon (DOC), nitrogen (DON) and phosphorus (DOP) completed over the last decade
79 now include > 10^4 analyses, and our knowledge of DOM elemental composition is
80 therefore relatively comprehensive (Hansell et al., 2009, 2012). In contrast, our
81 understanding of DOM molecular composition is often benchmarked as the inventory of
82 dissolved compounds (simple sugars, amino acids, lipids, vitamins, pigments, etc.) that
83 can be isolated from seawater. Viewed from this perspective, < 10% of DOM has been
84 characterized, and it is fair to say that our knowledge of DOM has improved only
85 marginally over the last decade and a half. However, it is often other features of
86 composition, such as the distribution of major carbon, nitrogen and phosphorus
87 functional groups, the identity of major classes of compounds that contribute to labile and
88 refractory fractions of DOM, or changes in the degree of oxidation, that are most
89 informative to understanding the sources, sinks, and cycling of DOM. Viewed from this
90 perspective, our understanding of DOM composition has advanced significantly to the
91 point where between 60-70% of DOM has now been "characterized".
92 This chapter summarizes recent advances in our knowledge of DOM composition,
93 with a particular emphasis on studies completed over the last decade that utilize high field

nuclear magnetic resonance, high resolution mass spectrometry, proteomics and related immunochemical assays. A number of excellent reviews and workshop reports summarize the field of DOM composition up to the early 2000's (McNichol and Aluwihare, 2007; Mopper et al., 2007; Aluwihare and Meador, 2008), and other chapters in this book describe progress in DOM elemental composition (Carlson and Hansell chapter), isotopic composition (Beaupre chapter), dissolved organic nitrogen (Sipler and Bronk chapter) and phosphorus (Karl and Björkman chapter), chromophoric DOM (Mopper et al. chapter, Stedmon and Nelson chapter), and DOM cycling in river and coastal systems (Raymond and Spencer chapter). These topics are integral to DOM composition and cycling, and specific aspects are included in the discussion below, but the reader is referred to these chapters for comprehensive discussions on these topics.

In practical terms, all studies of DOM composition begin with sampling, which aside from providing the material used in chemical and spectral analyses, also selectively defines the chemical fraction and spatial/temporal features of the DOM that is characterized. Because sampling is so integral to the interpretation of DOM composition, this chapter begins with a summary of sampling methods. From there, the chapter is organized into discussions of carbohydrates, proteins and aliphatic organic matter, the major components of DOM that have been identified to date. Finally, the results from these studies are discussed within the broader perspective of how composition impacts the cycling of DOM in the water column.

2.2 Isolation of dissolved organic matter from seawater.

Dissolved organic matter is operationally defined as the fraction of organic matter not retained by filtration. However, the specific choice of filter is determined by the preferences of the analyst and may be influenced by the subsequent suite of analyses that are to be performed. There is no universally agreed upon filter type or pore size that distinguishes dissolved and particulate phases. Many studies of marine particles have utilized Whatman GF/F glass fiber filters with a nominal pore size of 0.7 μm due to the ease with which these filters can be cleaned and to their excellent flow characteristics, facilitating their adoption for DOM studies where large volume samples were often required. However, some marine bacteria and viruses are < 0.7 μm and pass through

GF/F filters to be included in the "dissolved" fraction. Membranes with smaller pore sizes (0.1-0.2 μm) effectively exclude bacteria, while much smaller pore sizes (10-15 nm) are needed to exclude viruses. "Dissolved" is therefore a non-specific term that can include bacteria-sized particles, colloidal organic matter, and truly dissolved species.

Although the concentrations of some organic compounds (amino acids, simple sugars, low molecular weight acids, ketones, and aldehydes) can be measured directly in seawater, > 90% of DOM needs to be concentrated and isolated before spectral and further chemical characterization can proceed. Separation of DOM (~ 0.5-1 mg/L) from salt (~35 g/L) poses the major challenge for DOM isolation, and no single approach recovers all DOM from seawater. Therefore, a number of different strategies have been developed that capitalize on either the larger molecular size or the lower polarity of DOM relative to sea salt. Advances in spectroscopic and spectrometric analyses have in many cases reduced sample requirements from mg to μg or even ng amounts of material, and have mitigated some of the need to obtain DOM as a salt free preparation. For example, samples for mass spectral analyses can be obtained from only a few liters of seawater, and proton nuclear magnetic resonance (^{1}H NMR) spectra have now been reported for unprocessed seawater (Dittmar et al., 2008a; Lam and Simpson, 2008). Presently, these approaches are limited to qualitative analyses of DOM; water suppression leads to biases in the determination of carbohydrate functional groups in ^{1}H NMR, while matrix effects and differences in ionization efficiency complicate the quantitative interpretation of mass spectra. As analytical techniques continue to advance, these limitations will be addressed, but for the immediate future, our ability to isolate only a portion of DOM will continue to limit our understanding of DOM composition.

2.2.1 Isolation of hydrophobic DOM by solid phase extraction

Simple passage of filtered seawater across a solid hydrophobic surface or mineral phase leads to the adsorption and concentration of DOM (Fig. 2.1). Since the basis of the method is physisorptive attraction between DOM and the solid phase, the approach selectively concentrates the hydrophobic or surface-active fraction of DOM with distinct characteristics that are not representative of total DOM. For example, colored dissolved organic matter is efficiently extracted by contact with polystyrene or octadecyl-silica (C-

18) resins, but the absorption and fluorescent properties of the extracted samples are significantly different from the original seawater (Green and Blough, 1994). Early work on DOM solid phase extraction (SPE) explored charcoal, freshly precipitated iron oxy-hydroxides, and synthetic hydrophobic resins as substrates, but over the past two decades commercially available octadecyl-bonded silica (C-18), cross-linked polystyrene (XAD-2, -4, and -16) and their derivatives (PPL, Isolute ENV, and polyacrylate (XAD-8)) have become the sorbents of choice for these studies (Mopper et al., 2007).

To maximize sample recovery, filtered samples are often acidified with hydrochloric acid to pH 2-2.5. At lower pH, most carboxylic acids and phenols are protonated, reducing their aqueous solubility and enhancing their adsorption, thereby leading to a higher recovery of carbon. The extraction efficiency will depend on the speed at which seawater is passed through the column, and the amount of sorbent used per volume of seawater. A recent study used 1g sorbent per 1-2 mg of total DOC at 20 column volumes per minute, but the effects of flow rate and sorbent/sample ratio have not been investigated in detail (Dittmar et al., 2008b). After collection, the sample is rinsed of salt using pH 2, ultra-pure water, and recovered by elution with methanol and/or methanolic or aqueous sodium or ammonium hydroxide. In performing SPE, the sample is subjected to large changes in pH, which have unknown effects on the sample composition.

The diversity of SPE products available to the analyst has led to a few comparisons of carbon recovery and the elemental, spectroscopic and isotopic characteristics of SPE-DOM (Macrellis et al., 2001; Dittmar et al., 2008a). DOC and analyte recovery was highly dependent on the choice of solid phase. In one study, PPL (functionalized polystyrene/divinyl benzene) was found to be more efficient than C-18 (octadecyl-functionalized silica with 500Å pore size) in extracting DOC from surface seawater near the North Brazilian Shelf, adsorbing on average 62% of total DOC, with a lower C/N (20) and less depleted $\delta^{13}C$ value (-23.4‰) than recovered by C-18 (37%, 37 and -24.8‰, respectively). Given the large difference in recovery, C/N ratio and isotope value it would seem that PPL and C-18 extract different but overlapping fractions of DOM. However, the ^{1}H NMR spectra of the two samples were nearly identical. In this particular study, differences in extraction efficiency may have been accentuated by the

187 presence of terrestrial organic matter sourced from the nearby continental margin.
188 Extraction efficiencies for open ocean seawater have not been widely reported, but are
189 generally lower (10-20%).
190
191 *2.2.2 Isolation of high molecular weight DOM by ultrafiltration*
192 "Molecular" or "ultra-" filtration exploits the larger hydrodynamic diameter of
193 high molecular weight DOM compared to most dissolved inorganic species to achieve a
194 separation of organic matter from seawater. In this technique, hydrostatic pressure is
195 applied across a semi-permeable membrane perforated with very small pores, typically 1-
196 15 nm in diameter. Salts, water, and organic matter of a hydrodynamic diameter smaller
197 than the filter pore size pass through the membrane (as the permeate) while high
198 molecular weight organic matter is retained and concentrated in the original sample (as
199 the retentate; Fig. 2.1). Accumulation of organic matter on the filter surface rapidly leads
200 to membrane polarization, which is reduced by applying a second (tangential or cross)
201 flow perpendicular to the direction of filtration. The sample is concentrated to a fraction
202 of its original volume, diluted with ultra-high purity, salt-free water, and filtered again.
203 This "diafiltration" process is repeated until the salt content is reduced to a fraction of the
204 organic matter concentration. Once this has been achieved, the remaining water is
205 removed by lyophilization or rotary evaporation, and the sample recovered.
206 Ultrafiltration concentrates a hydrophilic, high molecular weight fraction of DOM
207 (HMWDOM). The amount and chemical characteristics of HMWDOM recovered is
208 highly dependent on the membrane material (cellulose, polysulfone, etc.) and pore size,
209 the strength of the cross flow, the ratio of original to final sample volume (concentration
210 factor), and a number of other operational parameters. Plots of water volume filtered
211 against DOC concentration show that ultrafiltration with a 1 nm pore-sized membrane
212 typically retains ~30% of DOC, but losses associated with high concentration factors and
213 diafiltration lead to far lower physical recoveries, typically 10-15% for final isolates that
214 are 35-38% by weight carbon (Walker et al. (2011). Walker et al. (2011) applied a
215 permeation model to ultrafiltration data where seawater was concentrated by factors of >
216 1000 fold. High molecular weight components of DOM behaved ideally, e.g. even at
217 high concentration factors they are efficiently retained by the ultrafiltration membrane.

Hydrophobic, low molecular weight DOM (LMWDOM) that is nominally smaller than the membrane pore size, is also concentrated by ultrafiltration, probably due to membrane polarization and adsorption onto the membranes themselves. The amount of LMWDOM retained is highly variable, being sensitive to the membrane material, concentration factor and perhaps other operational factors. A number of studies report differences in the recovery and chemical properties of HMWDOM. These differences could be due to the variable retention of low molecular weight components. The selectivity inherent in ultrafiltration sampling, and the sensitivity of DOM recoveries to operation parameters that differ between systems and operators, suggests caution must be exercised when comparing data between studies.

2.2.3 Isolation of DOM by reverse osmosis/electrically assisted dialysis

A recent advance in DOM sampling is reverse osmosis/electrically-assisted dialysis (RO/ED; Vetter et al., 2007; Gurtler et al., 2008; Koprivnjak et al., 2009) In this technique, the sample is desalted by an alternating series of positive and negative ion exchange membranes under the influence of an electric potential (Fig 2.1). Anions pass through positively charged ion exchange membranes towards the anode, while cations pass through negatively charged ion exchange membranes towards the cathode. The resulting lower salinity sample is reduced in volume by reverse osmosis, then desalted a second time in a final ED phase. Recoveries of DOM range from 50 to >100% with an average carbon recovery of 76% (n=21), similar to the 70% recovered when SPE and ultrafiltration are used in series (Simjouw et al., 2005). Final preparations are ~ 25% salt by weight and have chemical characteristics of both hydrophobic organic matter isolated by SPE and hydrophilic DOM isolated by ultrafiltration.

2.3 Chemical characterization of dissolved organic matter

DOM includes simple biochemicals (amino acids, simple sugars, vitamins, fatty acids), complex biopolymers (proteins, polysaccharides, lignins) and very complex degradation products of unknown origin that so far have defied full characterization (humic substances, black carbon). The complexity and diversity of organic constituents

in DOM have pushed the limits of the chemical and spectral techniques brought to bear on their characterization. High resolution mass spectrometry, high field NMR, and new approaches to chemical degradation have significantly broadened and deepened our understanding of DOM composition, but have also highlighted the limits of even advanced spectral techniques.

Ultrafiltration, solid phase extraction, ED/RO, and direct chemical analysis of unfractionated seawater all access overlapping, but compositionally different fractions of DOM. NMR and chemical analysis of hydrolysis products have been most successful in characterizing polysaccharides and proteins in HMWDOM. High-resolution mass spectrometry, 2D NMR and chemical degradation approaches have found their most successful application in the characterization of hydrophobic DOM isolated by solid phase extraction. The following discussion is therefore organized around the characterization of carbohydrates, proteins, and hydrophobic humic substances that are the major components of DOM, highlighting the new approaches and methods that have come to the fore in the last decade.

2.3.1 Polysaccharides in DOM

^{13}C NMR analysis of surface water HMWDOM gives a characteristic spectrum (Fig. 2.2A) with major resonances assigned to carboxyl/amide carbon (~180 ppm; 5%), unsaturated C=C/aromatic carbon (broad peak centered at ~140 ppm; 5%), anomeric O-C-O (~100 ppm; 14%), O-alkyl C (~75 ppm; 56%), a broad peak centered at ~35-40 ppm (13%) from methylene and substituted methylene C, and two alkyl carbon peaks at 20 ppm (5%) and 26 ppm (5%). ^{1}H NMR spectra are similarly characteristic (Fig, 2.2B), with major resonances from anomeric (5.2 ppm; **H**C(-O)$_2$), and O-alkyl (3.5-4.5 ppm; HO-C**H**) protons, as well as methyl carbons from acetamide (2.0 ppm; HN-C(O)C**H**$_3$) and deoxysugars (1.3 ppm; C(H$_2$)-C**H**$_3$). In addition, ^{1}H NMR spectra have a distinct signal at 2.7 ppm which is tentatively assigned to N-methyl-acetyl (C**H**$_3$-NH-C(=O)CH$_3$) on the basis of chemical shift comparisons with literature values, but further corroborative evidence is lacking. The proton and carbon NMR spectra are complimentary, each showing a majority of functional groups can be assigned to carbohydrates. The positions of carbohydrate peaks change little between samples, but

changes in their relative intensities are observed with depth (Benner et al., 1992; Hertkorn et al., 2006), sampling location (Aluwihare et al., 1997), and across salinity gradients (Abdulla et al., 2010a,b), supporting the idea of at least two major components to HMWDOM; a polysaccharide fraction referred to as acylated polysaccharide (APS; Aluwihare et al., 1997) or heteropolysacharide (HPS; Hertkorn et al., 2006; Abdulla et al., 2010a,b), which includes anomeric, O-alkyl, amide, and methyl carbon (from acetate and deoxy sugars), and a carboxylic acid-alkyl carbon-rich fraction referred to as carboxyl-rich aliphatic matter (CRAM) or carboxyl-rich compounds (CRC) reminiscent of aquatic humic substances.

The presence of distinct polysaccharide and CRAM/CRC fractions within HMWDOM can be demonstrated by passing HMWDOM samples through hydrophobic C-18 resin at low pH or through anionic exchange resin at neutral pH to selectively remove most of the CRAM/CRC fraction (Fig. 2.3A; Panagiotopoulos et al., 2007), and through correlation spectroscopy (Fig. 2.3B; Abdulla et al., 2010a,b; Abdulla et al., 2013) In correlation spectroscopy, the variable intensities of major resonances are correlated with a second variable (salinity, depth, location) to derive synchronous and nonsynchronous changes in spectral characteristics. Signal fluctuations that are synchronous indicate a common chemical constituent, while nonsynchronous signals indicate chemically distinct components. Correlation spectroscopy therefore identifies functional group relationships within the different fractions of DOM, but requires that different fractions of HWMDOM vary independently across changes in depth, location, salinity, *etc*. For example, Abdulla et al. (2013a,b) used two-dimensional (2D) correlation analysis on a suite of samples from the Elizabeth River/Chesapeake Bay estuary to identify synchronous changes in ^{13}C NMR signal intensity. Strong correlations were observed between intense signals from O-alkyl carbon at 74 ppm, anomeric carbon at 103 ppm, amide carbon at 178 ppm, and two alkyl carbons at 20 and 26 ppm. These functional groups arise from the HMWDOM polysaccharide fraction. The carboxyl-rich component (CRAM/CRC) showed correlation between signals in the methylene and substituted carbon region (29-50 ppm), unsaturated C=C/aromatic region (115-160 ppm), carboxyl carbon at 183 ppm, and carbonyl (aldehyde and ketone) carbon at 190-200 ppm. The negative correlation between carbohydrate resonances at 110 ppm and 74 ppm with

311 aliphatic signals between 30-46 and unsaturated/aromatic signals centered at 130 ppm
312 indicates that carbon functional groups in these regions of the spectrum are primarily
313 associated with CRAM/CRC. HMWDOM polysaccharides have little to no aliphatic
314 component other than carbon associated with acetate and deoxysugar carbon (Fig. 2.2A).
315 Full characterization of any polysaccharide is challenging, and typically includes
316 acid hydrolysis to determine simple sugar composition, methylation and reductive
317 cleavage to determine branching, and spectroscopic or spectrometric characterization of
318 partially degraded oligosaccharides to determine sequence. For HMWDOM, these
319 approaches have proved to be only partially successful. Hydrolysis of HMWDOM using
320 a wide variety of acids and hydrolysis conditions yields a characteristic suite of seven
321 major neutral sugars including arabinose and xylose (pentoses), glucose, galactose, and
322 mannose (hexoses), fucose and rhamnose, (6-deoxy-hexoses) (Sakugawa and Handa,
323 1985; McCarthy et al., 1996; Aluwihare et al., 1997; Panagiotopoulos and Sempéré,
324 2005), and similar amounts of the amino sugars glucosamine and galactosamine (Kaiser
325 and Benner, 2000; Aluwihare et al., 2002; Benner and Kaiser, 2003). Remarkably, the
326 relative proportions of these sugars is largely conserved across samples collected in
327 different ocean basins, at different times, and at different depths(Sakugawa and Handa,
328 1985; McCarthy et al., 1996; Aluwihare et al., 1997). However, small variations in the
329 ratio of neutral sugars have been attributed to spatial/temporal changes in HMWDOM
330 composition (Boon et al., 1998; Goldberg et al., 2009, 2010). Quantitatively, the seven
331 neutral and two amino sugars represent only a minor fraction, between 10-20%, of the
332 total HMWDOM carbohydrate. The composition of most HMWDOM polysaccharide,
333 even to the level of simple sugar compliment, is therefore unknown.
334 Sugars in HMWDOM have also been characterized by direct temperature
335 resolved mass spectrometry (DT-MS; Boon et al., 1998; Minor et al., 2001). In DT-MS,
336 the sample is rapidly heated under vacuum. Thermal decomposition of the sample leads
337 to the release of simple, volatile degradation products that are characteristic of the type of
338 organic matter undergoing thermolysis. DT-MS of model compounds (proteins, lipids,
339 carbohydrates and nucleic acids) allow for the assignment of diagnostic masses for
340 different compound classes. DT-MS spectra of HMWDOM display ions for hexoses,
341 pentoses, and deoxysugars, that were attributed to N-acetyl-amino-, and monomethyl-

342 and dimethy-, and methyl-deoxysugars. Ions from N-acetyl-aminosugars were often the
343 most intense features of the mass spectra, consistent with the assignment of the large
344 signal at 2 ppm in the ^{1}H NMR spectrum as -C(=O)C**H**$_3$ (Fig. 2.2B). No ions for acetic
345 acid were observed, and the study concluded that nitrogen, not oxygen, was the site of
346 acetylation. Masses indicative of deoxy- and methyl-sugars were also prominent, and
347 these sugars make substantial contributions to the uncharacterized portion of
348 HMWDOM. HMWDOM polysaccharides are introduced into the mass spectrometer by
349 thermal desorption, which occurs in two distinct stages. The bimodal thermal evolution
350 profile is indicative of at least two fractions of carbohydrate (Boon et al., 1998). Both
351 fractions include the same suite of sugars, but the relative intensity of ions derived from
352 furfural (from uronic acids or deoxysugars) was enhanced and the specificity of the
353 spectra decreased in the high temperature fraction. No evidence was found in either
354 fraction for extended homopolysaccharides: chitans, glycans, xylans, or arabino-galactans
355 that are typical of many storage and some structural polysaccharides. DT-MS data
356 suggest HMWDOM polysaccharides are very heterogenous, include a large fraction of
357 deoxy- and N-acetyl aminosugars, and are highly branched and cross-linked.
358 Branching into two and three-dimensional polysaccharides can be assessed by
359 selective permethylation of the polysaccharide to protect non-linked sites, followed by
360 hydrolysis. Hydrolysis leaves methylated sites intact, but results in a suite of simple
361 methylated sugars that can be identified and quantified by chromatography. Linkage
362 analysis shows that of the sugars that can be recovered after acid hydrolysis (e.g., 10-20%
363 of the total polysaccharide), 40% have only terminal linkages, 40% are linked without
364 branching, and 20% are branched with one branch point. All of the seven major neutral
365 sugars characteristic of HMWDOM (glucose, galactose, mannose, fucose, rhamnose,
366 xylose and arabinose) have terminal linkages, but only a few sugars are branched. Major
367 linkage patterns for non-branched sugars include 1,3 and 1,4 linkages, with only small
368 amounts of 1,2 branching (Sakugawa and Handa, 1985; Aluwihare et al., 1997). The
369 degree of branching in HMWDOM polysaccharides is unusually high. Highly branched
370 polysaccharides are typical of structural biopolymers found in microbial cell walls. The
371 high degree of branching may impart some resistance to microbial degradation that
372 persists and allows these polymers to accumulate as DOM.

373 The distinct peaks at 2.0 ppm in ^{1}H NMR and 26 ppm in ^{13}C NMR spectra (Fig.
374 2.2 A, B) are assigned to the methyl group of N-acetylated sugars (Aluwihare et al.,
375 2005; Quan and Repeta, 2007). Correlation analysis (Fig. 2.3B; Abdulla et al., 2010a,b)
376 shows synchronous changes in resonances in amide carbon at 180 ppm, anomeric carbon,
377 O-alkyl carbon and methyl carbon at 26 and 20 ppm, in support of this assignment.
378 Based on integration of the ^{13}C- and ^{1}H NMR spectra (Fig. 2.2), acetate contributes 5-8%
379 of the polysaccharide carbon, larger than any other molecular component of HMWDOM
380 polysaccharide identified to date. On this basis, approximately one out of every four
381 sugars in HMWDOM polysaccharide would have N-linked acetate. Aluwihare et al.
382 (2005) inferred that N-acetyl amino sugars are incorporated into a family of related
383 acylated polysaccharides (APS) that includes major neutral sugars and amino sugars, but
384 correlation analysis suggests a somewhat higher ratio (6:1) of neutral to amino sugars,
385 and that there are at least two distinct fractions of neutral and amino polysaccharides.
386 Correlation analysis distinguishes acylated amino sugar containing polysaccharide (APS)
387 from (non-acylated) heteropolysaccharides on the basis of changes in the asymmetric
388 amide stretching the IR spectrum at 1660 cm^{-1}. In a suite of samples through a coastal
389 estuary, Abdulla et al. (2010a) found that as HMWDOM samples become increasing
390 marine, with a relative increase from 50% to 70% in heteropolysaccharide content but
391 little change in the acylated amino sugar containing polysaccharide component,
392 suggesting that the major heteropolysaccharide and aminosugar components of
393 HMWDOM behave independently. A more detailed characterization of HMWDOM and
394 a better understanding of spatial/temporal changes in HMWDOM cycling will be needed
395 to reconcile these two interpretations of polysaccharide composition.
396 The contribution of N-acetyl-aminosugars to HMWDOM polysaccharide has been
397 quantified indirectly by monitoring the effects of mild acid hydrolysis on ^{1}H- and ^{15}N-
398 NMR spectra (Aluwihare et al., 2005). ^{15}N NMR spectra of HMWDOM are
399 characterized by a large peak from amide-N at 124 ppm and a smaller peak at 35 ppm
400 from methyl- and amino-N (McCarthy et al., 1997; Aluwihare et al., 2005). The two
401 common classes of biochemicals most likely to contribute to amide-N are proteins,
402 polymers of amino acids linked through an amide functional group, and N-acetyl amino
403 sugars such as chitin or peptidoglycan. Hydrolysis of either will convert amide-N to

amino-N, however for proteins this results in depolymerization while in N-acetyl amino sugars it does not. If acetate occurs primarily as N-acetyl amino sugars, then the amount of amino acids plus acetic acid released by hydrolysis should equal the conversion of amide-N to amino-N measured by ^{15}N NMR. If conversion exceeds the sum of amino acids and acetic acid, then other biochemicals must contribute to amide-N. Alternatively, if the conversion is significantly less than the sum of amino acids and acetic acid, then a significant fraction of acetate is bound as (O-linked) esters.

Hydrolysis of surface (5-23 m) and midwater (600-1000 m) samples showed good agreement between the conversion of amide-N to amino-N and the production of amino acids and acetic acid (Fig. 2.4). Between 97-116% of the new amino-N could be accounted for as the sum of amino acids and acetic acid. Of this, the majority (72-90%) was attributed to hydrolysis of N-acetyl amino sugars, while the balance (11-44%) was attributed to protein hydrolysis. Critical to this interpretation is the assumption that quantitative agreement between ^{15}N NMR and molecular level acetic acid analysis signifies that acetic acid is derived from N-acetyl amino sugars. The experiment does not show this directly, but given results from DT-MS that only acetamide is generated by HMWDOM thermolysis, fortuitous agreement between the two techniques seems unlikely.

Detailed characterization of methyl sugars followed their detection in DT-MS spectra by nearly a decade. Hydrolysis of HMWDOM yields an O-methylated sugar fraction that can be purified by chromatography and characterized in detail by ^{1}H NMR and mass spectrometry (Panagiotopoulos et al., 2007; Panagiotopoulos et al., 2013). All seven major neutral sugars recovered by hydrolysis were found to have mono- and di-O-methylated homologues (Fig 2.5). In addition, many novel O-methyl sugars not yet identified in the nonmethylated fraction, including O-methyl heptose, O-methyl di-deoxy hexoses and yersiniose, a dideoxy-4-C-(1-hydroxyethyl)-D-xylo-hexose, occur in small amounts. The presence of methyl sugars does not impact the interpretation of linkage analysis, since methylation prevents linkage through a particular carbon, and the product in each case is a methyl sugar. O-methyl sugars are common in algal and bacterial structural polysaccharides, and as such have little biomarker value, but their occurrence in HMWDOM and the complexity of the O-methyl sugar mixture suggests a broad suite

435 of structural polysaccharides may co-exist in HMWDOM. Treatment of HMWDOM
436 with periodate at high temperature yields methanol as a major oxidation product (Quan
437 and Repeta, 2007). Assuming all this methanol is sourced from O-methyl sugars, O-
438 methyl sugars contribute an important fraction of HMWDOM, beyond the amount
439 released by acid hydrolysis. Quantitative analysis of methanol after periodate oxidation
440 could be useful in assessing the contribution of methyl sugars to non-hydrolyzable
441 HMWDOM polysaccharide.
442 Attempts to further characterize HWMDOM polysaccharides have been met with
443 limited success. For reasons that are still unknown, even aggressive hydrolysis by strong
444 acid does not appear to depolymerize HMWDOM, and ~70% of the polysaccharide
445 fraction remains relatively uncharacterized (Panagiotopoulos and Sempéré, 2005).
446 Information on the non-hydrolyzable portion of HMWDOM polysaccharide can be
447 obtained from 2D homo- and heteronuclear NMR correlation techniques (Fig. 2.6). For
448 example, the ^{1}H NMR correlation spectroscopy (COSY) spectrum of non-hydrolyzable
449 HMWDOM polysaccharide shows strong cross peaks between methyl, H-6 protons
450 (C**H**$_3$-) and carbohydrate H-5 (**H**C-OH) from 6-deoxysugars. Cross peaks are also
451 observed between 2-3 ppm and 3-4 ppm from 2-, 3- or 4-deoxysugars (Fig. 2.6).
452 Deoxysugars are recovered from HMWDOM hydrolysis products only in low yields
453 (~2% of total carbon), but the 2D NMR suggests a much higher contribution to
454 HMWDOM carbohydrate.
455 Each class of sugar (hexose, pentose, deoxyhexose, aminohexose, methylhexose)
456 identified by DT-MS has a different molecular weight easily distinguished by mass
457 spectrometry, making this is an attractive approach for understanding the sequence and
458 arrangement of sugars within DOM (Boon et al., 1998; Minor et al., 2001). However, a
459 number of issues including the low ionization efficiency of carbohydrates relative to
460 other classes of organic matter, incomplete removal of inorganic salts, and a molecular
461 weight range that may easily exceed the mass range of most spectrometers (typically 2-4
462 kDa), need to be overcome before MS can be applied to its full potential (Sakugawa and
463 Handa, 1985; Schmidt et al., 2003). For example, high-resolution mass spectra for
464 HMWDOM show no ions with H/C and O/C elemental ratios characteristic of
465 polysaccharides (~1.7-2.0 and ~ 0.8-1.0 respectively; Hertkorn et al., 2006). Numerous

466 strategies have been developed in glycochemistry to enhance the MS detection of
467 polysaccharides by conjugation with proteins or fluorescent tags that are amenable to
468 ionization by electrospray and matrix assisted laser desorption ionization (ESI; MALDI).
469 These approaches might prove promising for DOM polysaccharides, and could facilitate
470 MS characterization. Separation of HMWDOM polysaccharides into defined fractions
471 could also facilitate spectral characterization. Appropriate methods for size exclusion
472 and ion chromatography for complex mixtures of oligo- and polysaccharides in the
473 molecular weight range of a few kDa and higher are limited, but have been applied to
474 HMWDOM (Sakugawa and Handa, 1985). Recent advances in strong anion exchange
475 chromatography at high pH also shows promise as an approach for HMWDOM
476 carbohydrate separations (Corradini et al., 2012).
477 Finally, some inferences as to the composition of different HMWDOM
478 polysaccharides can be drawn from changes in the temporal and spatial distribution of
479 sugars between samples. Multivariate analysis of DT-MS data from samples collected in
480 the U.S. Mid Atlantic Bight between 35^{o}N-43^{o}N and the Gulf of Mexico find the same
481 suite of ions from hexoses, pentoses, deoxy-, N-acetyl-amino- and methyl sugars in all
482 samples, but the relative abundances changed with sample location (Boon et al., 1998).
483 These differences were attributed to changes in the composition or relative abundance of
484 different polysaccharides. The most striking differences were between sugars desorbed at
485 low and high temperatures. The high temperature fraction from all samples showed a
486 remarkable similarity in composition, while the sugar distribution in the low temperature
487 samples showed much more diversity, and some clustering by sampling site. The results
488 suggest two distinct fractions of polysaccahrides co-exist in coastal seawater, a fraction
489 with highly similar composition that is ubiquitous at all sites, and a fraction of variable
490 composition influenced by local production.
491
492 *2.3.2 Proteins and amino acids in DOM*
493 Proteins account for up to 50% of the organic carbon and 80% of the organic
494 nitrogen in marine microbes. Grazing, release of extracellular enzymes, and viral lysis all
495 introduce proteins and amino acids into seawater, and on this basis alone, it is likely that
496 proteins contribute to DOM. Analytical methods to identify and quantify dissolved

497 proteins directly (proteomics) have only recently reached the point where they can be
498 applied to DOM, and the next decade should see a rapid expansion in our understanding
499 of the sources, cycling, and fate of proteins as these methods become more widely
500 applied. However, studies of the distribution, stereochemistry, and isotopic values of
501 amino acids released after DOM hydrolysis have already made major contributions to our
502 understanding of dissolved protein cycling, and have set the stage for the future
503 application of proteomics.
504 Sensitive methods for the detection of nanomolar concentrations of dissolved
505 amino acids were first applied to seawater in the early 1960's and 70's (Lee and Bada,
506 1975, 1977). Due to the low ambient concentrations of dissolved amino acids, and the
507 potential for contamination by laboratory glassware and reagents, early studies gave
508 variable results. Current analyses capitalize on the reaction of ortho-phthalaldehyde
509 (OPA) with primary amines in basic, aqueous solutions to form fluorescent, hydrophobic
510 products that can be retained and separated by high pressure liquid chromatography
511 (Lindroth and Mopper, 1979; Mopper and Lindroth, 1982). The reaction proceeds
512 rapidly and at high yields and has sub-nanomolar detection limits. Primary amines other
513 than amino acids (ammonia, urea, etc.) also react with OPA and are included in the
514 analysis. Some amino acids co-elute under some separation conditions, but with
515 appropriate calibration the method provides good quantitative measurements of dissolved
516 amino acids in seawater (Tada et al., 1998).
517 Dissolved amino acids are operationally classified by the methods used for
518 sample processing. Dissolved "free" amino acids (DFAA) are measured by the direct
519 reaction of OPA with seawater, and are thought to represent monomeric amino acids
520 present in a sample. In order to minimize contamination during sample processing, some
521 early studies did not use filtration to separate dissolved and particulate free amino acids
522 (Mopper and Lindroth, 1982). However, subsequent studies typically include a filtration
523 step (Fuhrman, 1987). Treatment of filtered seawater with acid hydrolyzes peptides,
524 proteins, and glycoproteins, and allows for the measurement of "total hydrolysable" or
525 "total dissolved" amino acids (THAA; TDAA, respectively; Lee and Bada, 1975, 1977).
526 The difference; THAA-DFAA represents dissolved combined amino acids (DCAA), the
527 fraction of amino acids bound as proteins, peptides and other amino acid polymers. Since

DFAA are typically more than an order of magnitude less abundant than DCAA, recent studies have focused only on total hydrolyzable or total dissolved amino acids (McCarthy et al., 1996; Yamashita and Tanoue, 2003b).

Open ocean profiles of DFAA in the equatorial Pacific and Sargasso Sea show very low values throughout the water column. Surface water concentrations (10-40 nM) are somewhat enriched relative to deep sea samples, which have lower and more constant values (<10-20 nM). THAA distributions follow a pattern similar to DFAA, with higher and more variable concentrations in surface waters (200-450 nM) and lower and more stable values below the euphotic zone (100-200 nM)(Fig. 2.7; Lee and Bada, 1975, 1977; McCarthy et al., 1996; Yamashita and Tanoue, 2003b; Kaiser and Benner, 2009) Semi-enclosed seas, coastal and near-shore sites have higher concentrations of both DFAA and THAA.

Overall, spatial patterns of THAA concentrations reflect changes in DOC concentrations. THAA carbon to total DOC ratios (THAA-C/DOC) vary between sites and depth, but generally fall within 1-4% for surface waters and 0.4-0.8% at depths > 1000 m (McCarthy et al., 1996; Yamashita and Tanoue, 2003a; Kaiser and Benner, 2009). THAA contribute a larger portion of DON (1.4-11%; McCarthy et al., 1996; Tada et al., 1998; Kaiser and Benner, 2009), and are the largest component of DON characterized to the molecular level. A decrease in the ratio of THAA-C to DOC has been observed between highly productive coastal waters and the open ocean along a line extending from Japan (Yamashita and Tanoue, 2003a). THAA carbon to DOC ratios fall from 4% in near-shore surface waters to 2% in offshore surface waters. Similar patterns have been observed in the Baltic Sea, Chesapeake Bay, Biscaye Bay (Florida) and in the Laptev Sea (Mopper and Lindroth, 1982). Nutrient and chlorophyll concentrations were quite high at all sites and higher rates of local primary production; more dynamic organic matter cycling closer to shore may result in relatively higher contributions of THAA to DOC.

Major amino acids include glycine, alanine, glutamic acid, serine, aspartic acid, arginine and threonine, which typically contribute >90% of THAA (Fig. 2.8). Other protein amino acids individually represent < 5 mole % of THAA, although contributions from valine and leucine are sometimes in excess of this amount. Tryptophan decomposes

559 under the acid and temperature conditions typically used for THAA analysis, and can be
560 measured in samples only when alkaline conditions are used for hydrolysis. In open
561 ocean waters tryptophan contributes ~1 mol % of THAA, although somewhat higher
562 contributions were noted near-shore.(Yamashita and Tanoue, 2003b) The distribution of
563 amino acids in THAA is significantly different than particulate organic matter
564 (phytoplankton, suspended and sinking detrital material, Fig. 2.8), with higher
565 concentrations of aspartic acid and glycine, but lower concentrations of arginine, leucine
566 and isoleucine (Fig. 2.8).
567 Amino acid distributions at open-ocean and coastal sites generally do not show
568 large, systematic changes, however subtle changes have been detected through correlative
569 analysis. Using relative abundance as a measure of sample relatedness, Yamashita and
570 Tanoue (2003b) compared changes in the distribution of amino acids along a north-south
571 transect along 137^{o}E from Ise Bay, Japan into the northwest Pacific Ocean. Some amino
572 acids (for example glycine and alanine) are positively correlated in all samples, and on
573 this basis, amino acids were grouped into four categories. The positive correlations
574 within a particular group indicates similarities in the biogeochemical cycling of the
575 constitutive amino acids, while differences in the correlations between groups suggest
576 divergence in THAA cycling due to differences in either the macromolecular form of the
577 peptides or the way THAA are processed by microbial degradation. Amino acid
578 distributions have also been analyzed by principal component analysis (PCA) to
579 quantitatively differentiate patterns of amino acid distribution. Cross correlation of the
580 first and second PCA scores for each acid showed general groupings based on sample
581 location and depth (bay, coast, open-ocean, surface, and deep water), and cross plots of
582 factor coefficients grouped acids into four classes with the same make up as found for
583 correlative analysis.
584 Amino acids occur in two enantiomeric forms (D- and L-amino acids). Proteins
585 are made exclusively from L-amino acids, but many bacteria utilize D-amino acids in
586 cellular regulatory functions and in bacterial cell wall biopolymers (Cava et al., 2011).
587 Enantiomeric amino acids can be chromatographically separated and quantified in THAA
588 analysis, and the composition and distribution of D-amino acids have been used as a
589 biomarker for the contribution of bacterial cell wall material to DOM (Lee and Bada,

590 1977; McCarthy et al., 1998; Kaiser and Benner, 2008). Lee and Bada (1977) reported
591 enantiomeric (D:L) ratios of aspartic acid (0.07-0.44), glutamic acid (0.04-0.07), alanine
592 (0.05-0.14), valine (0.02-0.04), isoleucine (<0.01-0.22) and leucine (0.02-0.07).
593 Subsequent studies have reported D:L ratios for serine of 0.1-1. McCarthy et al. (1998)
594 found the HMWDOM fraction has higher D:L ratios for glutamic acid (0.08-0.15) and
595 alanine (0.32-0.55) than THAA. These ratios are greater than D/L ratios in cellular
596 organic matter and POM, and are indicative of selective preservation of D-amino acid
597 containing bacterial structural polymers relative to proteins in THAA (McCarthy et al.,
598 1998; Dittmar et al., 2001; Nagata, 2003; Kawasaki and Benner, 2006, 2008).
599 The high relative abundance of D-amino acids in THAA and HMWDOM has led
600 to a series of investigations designed to assess the contribution of bacterial cell wall
601 material to DOM. Bacteria are abundant at all depths in the ocean, and the selective
602 preservation of D-amino acids indicated by high D/L ratios suggests that cell wall
603 biopolymers are more resistant to microbial degradation than proteins, and are therefore
604 likely to be persist in DOM (McCarthy et al., 1996; Kaiser and Benner, 2008; Calleja et
605 al., 2013). Kaiser and Benner (2008) measured the abundance and distribution of D-
606 amino acids and muramic acid (a constituent of peptidoglycan in bacterial cell walls) in
607 marine heterotrophic and cyanobacteria in order to make a quantitative assessment of the
608 peptidoglycan and other D-amino acid containing bacterial cell wall constituents to
609 DOM. In purified peptidoglycan, the ratios of muramic acid to D-glutamic acid and D-
610 alanine are ~1 and ~0.75, respectively. Ratios in marine POM and DOM above these
611 values were interpreted to signify the presence of other (non-peptidoglycan) D-amino
612 acid containing constituents, while ratios below these values signify the preferential
613 degradation of D-amino acids relative to muramic acid. Muramic acid was non-
614 detectable (<1.2 nM) in filtered seawater, even though total D-amino acids concentrations
615 ranged between 8-26 nM. These high relative concentrations suggest that D-amino acids
616 in DOM are either derived from peptidoglycan degradation products or are constituents
617 of bacterial polymers other than peptidoglycan.
618 Tanoue and colleagues pioneered the application of gel electrophoresis and N-
619 terminal sequencing to characterize intact proteins in DOM (Tanoue et al., 1995; Tanoue,
620 1995; Tanoue et al., 1996; Yamada and Tanoue, 2003). Dissolved proteins can be

concentrated and desalted using ultrafiltration (>10 kDa), then partially purified by precipitation with cold trichloroacetic acid or methanol/chloroform/water (Tanoue, 1995; Powell and Timperman, 2005). Care must be exercised throughout the concentration steps to minimize contamination from lysed cells or bacteria growth, as well as from losses of proteins due to precipitation or adsorption onto filters and other surfaces. The insoluble protein pellet from trichloroacetic acid precipitation was washed of residual polysaccharides and lipids with ethanol and diethyl ether, then analyzed by gel electrophoresis.

Electrophoretograms of dissolved proteins were compared to a suite of standard marker proteins separated on the gel electrophoresis plate by molecular size (Fig. 2.9). Samples from the northcentral and southwest Pacific Ocean and the Gulf of Mexico show proteins with a wide range of sizes corresponding to molecular weights from < 14kDa to > 66 kDa (Tanoue et al., 1995; Tanoue, 1995; Tanoue et al., 1996; Powell et al., 2005). Major proteins were concentrated in 25-30 bands, some of which were present in all samples, while others changed with sample location and depth. Surface waters <50 m generally showed low numbers and concentrations of recognizable protein bands. The number and intensity of bands increased with depth (75-200m); below 200m, gels were heavily stained, with a high degree of background staining from unresolved proteins and perhaps humic substances. Proteins with putative molecular weights of 48 kDa and 37-40 kDa were clearly visible at many of the stations irrespective of depth, while proteins designated as 66-63 kDa, 44 kDa, 41 kDa, 31-34 kDa, 26 kDa, 23 kDa, and 15 kDa varied with depth and sampling location, but were present in a number of samples. The strikingly similar patterns that appear in electrophoretograms of dissolved proteins led Tanoue et al. (1996) to conclude that the processes that transfer proteins from cellular material and allow for their accumulation in DOM are similar across broad expanses of the ocean.

The major protein band at ~48 kDa present in all samples was recovered from six samples collected between 45-462m and the N-terminal sequence of 14-15 amino acids determined (Tanoue et al., 1995). Later analysis of these samples expanded the sequence to 24 amino acids (Yamada and Tanoue, 2003). All 48 kDa bands yielded the same N-terminal sequence of amino acids, indicating that all bands represented the same protein.

652 The sequence shared 100% homology with porin-P and porin-O of the gram-negative
653 bacterium *Pseudomonas aeruginosa* (Tanoue et al., 1995; Yamada and Tanoue, 2003).
654 Porin-P and porin-O are membrane proteins expressed to facilitate cross membrane
655 transport of small hydrophilic substrates, often under conditions of phosphate stress. The
656 bacterial community composition at the sampling sites was not determined, but genomic
657 analysis of bacterioplankton at Station ALOHA, one of the stations sampled by Tanoue,
658 yielded 16s sequences of *Alteromonas*, *Vibrio* and *Pseudomonas* spp., bacteria that are
659 closely related to *P. aeruginosa*. Similar biosynthetic pathways between indigenous
660 bacteria and *P. aeruginosa* might lead to porins of comparable homology. Recognizing
661 that existing databases contain sequences from only a small number of proteins, Tanoue's
662 data suggests that bacterial proteins such as porin-P contribute to DOM. Porin P has been
663 shown to be resistant to proteases, which together with a potentially ubiquitous and
664 abundant source, may explain its appearance in all samples analyzed by gel
665 electrophoresis in Tanoue's studies. Likewise a 40 kDa protein from the North Pacific
666 had 100% homology with the family of outer membrane proteins (OmpAs) of
667 *Acinetobacter* spp., however sequencing of the 30 kDa, 37 kDa, and 39 kDa proteins did
668 not exhibit homology with any known proteins in searchable databases, and these
669 proteins could not be identified
670 Suzuki et al. (1997) and Yamada et al. (2000) developed and applied an
671 immunochemical assay against bovine serum albumin modified with the N-terminal 14
672 oligomer of *P. aeruginosa* porin P (α-48 DP N-14), and the whole outer membrane
673 protein Omp35La from *Vibrio anguillarum*. Polyclonal antibodies developed against
674 these antigens were used as sensitive screens for porin P and related proteins in DOM.
675 Western blots of DOM proteins showed cross reaction between the α-48 DP N-14 probe
676 and the 39 kDa, 48 kDa and 60 kDa bands, and between the Omp35La probe and the 18
677 kDa, 34 kDa and and 70 kDa bands. Cross reaction of the α-48 DP N-14 probe and the
678 39 kDa protein is not fully understood, as a subsequent investigation showed this protein
679 to be glycosylated, and therefore probably not a porin P homologue (Yamada and
680 Tanoue, 2003). Cross reactivity for the α-48 DP N-14 probe was also observed for
681 natural populations of bacteria in all samples, although the number of bacteria cells that
682 cross reacted were 2-6 orders of magnitude less than enumerated by total bacterial cell

683 counts. The results raise the possibility that the sources and composition of proteins
684 dissolved in seawater might be highly specific.
685 Erdman degradation was used to partially sequence the 48 kDa protein in DOM,
686 but HPLC-MS techniques offer the possibility of more comprehensive sequencing of
687 dissolved proteins in environmental samples (Powell et al., 2005). In this approach,
688 proteins purified by gel electrophoresis or capillary zone electrophoresis are partially
689 digested by exposure to trypsin, a protease, and the peptides separated by HPLC and
690 sequenced by MS. Fragment ion masses are used to reconstruct the peptide amino acid
691 sequence that is then compared to sequence information stored in databases of known
692 proteins. Using this approach, Powell et al. (2005) distinguished families of proteins,
693 showing that proteins from both bacterial membranes (fatty acid synthetase, luminal
694 binding protein) and enzymes (ribulose bisphosphate carboxylase, anthranilate
695 synthethase) were present in DOM (Powell et al., 2005).
696 Bottom-up proteomics and amino acid D/L ratios both highlight the contribution
697 of bacterial proteins to DOM. Another way to assess the sources, cycling, and
698 distribution of dissolved proteins is to target abundant proteins using 2D gel
699 electrophoresis and sensitive immunoassays such as ELISA (enzyme-linked
700 immunosorbent Assay) and MSIA (mass spectrometry immunoassay; Orellana et al.,
701 2003; Jones et al., 2004; Orellana and Hansell, 2012). In their proteomic data, Powell et
702 al. (2005) reported short peptide sequences suggestive of ribulose-1,5-bisphosphate
703 carboxylate/oxygenase (RuBisCo). RuBisCo is one of the most abundant proteins on
704 Earth, and is essential in catalyzing carbon fixation in vascular plants, algae,
705 photoautotrophic and chemoautotrophic bacteria. RuBiscCo is abundant in particulate
706 matter located in the euphotic zone, where grazing, viral lysis, and other processes
707 transfer some particulate RuBisCO into DOM. Some of the DOM proteins visualized by
708 electrophoresis and staining, particularly in the range of known RuBisCo subunit proteins
709 of 55 and 13 kD, probably result from this cycling. Orellana and Hansell (2012) used a
710 synthetic protein incorporating RuBisCo sequences to develop an immunoassay for anti-
711 RbcL to measure RuBisCo concentrations in ~800 samples from the North Pacific Ocean.
712 The large number of samples analyzed in this study, and sensitive detection limits (< 1
713 ng RuBisCo L^{-1}), highlights the potential power of immunological approaches to track

714 the distribution and cycling of biologically important proteins. They found RuBisCo in
715 all samples from the surface to depths > 4000 m. RuBisCo is synthesized in the euphotic
716 zone, and the presence of high concentrations of RuBisCO (5-20 ng/L) throughout the
717 deep ocean ties meso- and bathypelagic RuBisCO distributions to export production (a
718 small amount of RuBisCO may be synthesized at depth from chemoautrophy, but this
719 contribution is thought to be small). As large particles sink from the euphotic zone,
720 microbial remineralization and physical disaggregation release smaller particles and
721 inject DOM into underlying waters. High relative concentrations (15-20 ng L^{-1} between
722 2000-4000 m) of RuBisCO in the deep equatorial and subarctic Pacific coincide with
723 higher carbon export in these regions. Low relative concentrations of RuBisCo ($\leq$ 10 ng
724 L^{-1} between 2000-4000m) below the northern and southern subtropical gyres were
725 attributed to the low carbon export fluxes that characterize these regions. The coupling
726 of deep water RuBisCo concentrations to surface processes implies a rapid turnover of
727 RuBisCo related proteins, but spatial differences in deep RuBisCo concentrations also
728 trace deep water mass flows. If correct, then the residence time of some deep RuBisCo is
729 on the order of years to decades, a timescale typically associated with semi-labile DOM
730 (Section 4.2).
731
732 *2.3.3 Humic substances in solid phase extractable DOM (SPE-DOM)*
733 Simple ^{1}H and ^{13}C NMR spectra along with elemental analysis of hydrophobic
734 SPE-DOM made in the 1970's and 1980's showed SPE-DOM is distributed throughout
735 the water column, is rich in COOH and aliphatic carbon, and has a COOH/aliphatic
736 carbon ratio of 1:4-5 (Hedges et al., 1988). Natural products with such a high ratio of
737 COOH/alkyl carbon are rare in nature, and the SPE-DOM fraction is therefore thought to
738 result from extensive transformations of marine lipids, carbohydrates and proteins.
739 Recent studies refer to this fraction of DOM as "carboxyl rich aliphatic material"
740 (CRAM), but it has alternatively been referred to as hydrophobic DOM, solid phase
741 extractable (SPE) DOM, carboxylate rich carbon (CRC), or marine humic substances
742 (HS). For simplicity, this fraction of DOM will hereafter be referred to as SPE-DOM,
743 since all studies rely on isolation by adsorption onto a solid hydrophobic resin (XAD, C-
744 18, PPL), and recent work has begun to distinguish distinct components within SPE-

745 DOM and assign characteristic molecular features to specific terminology (CRAM,
746 thermogenic DOM, *etc*.). However, in the literature, different terminologies are still in
747 use. SPE-DOM as been compared to humic substances isolated from soils and
748 freshwaters, but the marine version has a lower aromatic and olefinic content, a higher
749 C/N ratio, and a carbon staple isotope ($\delta^{13}C$) value of ~21-22 ‰, all of which suggested a
750 autochthonous source (Gagosian and Steurmer, 1977; Hedges et al., 1988; Druffel et al.,
751 1992). Although only a handful of measurements exist, SPE-DOM is highly depleted in
752 radiocarbon (-310 to -587 ‰), and is considered to represent recalcitrant fractions of
753 DOM resistant to microbial oxidation (Druffel et al., 1992).
754
755 *2.3.3.1 Characterization of SPE-DOM by high-field nuclear magnetic resonance*
756 The processes that lead to the formation and removal of SPE-DOM in the ocean
757 are not known, but high field NMR and high resolution MS have added unprecedented
758 detail to our knowledge of its composition (Hertkorn et al., 2006; Dittmar and Koch,
759 2006; Hertkorn et al., 2012; Helms et al., 2013). ^{1}H NMR spectra are characterized by
760 broad peaks between 0.8-10 ppm with substantial signal overlap (Fig 2.10). Major
761 signals have been assigned to aliphatic C**H**$_3$ and C**H**$_2$, carbonyl-rich aliphatics,
762 particularly methine protons ((C)$_2$-C**H**-COOH), methoxy protons (C**H**$_3$O), carbohydrate-
763 derived methines ((C)$_2$-C**H**-OH) and (O-C**H**-O)), and protons on sp^2 hybridized olefinic
764 and aromatic carbon. When ^{1}H NMR spectra of samples collected in a depth profile from
765 5m to 5446m were normalized to 100% total area (0-10.5 ppm), the spectra showed
766 nearly coinciding aliphatic terminal (-CH$_2$-C**H**$_3$; $\delta \sim 0.9$ ppm) methyl abundance, variable
767 methylene (-C**H**$_2$- > 4 bonds from a heteroatom) abundance, and progressively increasing
768 amounts of H associated with methylated, alicyclic rings with depth. Signals associated
769 with acylated polysaccharides (N-C(O)-C**H**$_3$; **H**-C-OH, O-C**H**-O, C**H**$_3$O-C) decreased
770 with depth.
771 Although signal overlap limits molecular definition in 1D ^{1}H NMR spectra, 2D
772 COSY spectra provide unprecedented definition of overlapping signals. About 4500 off-
773 diagonal cross peaks have been observed for SPE-DOM collected in surface waters, of
774 which ~75% were derived from sp^3 -hybridized carbon (H**C**$_{sp3}$-**C**$_{sp3}$H, H**C**$_{sp3}$ (O)-**C**$_{sp3}$H,
775 and H**C**$_{sp3}$ (O)-**C**$_{sp3}$(O)H), and 25% from sp^2 hybridized carbon (H**C**$_{sp2}$-**C**$_{sp2}$H; δ_H >5

776 ppm; Hertkorn et al., 2012). Assuming an average spin system of ~ 3.5 protons, the
777 COSY spectra of SPE-DOM suggests a mixture of at least several hundred distinct
778 molecular species. With depth, the COSY spectra of SPE-DOM become progressively
779 attenuated, however the position of major peaks remains the same. SPE-DOM
780 composition is highly conserved with depth, but the attenuation of COSY cross peaks
781 suggests subtle changes in composition that lead to faster transverse relaxation of NMR
782 signals and/or increasing molecular diversity associated with DOM aging (Hertkorn et
783 al., 2012).
784 ^{13}C NMR spectra and 2D heteronuclear ^{1}H/^{13}C NMR spectra are consistent with
785 these assignments, allowing for a better quantitative assessment of how carbon functional
786 groups are distributed within SPE-DOM. ^{13}C NMR spectra also provide some unique
787 insights not available through ^{1}H NMR alone. All ^{13}C NMR spectra show signals from
788 carbonyl (**C**=O; 220-187 ppm), carboxyl (**C**OX; where X= -O, -N, -CH_3; 187-167 ppm),
789 aromatic **C**-X (where X = O, N) and aromatic **C**-H (167-145 and 145-108 ppm
790 respectively), carbohydrate carbon (anomeric O-**C**H-O, 108-90 ppm and O-alkyl H**C**-
791 OH, 90-47 ppm), and aliphatic carbon (47-0 ppm; Hertkorn et al., 2006, 2012) The
792 relative amount of carboxylic acids and ketones increases from surface to deep water, and
793 the amount of labile carbohydrate carbon declines, indicating a selective removal of
794 carbohydrates and gradual oxidation of the non-carbohydrate fraction. Methine carbon
795 associated with aliphatic branched functional groups (C_3-**C**-H) increased relative to
796 aromatic and carbohydrate associated carbon from 46% in surface waters to 57% at 5446
797 m. The highly branched nature of marine SPE-DOM is also indicated by the relatively
798 intense adsorption bands between 2970-2980 cm^{-1} (aliphatic methyl stretch) and 2944
799 cm^{-1} (aliphatic methyl stretch) in the infrared (Esteves et al., 2009). NMR and IR spectra
800 indicate that aromatic carbon was not abundant at any depth (< 5%), and some aromatic
801 carbon associated with downfield NMR signals (δ_c =164 ppm) display a cross beak with
802 aromatic protons (δ_H = 8.2 ppm) that indicate nitrogen heterocycles (Esteves et al., 2009;
803 Hertkorn et al., 2012). Only a minor fraction (15%) of methyl groups were purely
804 aliphatic (-CH_2-**C**H_3), while a major fraction (70%) were shifted downfield to between 1-
805 1.6 ppm. The downfield shift in most methyl groups suggests proximity (< 3 C bonds
806 away) to carboxyl carbon. The carboxyl carbon peak itself is Gaussian shaped and

displays a sizable chemical shift range (6 ppm at half height) indicating high diversity and little preference or regularity in its chemical environment.

In summary, ^{1}H and ^{13}C NMR spectra show SPE-DOM is a highly complex, yet well defined mixture of molecular components, that includes carbohydrates and a carboxy-rich aliphatic (CRAM) fraction, along with a minor amount of extended aromatic and aromatic N-heterocycles. The CRAM fraction appears to become more highly branched with depth, either from transformations associated with aging, or from selective removal of less highly branched carbon. The major change in the distribution of carbon functional groups in SPE-DOM with depth results from the progressive loss of carbohydrate and the conservation of CRAM (Hertkorn et al., 2012).

2.3.3.3 Characterization of SPE-DOM by high resolution mass spectrometry

High resolution mass spectra of SPE-DOM have been reported since the 1970s (Gagosian and Steurmer, 1977), but the introduction of Fourier Transform Ion Cyclotron Resonance (FT-ICR) and more recently Orbitrap mass spectrometers, each capable of measuring ions at both very high mass accuracy and resolution, has changed our ability to characterize SPE-DOM at the molecular level (Kido Soule et al., 2010; Zubarev and Makarov, 2013). Coupled to electrospray ionization (ESI) these instruments provide the necessary resolution to distinguish the several thousand ions with unique masses within DOM between 200-2000 Da (Fig. 2.11). Due to the high mass resolution and accuracy (typically < 1 ppm for ions < 400 Da), elemental formulas for most ions can be assigned with a high level of confidence. Since the number of isomers for any given mass increases rapidly with molecular weight, each unique mass probably represents a mixture of different isomers. High resolution MS therefore does not allow for the full identification of new compounds, however it has led to the discovery of important new compound classes, and it is proving to be a very powerful technique for detecting changes in DOM composition between samples. To fully exploit the large amount of data provided by high resolution MS, analysts use a number of computational tools to extract information about DOM composition. Typically, elemental formulas with all possible combinations of atoms are calculated and matched to all ions to within a mass precision determined by the operational resolution of the particular instrument.

838 Depending on the approach used 45-97% of observed masses can often be assigned
839 molecular formulae. Elemental formulae with only C, H, and O dominate the molecular
840 formulae of assigned masses, with fewer elemental formulae assigned to compounds
841 having nitrogen (CHNO), sulfur (CHOS) and both nitrogen and sulfur (CHNOS).
842 In performing these calculations, some assumptions are needed. First, the type
843 and likely number of atoms within a formula are inferred. For example, in a recent study
844 of SPE-DOM in the southwest Atlantic Ocean, Flerus et al. (2012) constrained molecular
845 formula calculations for masses between 200-600 Da within ^{12}C (0-∞), ^{13}C (0-1), ^{1}H (0-
846 ∞), ^{16}O (0-∞), ^{14}N (0-∞), ^{32}S (0-1). For positive ions ^{23}Na (0-1) is also allowed to
847 account for sodiated DOM ions. The resulting mass list is filtered to remove ^{13}C isotopes
848 (mass difference between peaks of 1.003 Da), and further filtered by making assumptions
849 about nitrogen, the H/C ratio, and the number of double bonds (Koch et al., 2007). The
850 power of high resolution mass spectrometry lies in its ability to distinguish between
851 elemental formula with the same nominal masses. For example, the functional group
852 **CH_3**-C**H**-R- has the same nominal mass (16 Da) as the functional group **O**=C-R-, but
853 differs in exact mass by 36.4 mDa (16.0313 vs 15.9949), which is well within the
854 resolution of high field instruments. High resolution MS data allow mass lists to be
855 grouped into "pseudo-homologous" series that differ by a specified functionality (e.g., -
856 CH_2- or -CO_2-). The measured mass is converted to a "Kendrick mass" where each CH_2
857 unit is defined as 14.000 Da instead of its exact mass of 14.01565 Da. The difference
858 between the exact mass and Kendrick mass is then assessed as the Kendrick Mass Defect
859 (KMD, where KMD = exact mass- Kendrick Mass). The KMD will be constant for
860 compounds within a series that differ only by the number of -CH_2- groups. The
861 elemental formula of the lowest mass member within a series is determined, usually with
862 a high degree of confidence, thereby determining the molecular formulas for all other
863 members of the series. Analysis of mass data from a number of sites shows that most
864 masses can be grouped into pseudo homologous series with mass differences of 14.0156
865 (CH_2), 2.0157 (H_2; double bond series), and 0.0364 (replacement of CH_4 with oxygen).
866 Once elemental formulae have been determined, the data are reduced to their
867 elemental H/C and O/C ratios and visualized in a van Krevelen plot (Fig. 2.12). In a van
868 Krevelen plot, the H/C and O/C ratio of each ion can be compared to the elemental ratios

of likely biochemical precursors, to other samples grouped according to sample location or type, or queried with respect to differences in molecular weight, ionization mode and other features that provide information on DOM composition and cycling. Figure 2.12 shows a van Krevelen plot of FT-ICR-MS from Station ALOHA of the Hawaii Ocean Time-series (HOT). The sample is typical of many open ocean datasets, with the majority of compounds falling within a H/C range of 0.5-1.7 and an O/C ratio of 0.2-0.8 (Kujawinski and Behn, 2006; Koprivnjak et al., 2009; Kujawinski et al., 2009; Gonsior et al., 2011; Hertkorn et al., 2012). Surprisingly, this range of H/C and O/C falls outside the elemental ratios of most common proteins, carbohydrates, and lipids (Fig. 2.12), indicating either SPE-DOM has been extensively reworked and altered from its biochemical precursors, or that SPE-DOM mass spectra target a fraction of carbon that is not abundant in cells. Intensity weighted elemental data from a number of sites shows a narrower range of average values of between 1.3-1.4 for H/C and between 0.3-0.4 for O/C. Ratios may vary somewhat between different studies due to differences in sample handing or instrumental biases. Irrespective of these differences, all studies so far report fairly similar arrays of chemical formulae for SPE-DOM.

In one of the first reports of FTICR-MS data of SPE-DOM in the open ocean, Dittmar and Koch (2006) recognized a cluster of 244 ions with very low H/C and O/C ratios (0.5-0.9 and 0.1-0.25, respectively) and a high number of double bond equivalents (DBE; double bond equivalents, number or double bonds or rings). The high number of DBE and relatively low molecular weights (428-530 Da) that characterize these ions narrowly restricts the structural possibilities. Using conservative estimates of the number of DBE that can be assigned to oxygen, they postulated the low H/C, O/C group represents a class of condensed polycyclic aromatic compounds with 5-8 rings along with different degrees of alkyl substitution and oxygen functionality. As there are no known biogenic precursors for compounds of this type, these compounds most likely originate from thermogenic processes such as terrestrial biomass burning, fossil fuel combustion, and/or reactions of organic matter in hydrothermal systems (Dittmar and Koch, 2006; Dittmar and Paeng, 2009). The discovery of thermogenic polycyclic aromatic compounds in DOM was a significant contribution to our understanding of DOM sources and cycling. Although the potential for a contribution of thermogenic black carbon to

DOM had been recognized earlier from radiocarbon measurements, it was never characterized on the molecular level until the high resolution and specificity of FT-ICRMS was brought to bear on DOM characterization (Masiello and Druffel, 1998).

To quantify polycyclic aromatic carboxylic acids to DOM, an oxidative protocol designed to measure black carbon in soils was adapted to SPE-DOM (Dittmar, 2008). In the method, concentrated nitric acid at elevated temperature (170^{o}C) oxidizes polycyclic aromatic compounds in SPE-DOM to benzene polycarboxylic acids (BPCAs; Fig 2.13), which are separated by HPLC and quantified by on-line spectroscopic detection. Analyses of marine SPE-DOM yields a suite of substituted BPCAs with a relatively high fraction of benzene penta- and hexacarboxylic acids consistent with highly condensed polycyclic aromatic precursors. The distribution of BPCA isomers varied little between samples, and it is inferred that molecular structures for SPE-DOM are therefore similar, irrespective of sample depth or location. BPCAs represent 1-3% of SPE-DOM. Subsequent work used the method to quantify total polycyclic aromatic compounds (PCAs) in a meridional section across the Southern Ocean at 30^{o}E (Dittmar and Paeng, 2009). PCA concentrations ranged from 0.6-0.8 μM carbon, or about 1-2% of total DOC. Both high and low values were measured in surface waters, implying inputs and removal of PCAs on relatively short timescales. Due to the remoteness of the Southern Ocean from significant river inputs, atmospheric deposition and subsequent photochemical oxidation were considered to be the most likely sources and sinks for PCAs in this region. Radiocarbon in BPCAs from HMWDOM recovered by ultrafiltration was highly depleted (-880 to -918 ‰), with ages ranging from 17,000 to 20,100 ybp (Ziolkowski and Druffel, 2010). Concentrations were lower (90-330 nM) than reported by Dittmar and Peang (2009), probably due to lower recoveries of hydrophobic LMWDOM by the ultrafiltration method. However, the results overall support the idea that PCAs represent a refractory DOM fraction. Further studies designed to determine PCA structures are needed to better describe the sources, cycling, and sinks of PCAs.

Studies that compare FT-ICRMS spectra on a simple presence/absence basis of individual ions report a remarkable uniformity in a large fraction of ions from samples collected from different locations and different depths in the ocean. Koch et al. (2005) report that of the 1580 chemical formulae recognized in a suite of samples collected in

931 the Weddell Sea, ~30% were present in all samples. Only two formulae were found
932 exclusively in surface waters, and only 79 formulae were found only in deep (>3500 m)
933 water samples. Kujawinski et al. (2009) used statistical analysis of DOM collected in the
934 surface, deep and terrestrial-influenced coastal waters of the US Mid Atlantic Bight, also
935 finding only a very small number of indicator species among > 1000 formulae that could
936 be attributed to exclusively surface marine (32 formulae) or exclusively terrestrial
937 impacted (20 formulae) DOM. Finally, Flerus et al. (2012) found 54% of all masses were
938 present in 90% of 137 samples collected in the eastern Atlantic Ocean, while 74% of
939 mass were present in at least 100 samples. The uniformity in DOM molecular formulae
940 was attributed to refractory DOM with common compositional features that persists over
941 several millennia and is well mixed throughout the entire water column.
942 ESI-MS of uncharacterized, complex mixtures like SPE-DOM is inherently
943 qualitative. Ionization is selective and subject to matrix effects that are not fully
944 understood. Positive and negative modes yield highly overlapping but different sets of
945 ions due to different ionization efficiencies for carboxylic acids and other functional
946 groups. Only molecules that ionize are registered by the mass detector, and compound
947 classes with low ionization efficiencies (e.g., carbohydrates) are therefore under-
948 represented or can be absent from the mass spectrum (Hertkorn et al., 2006; 2012).
949 However, with careful control of sample processing and analysis, recent studies are
950 beginning to compare the intensity-weighted distribution of molecular formula within
951 sample sets to identify spatial and temporal changes in SPE-DOM composition. Using
952 this approach, Hertkorn et al. (2012) noted an increase in oxygen and a decrease in
953 carbon content between surface (5 m; 36% O; 50-52% C) and deep water (5446 m; 42%
954 O; 47% C) samples, which was attributed to progressive oxidation of DOM with
955 age/depth, in agreement with NMR data that also shows a progressive increase in relative
956 COOH and C=O % carbon with depth. However, Flerus et al. (2012) did not observe a
957 shift in O/C ratios between surface and deep water samples collected on the same cruise.
958 Hertkorn et al. (2012) noted that the abundance of formulae with CHO and CHNO
959 increased with depth relative to formulae containing sulfur (CHOS and CHNOS), in
960 contrast to Kujawinski et al. (2009) who reported an increase in both the number and
961 intensity-weighted number of sulfur containing compounds between the surface (0 m)

962 and deep (1000 m) Atlantic Ocean. Flerus et al. (2012) used the intensity-weighted
963 approach to distinguish masses that were relatively more abundant in surface waters from
964 masses that were uniformly present (when corrected for total DOC) throughout the water
965 column. They found that masses enriched in surface waters had a lower average mass
966 (300 vs 441 Da), and a lower range in DBE (2-11 *vs* 7-14), again supported by NMR data
967 suggesting a higher average degree of branching in deep water DOM (Flerus et al., 2012).
968 The intensity-averaged molecular weight increased from 411 Da in surface waters to 417
969 Da in deep waters, suggesting at best a very small increase in molecular weight with
970 water mass age (Hertkorn et al., 2012; Flerus et al., 2012).
971
972 **2.4 Links between DOM composition and cycling**
973 The current paradigm of marine DOM cycling draws from a synthesis of rate
974 measurements that span timescales from a few hours to several thousand years (Hansell,
975 2013; Carlson and Hansell chapter). On very short timescales, marine microbes produce
976 and consume DOM that is "labile" or "reactive". Annually, a large flux of carbon passes
977 through labile DOC, but at any given moment labile DOC represents only a small
978 fraction (< 0.2 Pg) of the global DOC inventory. Over longer timescales of months to
979 years, excess microbial carbon production and inputs of terrestrial carbon from
980 atmospheric deposition, rivers, and groundwater leads to net accumulation of "semi-
981 labile" or "semi-reactive" DOM in and immediately below the euphotic zone. Net
982 accumulation of semi-labile DOM in the upper water column, and net removal in the
983 mesopelagic ocean, give DOC profiles in temperate and tropical latitudes their
984 characteristic shape, with high values in the surface and lower values at depth. Globally,
985 semi-labile DOM contributes ~20 GT C, or 3% of the marine DOC reservoir (Hansell et
986 al., 2009; 2012). The annual flux of carbon through semi-labile DOM cannot be
987 measured directly, and estimates of residence time span at least an order of magnitude,
988 from a few months (the seasonal accumulation and export of semi-labile DOM from the
989 euphotic zone) to several years (radiocarbon measurements of semi-labile DOM
990 carbohydrates)(Repeta and Aluwihare, 2006; Hansell et al., 2009; 2012). This broad
991 range of rates reflects differences in local production and consumption, differences in
992 how rates are measured, how semi-labile DOM is defined, and the fraction of semi-labile

993 DOM that is tracked. Lability changes with nutrient conditions, temperature, light, and
994 consumer community structure.
995 In the deep ocean, DOC values are more stable and decrease only slowly along the
996 path of abyssal circulation.(Hansell et al., 2012) Radiocarbon measurements show deep
997 sea DOC to be several thousand years old (Williams and Druffel, 1987; Druffel et al.,
998 1992). Assuming production and removal of deep sea DOM is a first order process, the
999 turnover time of refractory DOC is ~16,000-30,000 years. The old radiocarbon age and
1000 the very slow net removal of deep sea DOC imply that most marine DOM is "non-
1001 reactive" or "refractory". The distinction between labile, semi-labile, and refractory
1002 DOM is purely operational. Studies define these terms differently, depending on the
1003 nature of the study and the preferences of the investigators. Other nomenclatures exist in
1004 the literature which make finer classifications of DOM reactivity (Hansell et al., 2012;
1005 Hansell, 2012). However DOM lability is defined, it is inferred from the broad range of
1006 timescales over which DOM cycles that composition and lability are linked in some way.
1007 One goal of DOM chemical characterization is to identify characteristic features of labile,
1008 semi-labile and refractory DOM and understand how composition is linked to cycling.
1009
1010 *2.4.1 Composition and the cycling of labile DOM*
1011 Grazing, viral lysis of infected cells, and a host of routine cellular physiological
1012 processes act to release labile DOM into seawater (Carlson and Hansell chapter). Labile
1013 DOM is also produced from the photochemical oxidation of refractory organic matter as
1014 it upwells from the deep ocean into the euphotic zone (Kieber et al., 1990; Mopper et al.,
1015 1991). Photochemical degradation products include low molecular weight organic acids,
1016 aldehydes and ketones that are readily assimilated by marine microbes (Mopper and
1017 Stahovec, 1986). The annual carbon flux through labile DOM is measured as
1018 heterotrophic bacterial production, under the assumptions of steady state production and
1019 consumption and that microheterotrophs are the dominant sink for labile DOM.
1020 Measurements of bacterial production are imprecise and do not include organic matter
1021 consumed through light driven consumption by photoautotrophs and photochemical
1022 oxidation to CO_2, or losses due to the adsorption of labile DOM onto sinking particles.
1023 Current estimates of bacterial production show that annually, some ~20% of global

primary production is released as labile DOM that is subsequently consumed through a "microbial loop" in which DOM is either respired or fixed again into microbial biomass (Fig. 2.14). While most studies have focused on the consumption of DOM by heterotrophic bacteria and more recently archea, there is abundant evidence that photoautotrophs also assimilate simple organic acids and other low molecular weight organic compounds. Some photoautrophs are auxotrophic for essential vitamins, and some use siderophores produced by heterotophic bacteria to supplement their requirements for iron (Vraspir and Butler, 2009; Helliwell et al., 2011). The exchange of labile DOM between auto- and heterotrophic microbes therefore limits and shapes microbial production and marine biogeochemical cycling in a very fundamental way.

Labile DOM constituents include easily characterized, low molecular weight biochemicals (simple amino acids, sugars, organic acids, ATP, vitamins, etc.) that are readily assimilated by marine microbes and simple biopolymers (proteins, unbranched homopolysaccharides, etc.) that can easily be hydrolyzed by extracellular hydrolytic enzymes. The high demand for labile organic substrates, nutrients, and metals by the microbial community keeps steady state concentrations of labile DOM constituents at nanomolar levels (Fuhrman, 1987; Skoog and Benner, 1997; Kaiser and Benner, 2009). As discussed in section 2.3.2, concentrations of dissolved free amino acids and THAA range from a few nM (for free amino acids) in the deep ocean, to 100s of nM (for THAA) in the surface open ocean. Radiocarbon tracer experiments show free amino acids are rapidly metabolized by heterotrophic bacteria, and the uptake and incorporation of the tritiated amino acid leucine is commonly used as a measure of bacterial production (Fuhrman, 1987). The lability of specific proteins and bacterial peptides that constitute THAA is unknown, but spatial and temporal changes in THAA concentrations along with experiments tracking extracellular peptidase activity by marine phytoplankton and bacteria show a significant fraction of THAA are metabolized over short time scales (Amon et al., 2001). Dissolved simple sugars likewise occur at low nM concentrations in the euphotic zone and are taken up quickly by bacteria (Rich et al., 1996). Total hydrolyzable neutral and amino sugars concentrations range from > 600 nM in open ocean surface waters to 30-60 nM at depth. It is unclear what fraction of DOM polysaccharides are labile. Extracellular, dissolved polysaccharides are universally

produced by marine algae and cyanobacteria when grown in laboratory pure culture (Aluwihare et al., 1997; Biddanda and Benner, 1997; Aluwihare and Repeta, 1999; Meon and Kirchman, 2001). A number of studies have explored carbohydrate degradation by inoculating filtered, spent culture media with heterotrophic bacteria and following simple sugar composition or DOM spectral characteristics over time. In these experiments homopolysaccharides are rapidly degraded by heterotrophic bacteria, but degradation is always selective; the composition of neutral sugars invariably changes over the course of the degradation experiments (Aluwihare et al., 1997; Meon and Kirchman, 2001). In the field, experiments using fluorescently labeled model compounds also show large changes in polysaccharide hydrolysis rates and substrate selectivity with location (Arnosti et al., 2011; Arnosti, 2011). Labile polysaccharides are readily produced and consumed during upper ocean carbon cycling, but steady state concentrations remain low as with other labile components of DOM due to tight coupling between production and consumption by marine microbes.

Although proteins and polysaccharides contribute the majority of carbon and nitrogen in living microbial biomass and marine particulate organic matter, microbes produce an enormous diversity of organic compounds as part to their metabolic systems. Untargeted characterization of DOM shows hundreds to thousands of different compounds can be recovered by SPE from pure cultures of marine photoautotrophs. Initial results suggest chemical diversity may track phylogenic diversity, such that the genomic variability in marine microbial communities may be matched by a similar chemical variability in labile DOM composition. Some labile DOM constituents may be generally available to the heterotrophic community, but others induce highly specific growth responses. For example, studies using defined radiolabeled substrates or labeled DOM produced in pure cultures of specific marine photoautotrophs show selective uptake by defined subclasses of marine heterotrophs (Sarmento and Gasol, 2012; Cottrell and Kirchman, 2000). DOM released by marine heterotrophs likewise enhances the growth of only certain marine autotrophs. A recent review highlights the interaction of marine bacteria and diatoms, while other studies have documented enhanced growth of the marine cyanobacteria *Prochlorococcus* in the presence of some heterotrophic bacteria (Sher et al., 2011; Amin

et al., 2012). *Prochlorococcus*-heterotophic mutualism is highly strain specific, some strains of bacteria enhance growth of only some strains of *Prochlorococcus*.

In the examples above, the DOM constituents that lead to enhanced growth have not been identified, but B vitamins and siderophores are two examples of labile DOM nutrients that are known to impact microbial community production and diversity. Approximately half of all marine microalgae, including many harmful algal bloom forming species, as well as many marine bacterioplankton, are auxotrophic for vitamins B_1 and/or B_{12} (Tang et al., 2010; Helliwell et al., 2011). B-vitamins co-limit and shape marine microbial production, so knowledge of the distribution of B vitamins is important to assessments of nutrient limitation (Tang et al., 2010; Bertrand et al., 2011; Bertrand et al., 2012). Early measurements of B vitamin distributions relied on bioassays, but recently, direct analysis of B vitamins by mass spectrometry has been reported. Concentrations of B_{12} reach low nM levels in some coastal waters, but fall to < 1 pM (detection limit) at open ocean sites due to low bacterial production and high uptake by B-vitamin auxotrophs (Sañudo-Wilhelmy et al., 2012).

Over 99% of dissolved iron in the ocean is complexed to organic ligands of unknown composition (Gledhill and van den Berg, 1994; Rue and Bruland, 1997; Boye et al., 2001; Gledhill and Buck, 2012). In many remote areas of the equatorial Pacific, northwest Pacific, and Southern Oceans iron concentrations fall to <100pM, creating enormous selective pressures for microbes to develop efficient Fe uptake and utilization strategies (Martin and Fitzwater, 1988; Martin et al., 1991; De Baar et al., 2005; Jickells et al., 2005; Follows et al., 2007; Dutkiewicz et al., 2009; Bragg et al., 2010; Barton et al., 2010; Boyd and Ellwood, 2010; Dutkiewicz et al., 2012; Miethke, 2013). Microbes that can access iron-organic ligand complexes have a distinct competitive advantage in iron-depleted regions of the ocean. One mechanism by which microbes can acquire iron is through the siderophores, strong iron-organic complexes that facilitate iron transport and uptake across the cell membrane (Vraspir and Butler, 2009). Like B vitamins, dissolved iron-organic complexes occur at extremely low concentrations that are difficult to measure. However, recent reports describe a number of siderophore and siderophore-like compounds in seawater at pM concentrations, and advances in analytical technologies should facilitate future measurements (Mawji et al., 2008; Mawji et al., 2011; Velasquez

et al., 2011; Gledhill and Buck, 2012; Boiteau et al., 2013). The distribution and cycling of vitamins and trace metal organic complexes are two developing areas of research that target specific, labile DOM constituents with measurable impacts on marine microbial communities. Studies of untargeted labile DOM composition and microbial interactions suggest that as yet unidentified labile DOM constituents may also influence an array of metabolic processes from cell-cell signaling (e.g., quorum sensing) to nutrient uptake. Understanding labile DOM composition is key to understanding many interactions between microbial communities, as well as many of the processes that limit and shape the microbial community production and diversity.

2.4.2 Composition and the cycling of semi-labile DOM

Traditionally, semi-reactive DOM has been defined as the fraction of DOC that is present in surface waters but that is not at depths > 1000m, the point where DOC concentration values begin to stabilize.[4] This definition arises from two principal observations; 1) DOC concentrations in temperate and tropical surface waters are elevated relative to deep ocean values, and 2) radiocarbon models of DOC age use a mix of modern and aged components to explain upper ocean Δ^{14}C-DOC values (Druffel et al., 1992; Hansell et al., 2009; 2012). However, semi-labile DOM can also be defined on the basis of turnover time relative to labile and refractory DOM fractions. Viewed this way, semi-labile DOM is any organic matter that cycles on seasonal to decadal timescales. This definition includes DOM in the deep ocean (> 1000 m) that is in quasi-steady state with its production (via dissolution of sinking particles, *in situ* microbial production, etc.) and removal (Repeta and Aluwihare, 2006; Orellana and Hansell, 2012). The timescales over which semi-labile DOM cycles are too long to be captured experimentally in laboratory or field incubation experiments without significant bottle effects, but too short to be captured by natural abundance radiocarbon measurements. Linking semi-labile DOM constituents to cycling pathways is therefore difficult, and the processes that result in the net accumulation of semi-labile DOM in the surface ocean, and net degradation at depth, remain largely unexplained.

Marine algae and bacteria synthesize semi-labile DOM polysaccharides and proteins, which in laboratory degradation experiments can persist for several years.(Fry et

al., 1996; Ogawa et al., 2001; Jiao et al., 2010) HMWDOM carbohydrate amendments to seawater simulate rapid increases in bacterial carbon utilization by a succession of bacterial taxa, suggesting resource partitioning of semi-labile DOM between different species of bacteria (McCarren et al., 2010). Coordinated, cooperative interactions by a variety of different bacteria may be necessary to degrade the complex, highly branched acylated polysaccharide that represents a large fraction of semi-labile DOM. The carbon respired by short-term incubation experiments of this type represents only a very small fraction (typically < 1%) of the carbon amendment, and the link between short term incubation results and semi-labile DOM degradation *in situ* is not clear. Longer incubations of nutrient amended surface waters show greater losses of DOC, but still fall far short of consuming a major fraction of the semi-labile DOC reservoir. In a series of experiments, Carlson and colleagues measured DOC respiration in a matrix of surface and 250 m water treatments that had been 0.2 μm filtered, amended with nutrients, and inoculated with either unfiltered (containing bacteria) surface or 250 m water (Carlson et al., 2002; 2004). No significant DOC respiration and only a slight increase in bacteria cell numbers were observed in surface water inoculated with surface water bacteria. However, significant respiration (up to 10% of total DOC) and 3x increases in bacterial cell numbers were measured in treatments of surface water with 250 m bacteria. The studies of Carlson and colleagues show that the bacterial community in surface waters has a limited capability to degrade polysaccharides and other components that contribute to semi-labile DOM, while mesopelagic bacterial communities have the requisite metabolic pathways to metabolize at least a fraction (up to 20%) of semi-labile DOM. The results of microbial degradation experiments have yet to be coupled to studies of semi-labile DOM composition. Characterizing the small amounts of semi-labile DOM that is consumed in these incubation will prove to be challenging, and developing improved experimental approaches to simulating semi-labile DOM degradation will be key to future progress in this area.

Metabolism of DOM by heterotrophic bacteria is selective and/or leads to subtle transformations of semi-labile DOM. A growing number of studies have measured differences in DOM composition between coastal and open ocean DOM or between surface and deep water DOM and tied these differences to the "apparent diagenetic state"

1178 or potential reactivity of semi-labile DOM. Goldberg and colleagues measured seasonal
1179 changes in DOC, total carbohydrates (TCHO) and dissolved combined neutral sugars
1180 (DCNS) as DOM accumulates in surface waters at the Bermuda Atlantic Time-series
1181 Study site (BATS; 31^{o} 40'N, 64^{o}10'W) and spatially in surface waters across the North
1182 Atlantic subtropical gyre between 7-43^{o}N (Goldberg et al., 2009, 2010). Values for
1183 DOC, THCO, and DCNS were highest during summertime stratification of the water
1184 column and in the mid-gyre (~ 24^{o}-27^{o}N). Recently accumulated DOM had higher
1185 carbohydrate yields (%TCHO) and higher mol% galactose and mannose+xylose than
1186 DOM at depth, which was characterized by higher mol % glucose. As semi-labile DOM
1187 is processed by bacteria, it becomes less amenable to chemical characterization and the
1188 distribution of DCNS changes (Amon and Benner, 2003; Goldberg et al., 2009; 2010).
1189 Patterns of amino acid and hexosamine distributions in particulate organic matter
1190 and sediments are also strongly imprinted with the combined effects of degradation and
1191 transformation. By comparing the distribution of amino acids in surface and subsurface
1192 sediments, and in fresh and recycled particulate organic matter, Dauwe proposed a
1193 degradation index that relates the composition of organic matter to lability (Dauwe et al.,
1194 1999). The degradation index assumes steady state deposition over time, so that the
1195 distribution of amino acids/hexosamines in contemporary surface sediments or fresh
1196 particulate matter is a good representation of the amino acid distribution of older
1197 sediments or more processed particulate organic matter at the time of synthesis. This
1198 concept has been applied to studies of DOM cycling to provide a measure of DOM
1199 degradation. For semi-labile DOM, it is assumed that the distribution of amino
1200 acids/hexosamines in coastal surface waters is indicative of the initial product, which is
1201 transformed as waters move offshore or into the deep sea. Yamashita and Tanoue (2003)
1202 observed decreases in the %THAA and increases in the relative amount of glycine and
1203 alanine in a suite of samples from near shore (fresh DOM) to offshore and greater depths
1204 (more recycled DOM), concluding that degradation had a major impact on the quantity
1205 and quality of THAA (Yamashita and Tanoue, 2003b). Likewise, Davis et al. (2009)
1206 measured the %THAA and degradation index in a suite of (organic matter) amended and
1207 unamended Arctic Ocean seawater samples, finding that %THAA changed rapidly in the
1208 days immediately following amendment, but stabilized and changed only slightly

thereafter. These changes were accompanied by minor changes in the amino acid degradation index, which varied in the upper 200 m of the water column but was invariant below this depth. These and other studies show that freshly produced organic matter has a relatively higher %THAA, which decreases on timescales of weeks to months, while the ratio of indicator amino acids can be used to track changes occurring over timescales of months to years.

Hubberten et al. (1994; 1995) used hydrophobic organic resins (XAD-2; a cross-linked polystyrene) to extract amino acids from the Greenland Sea and Southern Ocean. Seawater was filtered (Whatman GF/F), acidified to pH = 2 with hydrochloric acid, then passed through the XAD column.(Hubberten et al., 1994; 1995) Amino acids incorporated into hydrophobic substances are adsorbed onto the column, then recovered by sequentially rinsing with 0.2N NaOH and methanol. Each fraction was analyzed for amino acids. In all samples from < 1000m, TDAA concentrations always exceeded amino acids in the XAD fractions (XAD-AA; Fig. 2.7). However, the difference, the amount by which [TDAA] exceeded [XAD-AA], was greatest for surface waters and diminished with depth. Hubberten noted a linear correlation between chlorophyll-a [Chl-a] and THAA in surface waters. Extrapolation to [Chl-a]= 0 yielded a positive intercept for [THAA] that was similar to values of XAD-AA. For depths below 100m, concentrations of THAA and XAD amino acids were approximately equal. Both observations led Hubberten et al. to suggest that there are at least two fractions of hydrolysable amino acids in seawater, a labile fraction that is largely hydrophilic and present in surface waters and a semi-labile or refractory component of about 150-250 nM present throughout the water column. The distribution of amino acids in the XAD fraction was characterized and found to be similar to THAA, so no distinction of the two fractions could be made by amino acid distribution. No further characterization of XAD-AA was made, however proteins, peptides, and bacterial cell wall material have some hydrophobic character, and can be retained on hydrophobic resins under low pH conditions. The amino acids recovered by Hubberten and colleagues could have included amino acids bound in humic substances, proteins/cell wall biopolymers and their degradation products. The decrease in the ratio THAA/XAD-AA with depth suggests some change in the macromolecular form of amino acids, a point corroborated by amino

acid fluorescence data, which shows only tryptophan-like fluorophores in surface waters, but additional tyrosine-like fluorophores in deep water samples.(Yamashita and Tanoue, 2004)

Finally, DOM in filtered seawater spontaneously assembles into polymer gels, stable three-dimensional networks of DOM macromolecules that grow until they reach a size and density that allows them to sink or adhere to sinking particles ; Orellana chapter). Assembly is rapid and reversible, and gels are one mechanism by which semi-labile DOM can be removed from the surface ocean. As discussed in section 2.3.3, RuBisCo is produced in the euphotic zone, transported to the deep ocean by sinking particles, and released by DOM-POM exchange. In regions of high particle flux such as the equatorial Pacific, RuBisCo can be detected well into the deep ocean where it persists as semi-labile DOM. Gels stain positively for carbohydrates, proteins, and lipids and these other constituents of polymer gels are likely carried into the deep ocean as well. Peptidases, proteases, and ATPase enzymes have been identified in polymer gels through proteomic analyses (Orellana et al., 2007). No similar analyses of polymer gel carbohydrates have been reported, but bubble formation and collapse concentrates polymer gels into sea surface foam, and chemical analyses of natural sea foams have been made (Orellana et al., 2011). NMR spectra of natural sea surface foam and foam produced after the microbial degradation of spent algal culture media have spectral features characteristic of acylated polysaccharides that accumulate in surface water as semi-labile DOM carbohydrate. Combined neutral sugar distributions of semi-labile DOM and foam are also similar (Gogou and Repeta, 2010). ^{1}H NMR and ^{13}C NMR spectra of DOM collected by ultrafiltration, SPE, and ED/RO all show resonances assigned to semi-labile DOM carbohydrate as deep as 5200m, but further chemical and isotopic characterization is needed to link surface and deep reservoirs of semi-labile DOM (Benner et al., 1992; Sannigrahi et al., 2005; Quan and Repeta, 2007; Helms et al., 2013).

2.4.3 Composition and the cycling of refractory DOM

By definition, refractory DOM does not degrade *via* the typical microbial and chemical processes that recycle labile and semi-labile DOM. Understanding why

refractory DOM is so unique is therefore critical to a comprehensive description of the marine carbon cycle. The chemical composition of SPE-DOM is taken to be representative of refractory DOM. As discussed in section 2.3.3, SPE-DOM is a very complex mixture of at least several thousand different components with elemental H/C and O/C ratios that lie outside the range of common lipids, proteins and carbohydrates (Fig. 2.12). SPE-DOM is therefore not thought to have a direct biological source, but the case for direct biological production and selective preservation of refractory organic matter has been made for sediments, and given the very small flux of carbon (< 0.04 Pg year^{-1}) needed to support the radiocarbon age of refractory DOM, and the large annual flux of carbon through marine primary and secondary production, direct synthesis of refractory DOM cannot be discounted. The complex molecular features of SPE-DOM can be interpreted as the result of transformation of lipids, proteins and carbohydrates that become scrambled in such a way as to make them difficult for marine microbes to assimilate or metabolize. Refractory DOM is characterized by a high proportion of carboxylate and fused alicyclic ring carbon that shares structural characteristics with polycyclic lipids (Hertkorn et al., 2006). The mechanisms that could convert simple lipids to refractory DOM are a matter of conjecture, and more work is needed to assess both the feasibility of the formation pathway and its impact on microbial metabolism.

Although refractory DOM is not readily metabolized by marine microbes, a number of sinks that rely on physical/chemical processes have been identified. In a series of elegant experiments Mopper and co-workers detailed the photochemical oxidation of deep sea colored dissolved organic matter on exposure to light (Mopper and Stahovec, 1986; Kieber et al., 1990; Mopper et al., 1991). Photooxidation products include low molecular weight, labile, organic acids, aldehydes and ketones that are rapidly consumed by bacterial heterotrophs. Photochemical oxidation also decreases the adsorptive and fluorescent properties of DOM through the transformation or removal of unsaturated functional groups (Kieber et al., 1990; Weishaar et al., 2003). Subsequent studies have confirmed and expanded these observations and a photochemical sink and transformation pathway for otherwise refractory DOM is now firmly established. However, photochemistry is confined to the upper portion of the euphotic zone and the amount of carbon potentially mineralized by this pathway is very limited. Photochemical oxidation

of DOM probably leads to significant isotopic fractionation between products, but the isotopic value of DOM is similar to particulate organic matter, and it is unlikely that photochemical oxidation is the primary sink for refractory DOM.

Globally, the largest sinks for refractory DOM are in the deep sea (Hansell et al., 2009, 2012; Hansell, 2012; Hansell and Carlson, 2013). From an analysis of salinity and high precision DOC values in the deep Pacific Ocean, Hansell and Carlson (2013) were able to identify two regions of refractory DOC removal within the basin, a deep sink in the far North Pacific, and a mid depth sink in the tropical South Pacific. They estimated that these two sinks remove 7-29% of the 43 TG refractory DOC introduced into the deep global ocean by overturning circulation. Two processes, removal during hydrothermal circulation, and adsorption onto sinking particles, have been identified as sinks for deep sea refractory DOM. Hydrothermal fluids exiting permeable ocean crust at mid-ocean ridge crests and unsedimented/thinly sedimented ridge flanks have DOC concentrations that are lower by 20-25 μM than deep seawater (36-39 μM; typical vent fluid DOC concentrations are 11-19 μM; Lang et al., 2006; Lin et al., 2012). Global DOC losses in hydrothermal systems are low, < 0.0002 Pg C $year^{-1}$, but measurements are few and this may be an underestimate. The composition and lability of the ~20 μM DOC that exits with hydrothermal fluids has not been studied, but radiocarbon values of the HMWDOC fraction range from -772‰ to -835‰, significantly depleted relative to overlying seawater (McCarthy et al., 2010). Other processes such as microbial oxidation and removal by self-assembling organic gels may be active and need further study.

Radiocarbon values of suspended particulate matter decrease by almost 100 ‰ with depth in the ocean (Druffel et al., 1992;1998). Even at the low Stokes settling velocities calculated for μm sized particles (~ 1m day^{-1}), suspended particulate matter settles quickly enough that no appreciable gradient in radiocarbon values due to aging should be measureable. To explain the gradient in suspended POC radiocarbon values, Druffel and colleagues postulated that radiocarbon depleted, refractory DOM is adsorbed onto suspended particles. Adsorption forms the basis for SPE extraction of refractory DOM, and it would be surprising if a similar process does not occur in the water column that is permeated with mineral surfaces and organic particles. A number of factors including complex POM dynamics in the deep ocean, resuspension and advection of fine-

1333 grained sediments with depleted radiocarbon values from continental margins, and
1334 adsorption of refractory DOM onto filters used to collect particles, potentially influence
1335 the DOM-POM adsorption model. However, based on Druffel's data, Hansell calculated
1336 that adsorption could remove ~0.05 Pg C yr^{-1} from the deep ocean, enough to sustain the
1337 observed deep-sea gradient in DOC concentration (Hansell et al., 2009). No analyses of
1338 particle-adsorbed, refractory DOM have been attempted. Given the recent progress in
1339 SPE-DOM characterization, and the ~500 ‰ separation in radiocarbon values for newly
1340 synthesized POM (+ 50 ‰) and refractory DOM (-400‰), it might be feasible to test the
1341 adsorption/removal hypothesis through a combination of structural and isotopic analyses.
1342
1343 **2.5 Future research**
1344 Over the past decade, our understanding of DOM composition and cycling has
1345 advanced in a number of areas. Reverse osmosis/electrodialysis now provides a larger
1346 fraction of DOM for study than either ultrafiltration or solid phase extraction alone. High
1347 field, multi-dimensional NMR and high resolution MS are providing unprecedented
1348 details of DOM composition, and new techniques of data integration and visualization
1349 such as correlation spectroscopy are allowing marine chemists to couple different spectral
1350 datasets into a more integrated picture of DOM composition. This wealth of new
1351 information presents both opportunities and challenges to the DOM community. One
1352 challenge is to provide community-wide access to the very large amount of mass and
1353 NMR spectral data available through open-access databases. Presently, such data are
1354 often only summarized or provided as supplemental materials in published reports. A
1355 database of spectral information that includes details of the methodologies needs to be
1356 made available for interrogation by the wider scientific community if the full benefits of
1357 advanced methods of characterization are to be realized.
1358 Much more effort needs to be placed on the validation of results by bringing
1359 different analyses to bear on common samples or at common study sites. It is unlikely
1360 and perhaps undesirable for sampling methods to converge at this time on one technique
1361 that provides the highest recovery of DOM. Each method has particular benefits of cost,
1362 speed, throughput, and selectivity for different fractions of DOM. A better understanding
1363 of the sampling overlap between techniques would however help to interpret similarities

and differences in composition between SPE, ultrafiltration, and ED/RO samples. Most current studies focus on one or two methods of spectral characterization that are within the scope of expertise of particular analysts. Collaborative studies that integrate data from a suite of different spectral (MS, NMR, IR, etc.), chromatographic (HPLC, GC, etc.), elemental and isotopic (δ13C, Δ14C, etc.) analyses would allow for more robust interpretation of complex datasets. For specific components of DOM that have biomarker or tracer potential (thermogenic DOM, APS), more comprehensive isotopic and structural characterization, along with better methods for isolation and purification, would substantially improve existing models of DOM cycling.

Advances in technology have made in-depth studies of labile DOM composition and cycling feasible. Automated, high resolution multi-dimensional liquid and gas chromatographic systems coupled with high resolution MS and high throughput microcapillary NMR offer the potential to better characterize the exometabolome of labile DOM. A large number of model photoautotrophs and heterotrophs representing major ecotypes of marine cyanobacteria, algae, and bacterioplankton are now available as pure cultures with sequenced genomes. Labile DOM characterization of these cultures at different growth stages would provide valuable links between genomic and exometabolomic composition, as well as microbial dynamics in natural systems. Paired co-cultures studies further demonstrate that synergistic interactions between photoautotrophs and heterotrophs are probably common in the ocean. Little is known about the organic nutrients and substrates that stimulate these associations it is a fruitful area for further study, particularly when paired with transcriptomic and proteomic datasets. There are only a few reports of the distribution of vitamins and other bioessential organic compounds (siderophores, quorum sensing compounds, etc.) in seawater. These compounds have a demonstrable impact on microbial ecosystems, but their production and uptake are only poorly understood. Finally, labile DOM composition needs to be linked to genomic studies already underway at time-series study sites and in global surveys of microbial populations and water column chemical properties. Labile DOM composition might provide an important new input to global models of microbial metabolism, diversity, and community structure.

^{13}C NMR spectra of DOM collected by RO/ED provides the most comprehensive view of semi-labile and refractory DOM composition currently available (Fig. 2.15). These spectra show the presence of two major fractions, a semi-labile HMWDOM fraction with acylated polysaccharide (APS) as the major component, and a refractory fraction with carboxy-rich aliphatic matter (CRAM) as the major component. The NMR spectral, elemental (C/N/P), and partial chemical (monosaccharide composition, linkage pattern) characteristics of APS are known. This level of detail has allowed for the detection of APS throughout the water column, but has not allowed for the identification of major sources of APS, or provided either an explanation for why APS accumulates in the upper ocean or a better estimate of carbon flux through semi-labile HMWDOM. The major sinks for APS have also not been identified. Better characterization of APS using mass spectrometry and 2D NMR is an essential first step in addressing these questions, as are improved chemical techniques that can fully depolymerize APS for comprehensive monosaccharide and linkage analyses. A more detailed description of APS composition should allow for better distinction of APS sources in laboratory culture experiments, would help in the design and implementation of microbial degradation experiments, and experiments monitoring gel polymer formation as putative sinks for APS. Finally, there is evidence from the study of proteins in DOM for the transport of semi-labile DOM into the deep ocean. Determining the inventory of semi-labile DOM in the deep ocean, its radiocarbon value, and its sinks would provide important new insights into deep sea carbon cycling and perhaps bathypelagic microbial ecology.

Understanding refractory DOM may be the most formidable challenge for DOM composition and cycling. High resolution mass and high field NMR spectral analyses have yielded unprecedented details into refractory DOM composition, but the results need to be independently verified by other techniques and made more quantitative. For example, the current view of SPE-DOM composition is of a very complex mixture of low molecular weight carboxyl-rich aliphatic compounds. If correct, these compounds should be amenable to separation and characterization by multi-dimensional gas chromatography-mass spectrometry (GC-MS). 2D GC-MS has already proved to be a valuable tool in the characterization of petroleum, which is a mixture polycyclic alkanes

and alkenes, some of which incorporate nitrogen and sulfur, similar in many respects to the proposed composition of refractory DOM.

Better integration of carbon isotope analyses with structural characterization is also needed. The isotopic composition of thermogenic DOM should provide important insights into the origin and cycling of polycyclic aromatic compounds in DOM. Only one such set of measurements have been made, and more are needed (Ziolkowski and Druffel, 2010). Finally, there are only a few reports of deep sea DOM spectral characteristics. Given the large gradient in concentration and radiocarbon value through the deep ocean, it seems likely that aging and removal of DOM will impact DOM composition. A survey of DOM composition through the deep ocean may offer insights into the processes that cycle refractory DOM.

There is observational evidence for two deep ocean sinks of refractory DOM, removal during hydrothermal circulation of seawater through permeable crust and adsorption onto particles. Both sinks merit further study. The composition of DOM in vent fluids needs to be determined and compared with the isotopic and chemical composition of refractory DOM. Preliminary work suggests that hydrothermal circulation is not a large source or sink of refractory DOM, but further measurements are needed to verify this inference. Adsorption onto sinking particles has been proposed but not verified through experiments using molecular level analysis. Ultrafiltration and ED/RO or SPE allow for the concentration of deep sea POM and DOM that could be used in to experimentally track adsorption. Given the high level of detail that can now be achieved using advanced analytical methods, it may also be feasible to isolate compounds with chemical and isotopic characteristics of refractory DOM from suspended particulate organic matter. Such studies would help to verify the adsorption hypothesis. Nothing is known about microbial degradation of refractory DOM.

Finally, little is known about the role of deep sea microbes in DOM removal. Rates of microbial DOM cycling are thought to be very low and therefore difficult to simulate in laboratory experiments. However, using more sensitive and precise methods of DOM characterization that are now available, it may be possible to explore deep sea microbial/refractory DOM interactions to provide new insights into this potentially important aspect of the marine carbon cycle.

2.6 Acknowledgements

The author has had the good luck to work with a large number of talented scientists over many years whose enthusiasm, ideas, and laboratory work have contributed to this chapter. In particular this chapter has benefited from discussions with Lihini Aluwihare, Carl Johnson, Chritos Panagiotopolous, Mar Nieto Cid, Aleka Gogou, Chiara Santinelli, Robert Chen, Jamie Becker, Rene Boiteau, and Chris Follett. Tracy Quan. Hussain Abdulla and Eiichiro Tanoue provided many helpful comments and suggestions that significantly improved the manuscript. I would also like to thank the NSF Chemical Oceanography and National Science and Technology Center for Microbial Oceanography Research and Education (C-MORE) programs for their generous support over many years, and the Gordon and Betty Moore Foundation for their interest and support of microbial cycling and DOM.

Figure captions

Figure 2.1 Extraction methods for marine DOM. In solid phase extraction (left) the sample is passed through a column packed with an organic sorbent (polystyrene, octadecylsilyl coated silica gel, etc.). Physisorptive attraction between hydrophobic DOM and the sorbent leads to adsorption of DOM on the column, which in the photograph appears as a brown discoloration (due to the adsorption of colored dissolved organic matter). After the sample has been extracted, hydrophobic DOM is recovered by washing the column with methanol. In ultrafiltration (top, right), seawater is pressurized and passed through a filter with nanometer-sized pores (grey sheet in figure). Organic molecules with hydrodynamic diameters greater than the filter pore size (red ellipses) are retained, while salt, low molecular weight DOM, and water (blue circles) permeate through the filter. Once the sample has been concentrated to < 1-2 L, residual salts are removed by serial dilution with ultra-pure water followed by filtration. In reverse osmosis/electrically assisted dialysis (RO/ED; bottom right) the sample is processed in serial ED and RO steps. In the ED step, the sample is passed through stacks of cation and anion exchange membranes that are under the influence of an applied electric potential and washed by alternating flows of sample (seawater, black arrows) and ultra-pure water (freshwater; grey arrows). Anions (chloride, sulfate, etc.) pass through the positively charged membrane (blue panels) toward the cathode, while cations (sodium, potassium) pass through the negatively charged membranes (green panels) toward the anode. This transfers salts from the sample into the freshwater feed, lowering the salinity of the sample. The sample is then concentrated by reverse osmosis, and processed again by ED to further reduce the salt content of the sample. Figure adapted from http://www.osmo-membrane.de.

Figure 2.2 Nuclear magnetic resonance spectra of HMWDOM collected by ultrafiltration of surface seawater collected from the North Pacific Ocean using a polysulfone membrane with 1 nm pore size (nominal 1 kDa molecular weight cut-off). (A)^{13}C NMR spectra have major peaks from carboxyl (COOH, CON; ~175 ppm), aromatic and olefinic C (broad peak centered at ~ 140 ppm), anomeric (OCO; 110 ppm), O-alkyl C (HC-OH; 70 ppm), methine and substituted methylene C (~35-40 ppm), and two alkyl C peaks from acetamide (26 ppm) and 6-deoxysugars (20 ppm). (B)^{1}H NMR spectra show major peaks from anomeric protons (5.2 ppm), O-alkyl protons (3.5-4.5 ppm), acetamide methyl (2.0 ppm) and 6-deoxyl sugar methyl and methylene protons (1.3 ppm). These peaks sit atop a broad baseline between 0.9-4 ppm from substituted methine, methylene, and methyl protons from hydrophobic DOM.

Figure 2.3 (A) Overlay of ^{1}H NMR spectra from North Pacific Ocean HMWDOM before (black trace) and after (red trace) passage through an anion exchange resin. Ultrafiltration concentrates from seawater high molecular weight, acylated polysaccharides (APS) as well as low molecular weight, hydrophobic humic substances. These two chemically distinct fractions of DOM can be separated by solid phase extraction or ion exchange chromatography, providing relatively pure fractions of acylated polysaccharide (APS) and carboxyl-rich aliphatic matter (CRAM). (B) Contour map of synchronous changes in peak intensity for ^{13}C NMR spectra of HMWDOM

collected at estuarine and coastal marine sites. Positive correlations between functional groups appear in red as off-diagonal peaks. Negative correlations appear in blue, with the intensity of the colors scaled to the intensity of the correlation. Figure courtesy of Drs. Hussain Abdulla and Patrick Hatcher. Samples were collected using a polysulfone membrane with a 1 nm pore size.

Figure 2.4 ^{15}N NMR spectra of HMWDOM (polysulfone membrane with 1 nm pore size) before (top) and after (bottom) acid hydrolysis. HMWDOM nitrogen occurs primarily as amide-N (124 pm) with smaller amounts of amine-N (35 ppm). Major biopolymers that incorporate amide-N are proteins and N-acetyl-aminosugars. The contribution of proteins and N-acetyl-aminosugars in HMWDOM can be assessed by combining ^{15}N NMR spectral data with measurements of acetic and amino acids released after acid hydrolysis. Treatment of HMWDOM with acid converts most amide-N into amine-N. For surface waters, companion chemical analyses show that N-acetyl amino sugars contribute 40-50% of amide-N while proteins contribute 8-13% of amide-N. Figure adapted from reference 8.

Figure 2.5 Representative structures of monosaccharides isolated from HMWDOM hydrolysis products. Treatment of HWMDOM with acid yields a suite of hexoses (mannose, galactose, glucose), a pentose (arabinose), 6-deoxyhexoses (fucose, rhamnose), hexosamines (glucosamine, galactosamine), and a large number of methylated hexoses (3-methyl rhamnose, etc.) as well as some novel deoxysugars (3-deoxygluose).

Figure 2.6 2D NMR homonuclear correlation spectroscopy (COSY) of HMWDOM carbohydrate from the North Pacific Ocean (Fig. 2.2). In this example, strong cross peaks between H-5 x H-6 (red) and H-2, H-3, and H-4 (blue) show the presence of 6-, 4-, 3-, and 2-deoxysugars in HMWDOM. Additional strong cross peaks are observed between αH-1 x H-2, and βH-1 x H-2 (violet), showing different stereochemical geometries within the polysaccharide.

Figure 2.7 Distributions of total hydrolysable amino acids (THAA; left panel), D-amino acids (center panel) and SPE-amino acids and THAA (right panel). Data in the left and center panels are from the North Pacific (grey squares; Station ALOHA of the Hawaii Ocean Time-series (HOT) program) and North Atlantic (open circles; Bermuda Atlantic Time-series Study (BATS) program) Oceans. SPE-AA (filled triangles) and THAA (open triangles) data in the right panel are pooled datasets from the high latitude North Atlantic and Southern Oceans. Concentrations of THAA are high in the euphotic zone and fall through the mesopelagic zone. Concentrations stabilize in the deep ocean, >1000 m. D-amino acids concentrations are also highest in the euphotic zone, decrease to about 1000m and stabilize thereafter. SPE-AA are thought to represent amino acids and peptides that are part of refractory DOM, showing much less variation in concentration with depth. At 2000m, nearly all THAA is recovered as SPE-AA. Data from HOT and BATS are from reference 49. Data on SPE-AA and THAA in the right panel are from reference 140.

Figure 2.8 The relative distributions of individual amino acids within dissolved THAA, phytoplankton, suspended particulate matter, and sinking particles. Plankton, suspended, and sinking particle data are from the equatorial Pacific Ocean, while THAA is from Station Aloha, near Hawaii.(Lee et al., 2000; Kaiser and Benner, 2009) Sinking particle data are from short-term deployments of floating sediment traps. Data from long-term deployments of moored traps have higher concentrations of glycine (Gly), similar to THAA in DOM. All sample types have the same suite of amino acids. The major difference between dissolved and particulate amino acid distributions are the higher relative abundance of aspartic acid and glycine in THAA. Amino acids are: Asp (aspartic acid), Glu (glutamic acid), Ser (serine), His (Histidine), Thr (Threonine), Gly (Glycine), Arg (Arginine), Ala (Alanine), Tyr (Tyrosine), Val (Valine), Met (Methionine), Ile (isoleucine), Leu (leucine), Lys (lysine).

Figure 2.9 SDS-PAGE gel of dissolved proteins in seawater visualized by silver staining. Dark bands represent separated proteins. The left and right lanes are standard mixtures of known proteins used to calibrate the molecular separation of the gel. Sample proteins are from surface waters collected from the equator (Station 1) to 60^{o}S (Stations 4, 5) along 120^{o}E, then west across the Southern Ocean to approximately 30^{o}E (stations 6-9). Note the similarity in protein bands between samples. Major protein bands appear in samples at 48 kDa, 37 kDa, and 15 kDa. Figure used with kind permission from Dr. Eiichiro Tanoue.

Figure 2.10 ^{1}H NMR of SPE-DOM from 900m near Hawaii. NMR spectra of SPE-DOM differs from ^{1}H NMR spectra of HMWDOM by the absence of carbohydrates. Major resonances include methyl (**H$_3$**C-R; ~0.9-3.3 ppm), methylene (**H$_2$**CH$_2$-RR´; ~1.3-2 ppm), and methine (**H**C-R,R´,R´´; ~1.4- 4.5 ppm).

Figure 2.11 High resolution mass spectrum (positive ion) from SPE-DOM collected at 250 m, Station Aloha, near Hawaii. The mass spectrum of the infused sample (bottom) shows a complex distribution of ions with reoccurring mass differences of $\Delta m = 14.0156$ due to methylene homologues (Δ CH$_2$). Expansion of the series centered at 377 Da (upper left) shows a second homologous series with $\Delta m = 2.0157$ (H$_2$). Further expansion (upper right) shows the high mass resolving power that can be achieved, which allows for the assignment of elemental formulae, and the distinction of formulae of the same nominal mass. Here ions that differ by the substitution of CH$_4$ (16.0313 Da) for O (15.9949) yield a mass difference of 36.4 mDa.

Figure 2.12 van Krevelen plot of data in Figure 2.11 from 250 m, Station ALOHA. Each dot represents an ion for which a unique molecular formula could be assigned from the exact mass. Here the elemental ratios H/C and O/C calculated from molecular formulae are plotted and compared with elemental H/C and O/C ratios from classes of known biochemical (lipids, proteins, and carbohydrates). Most SPE-DOM formulae plot outside the region of known biochemicals, perhaps due to extensive degradation and transformation of organic matter during DOM formation, or from unknown DOM precursors. A distinct group of ions with H/C < 1 and O/C< 0.2 appear in some SPE-

DOM spectra; these have been assigned to polycyclic aromatic compounds (PCAs) of thermogenic origin (see text).

Figure 2.13 HPLC analysis of benzene polycarboxylic acids (BPCAs) derived from SPE-DOM. Treatment of SPE-DOM with nitric acid at high temperature degrades polycyclic aromatic compounds (top) into a series of benzoic acids that can be measured at high sensitivity by HPLC (bottom) and HPLC-MS.

Figure 2.14 The microbial loop of labile DOM cycling. Carbon dioxide is fixed by photoautotrophs (yellow and green cells, left), which excrete about 10% of total fixed carbon as DOC. Grazing (bottom left, right) and cell lysis after viral infection (upper left, right) release additional labile DOM to be consumed by heterotrophic bacteria and archea (blue cells, right). The microbial loop consumes labile DOM, converting it to carbon dioxide and nutrients. Heterotrophs also release essential vitamins, siderophores, and other organic compounds that facilitate the growth of photoautrophs. Figure courtesy of Dr. Jamie Becker.

Figure 2.15 ^{13}C NMR of DOM recovered by RO/ED (black trace) superimposed on spectra of HMWDOM (ultrafiltration; grey trace) and SPE-DOM (red trace) from surface water. The spectra of HMWDOM and SPE-DOM are scaled to the RO/ED peak at 70 ppm. To a good approximation, the distribution of carbon functional groups in the RO/ED sample is a mixture of acylated polysaccharides (APS), which dominate the ^{13}C NMR spectra of HMWDOM, and hydrophobic humic substances/CRAM that dominate the ^{13}C NMR spectra of SPE-DOM. Figure redrawn from Koprivnjak et al., 2009.

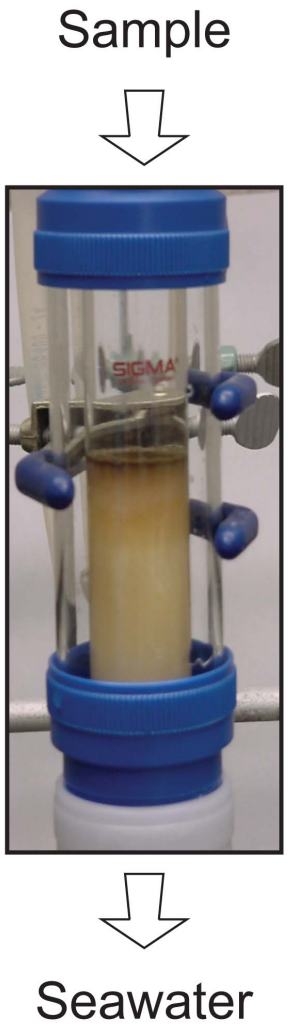
Sample
Seawater

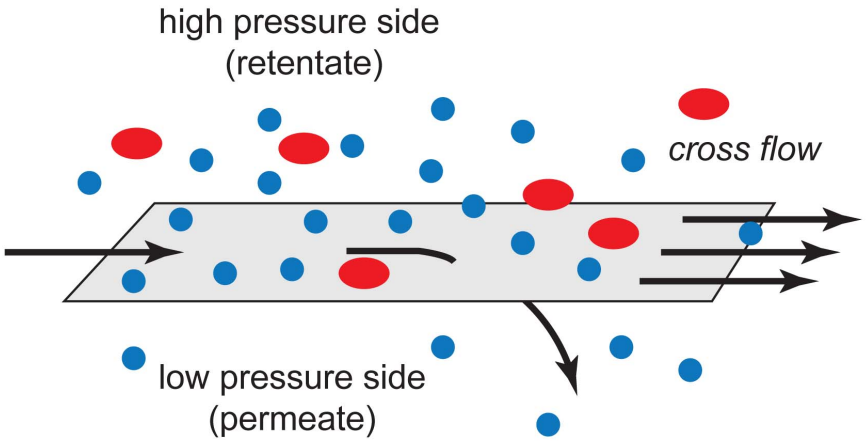
high pressure side
(retentate)
cross flow
low pressure side
(permeate)

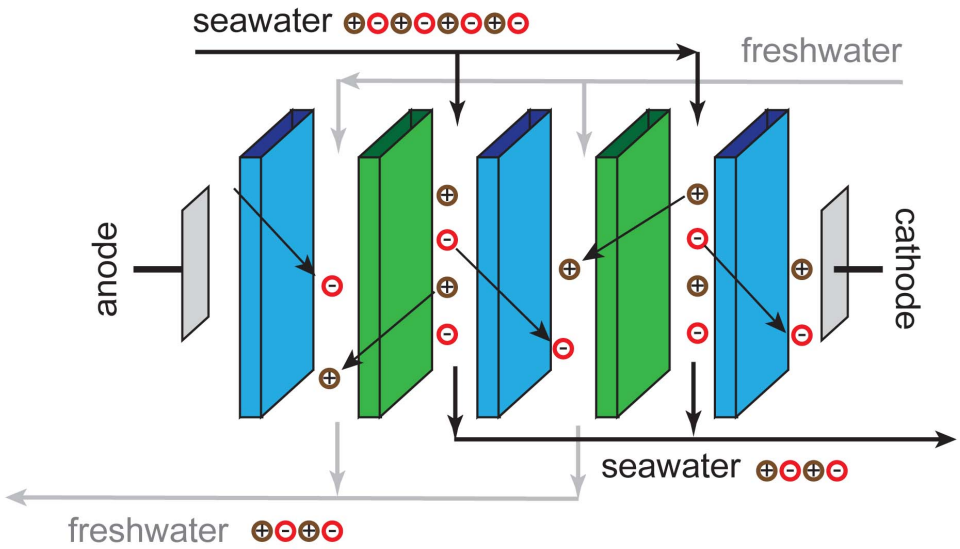
seawater
freshwater
anode
cathode
seawater
freshwater

Figure 1

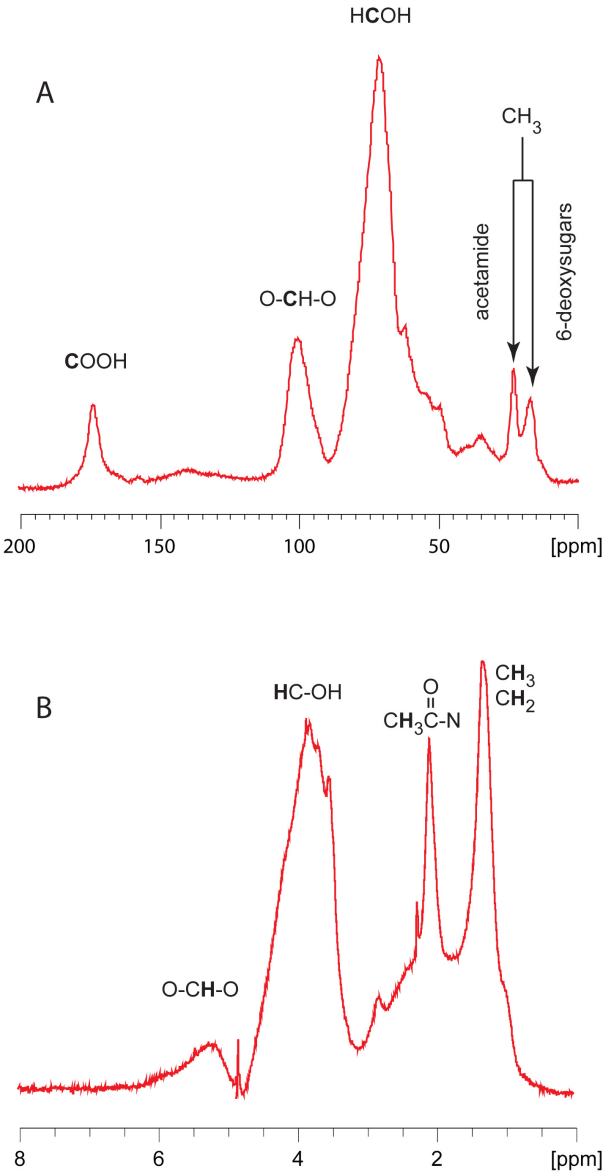
A
HCOH
CH3
acetamide
6-deoxysugars
O-CH-O
COOH
200
150
100
50
[ppm]
B
HC-OH
O
CH3C-N
CH3
CH2
O-CH-O
8
6
4
2
[ppm]

Figure 2

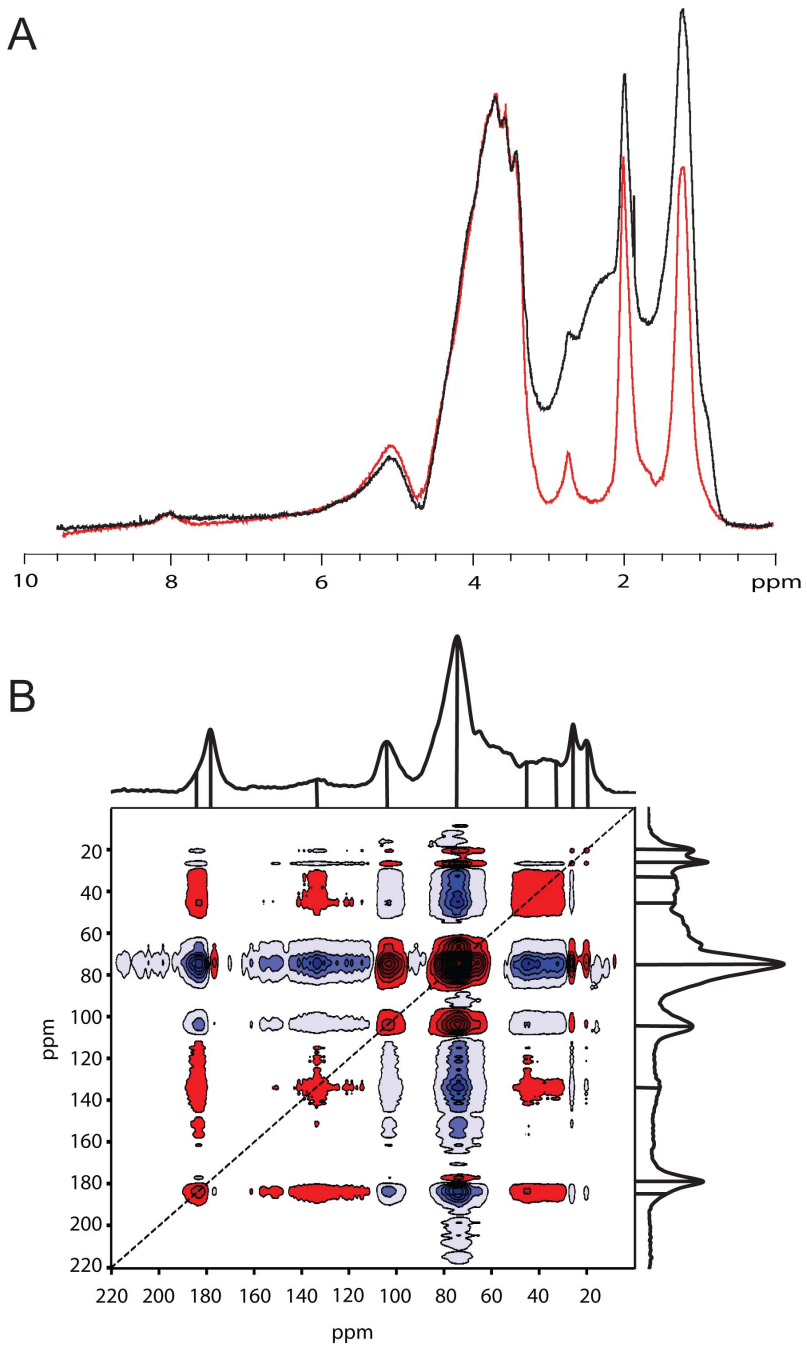
A
10
8
6
4
2
ppm
B
20
40
60
80
100
120
140
160
180
200
220
ppm
220 200 180 160 140 120 100 80 60 40 20
ppm

Figure 3

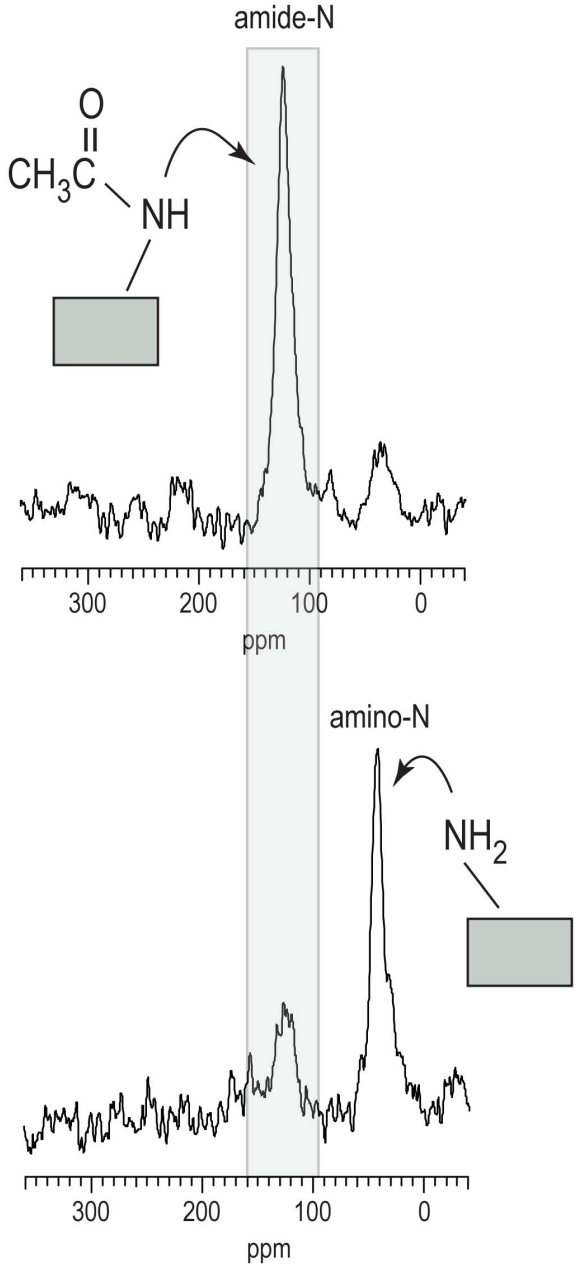
amide-N
O
CH3C
NH
300
200
100
0
ppm
amino-N
NH2
300
200
100
0
ppm

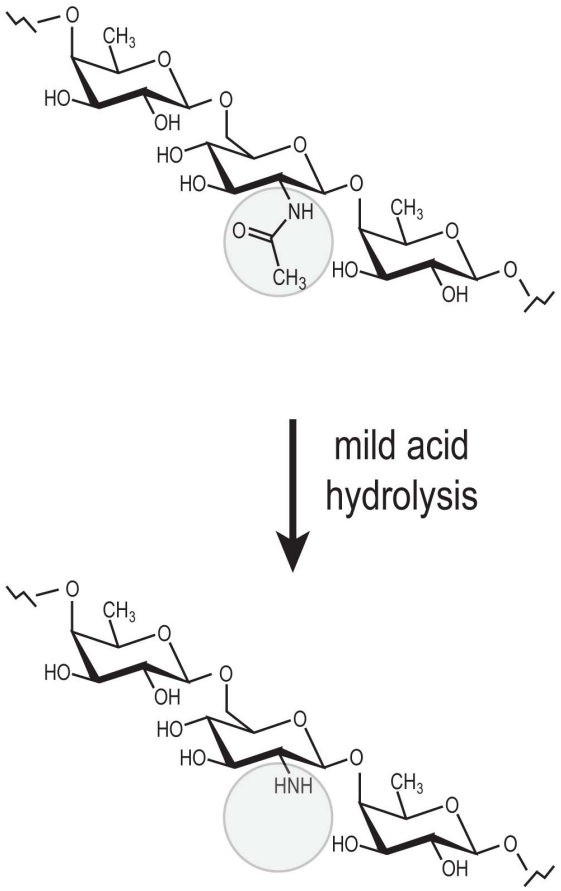
mild acid
hydrolysis

Figure 4

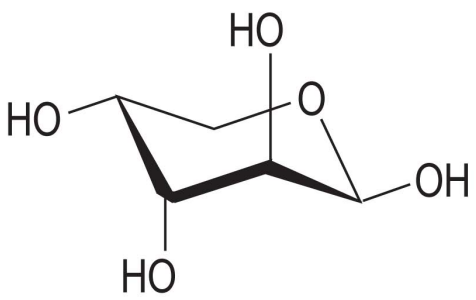

Arabinose

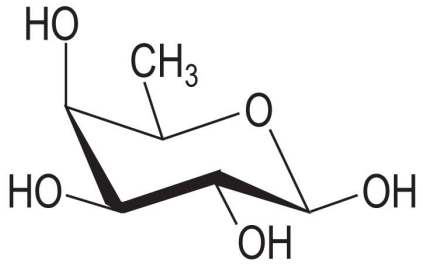

Fucose

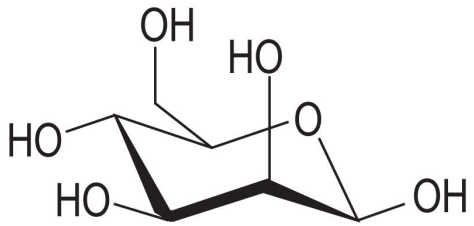

Mannose

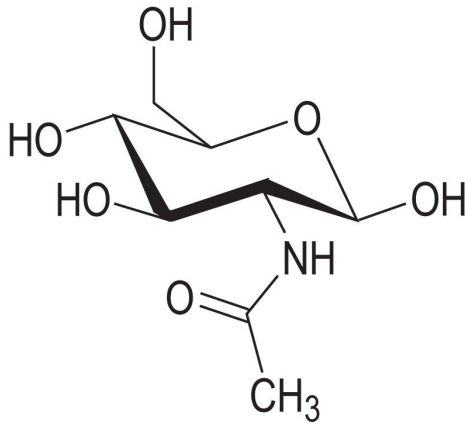

N-acetyl glucosamine

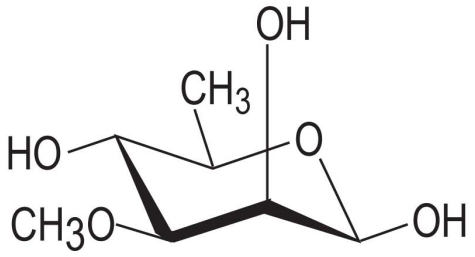

3-Methyl rhamnose

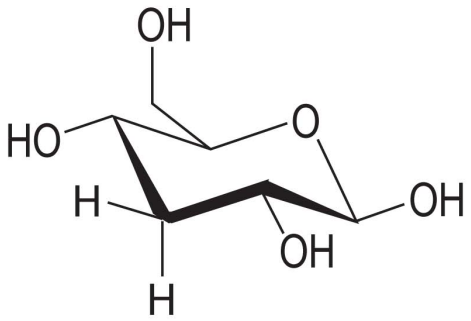

3-deoxyglucosamine

Figure 5

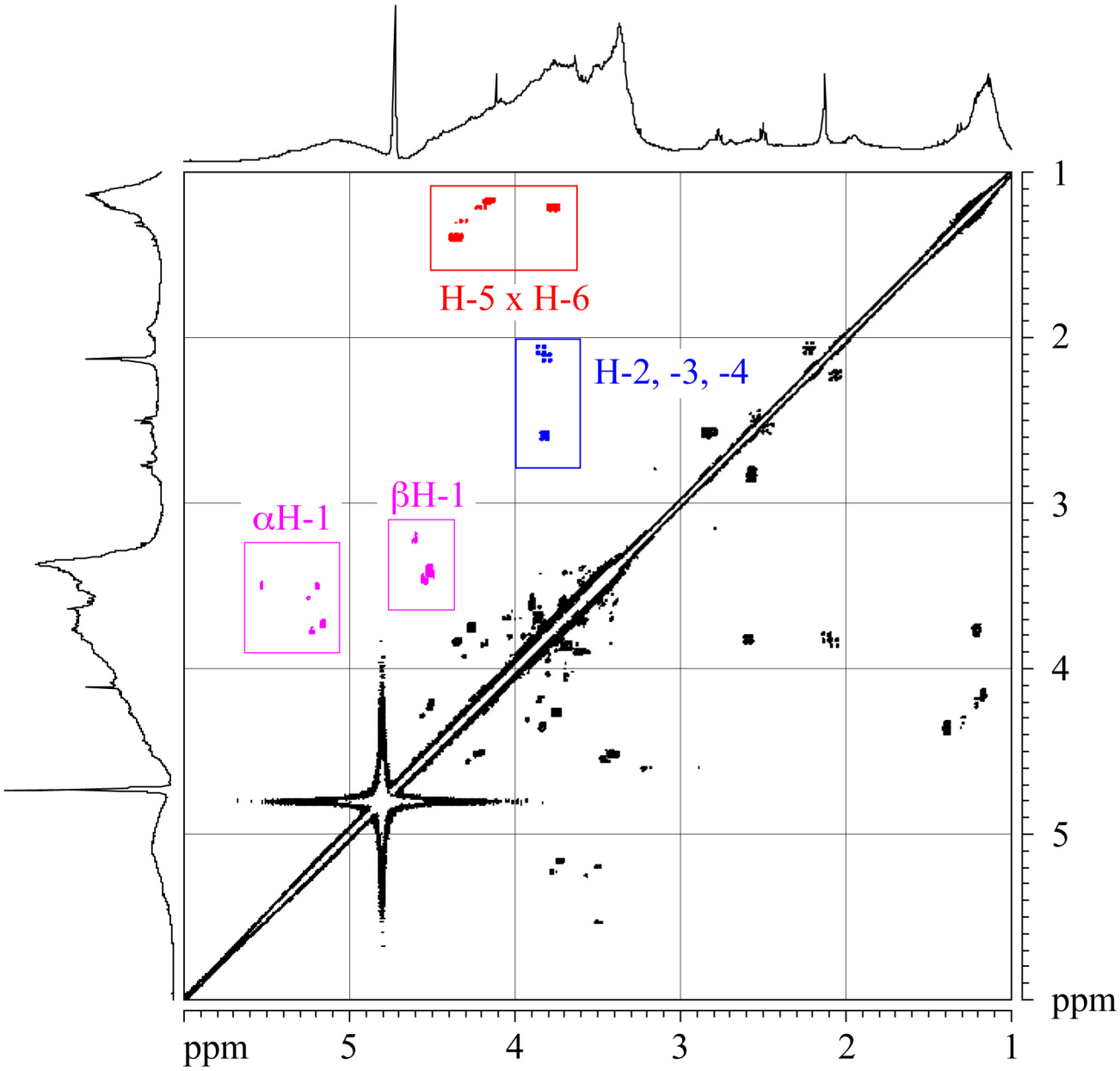

Figure 6

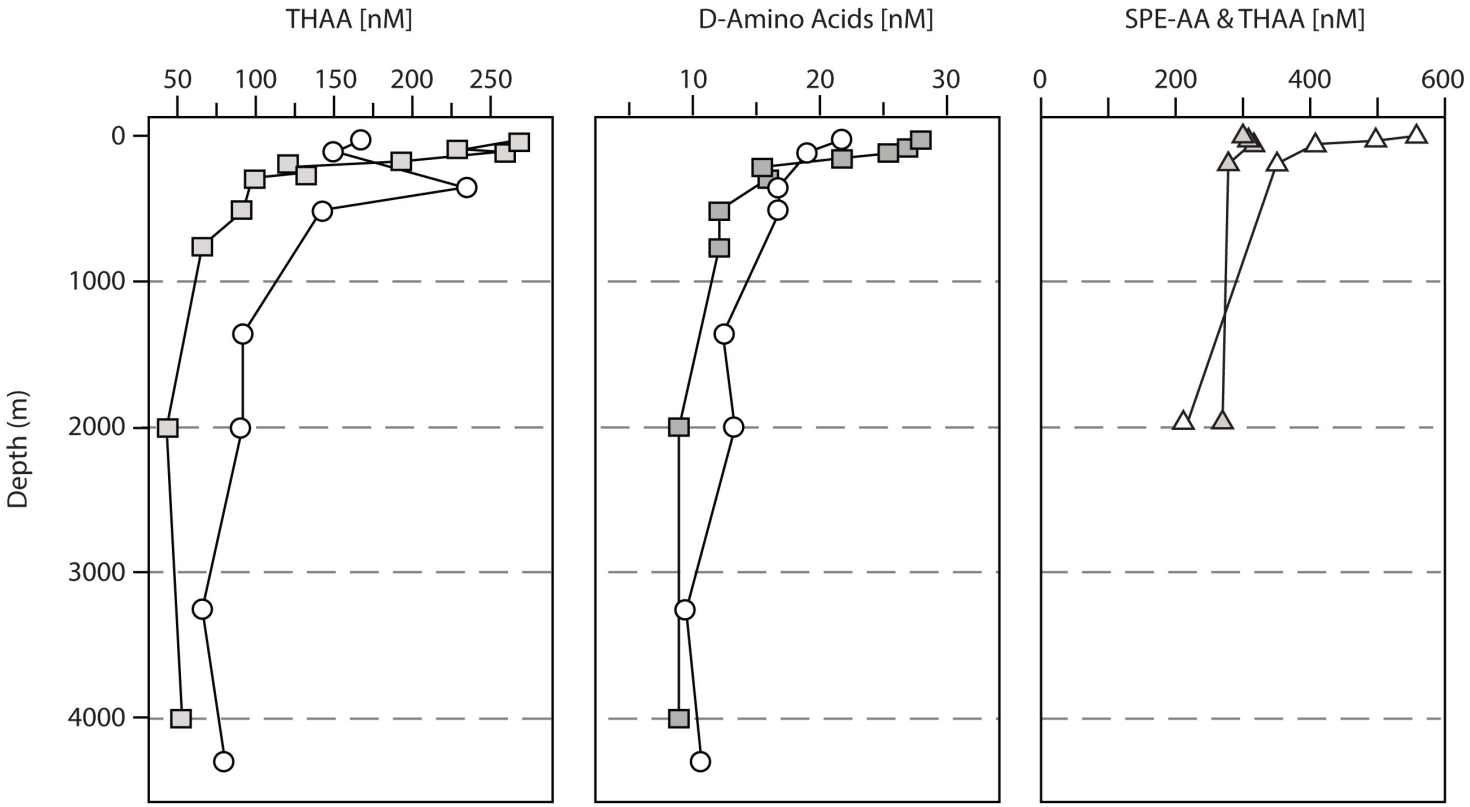
THAA [nM]
50
100
150
200
250
D-Amino Acids [nM]
10
20
30
SPE-AA & THAA [nM]
0
200
400
600
Depth (m)
0
1000
2000
3000
4000

Figure 7

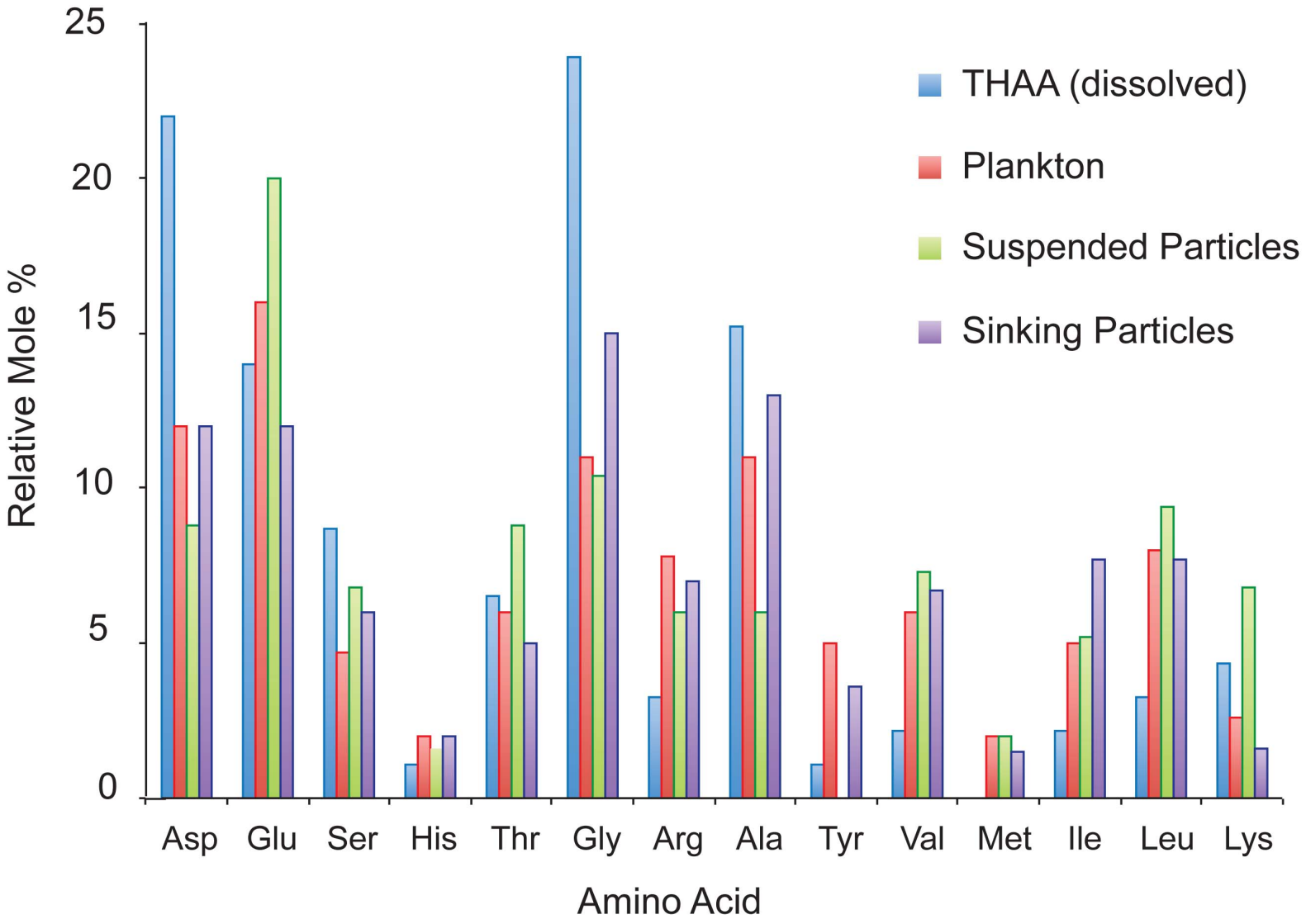
25
20
15
10
5
0
Relative Mole %
THAA (dissolved)
Plankton
Suspended Particles
Sinking Particles
Asp
Glu
Ser
His
Thr
Gly
Arg
Ala
Tyr
Val
Met
Ile
Leu
Lys
Amino Acid

Figure 8

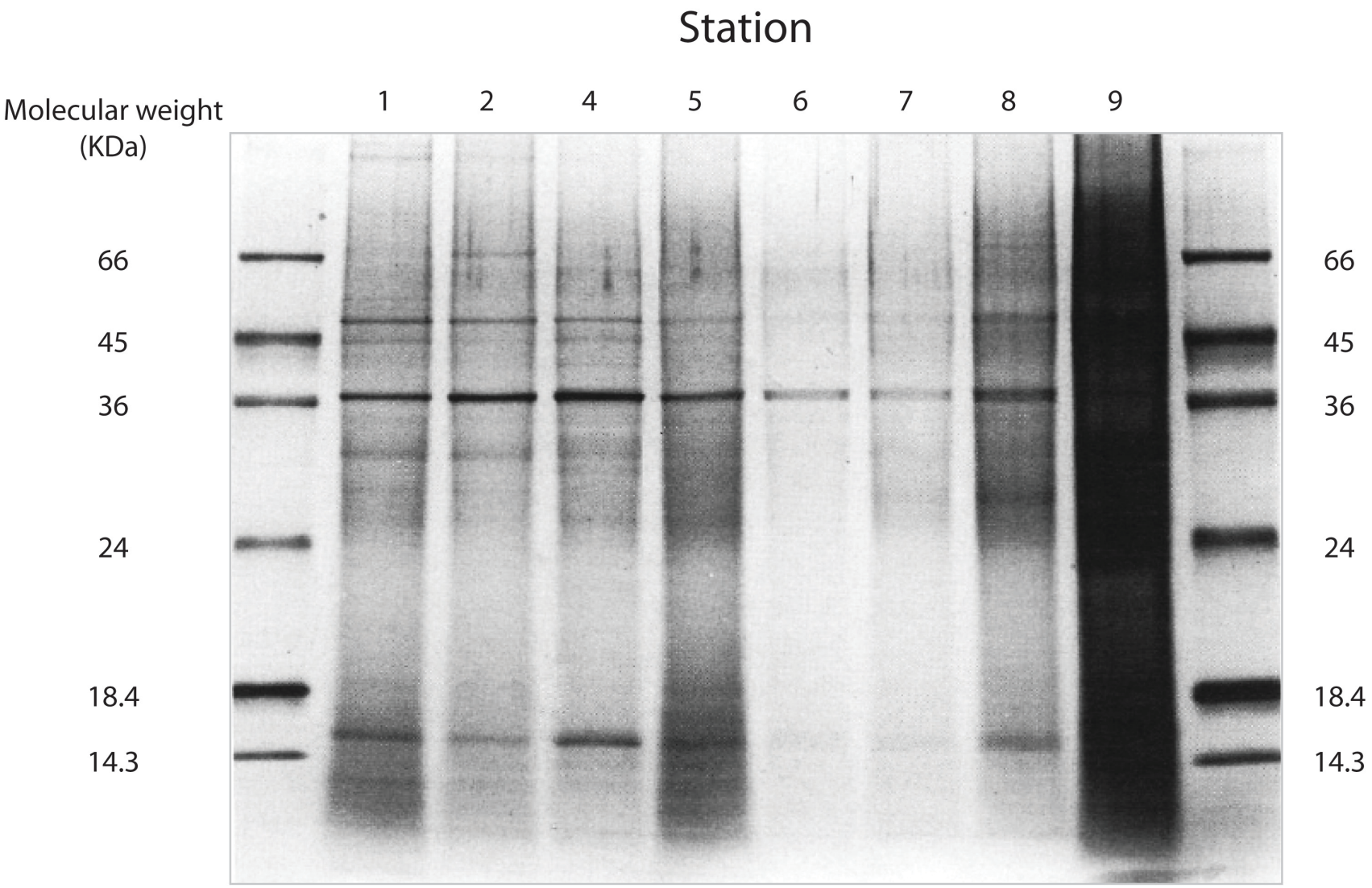
Station
1
2
4
5
6
7
8
9
Molecular weight
(KDa)
66
45
36
24
18.4
14.3
66
45
36
24
18.4
14.3

Figure 9

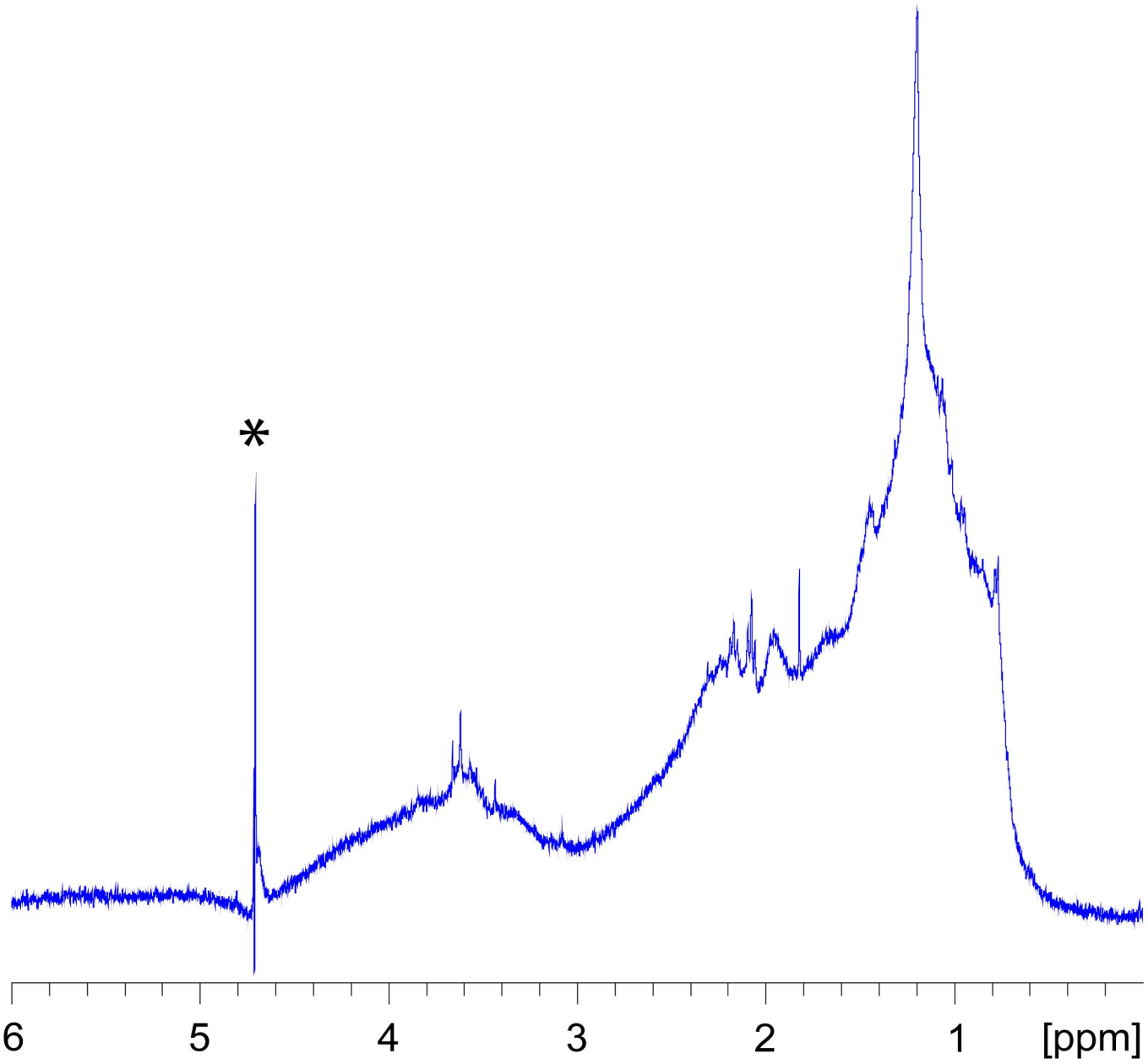

Figure 10

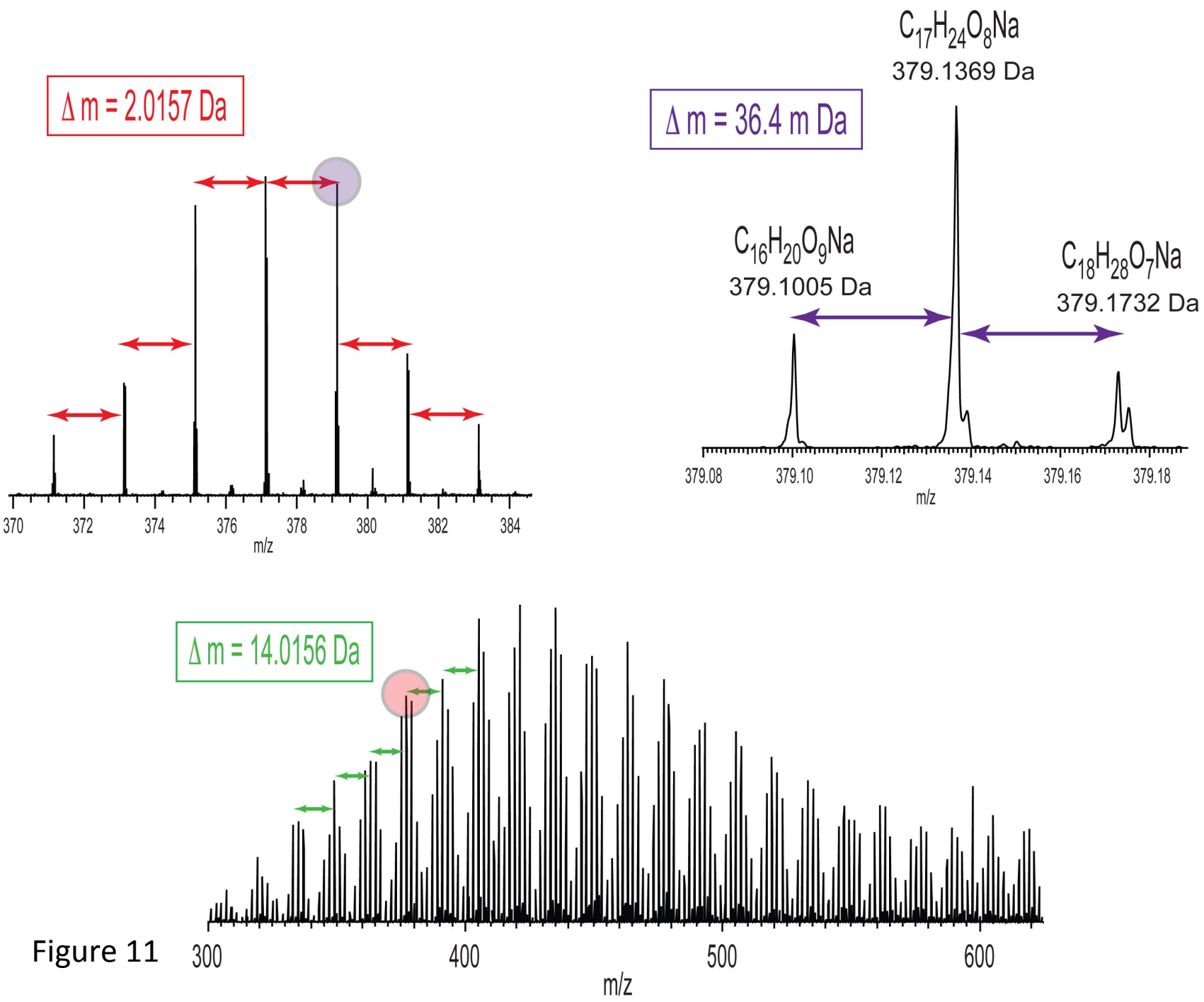
Δ m = 2.0157 Da
370
372
374
376
378
380
382
384
m/z
C17H24O8Na
379.1369 Da
Δ m = 36.4 m Da
C16H20O9Na
379.1005 Da
C18H28O7Na
379.1732 Da
379.08
379.10
379.12
379.14
379.16
379.18
m/z
Δ m = 14.0156 Da
300
400
500
600
m/z

Figure 11

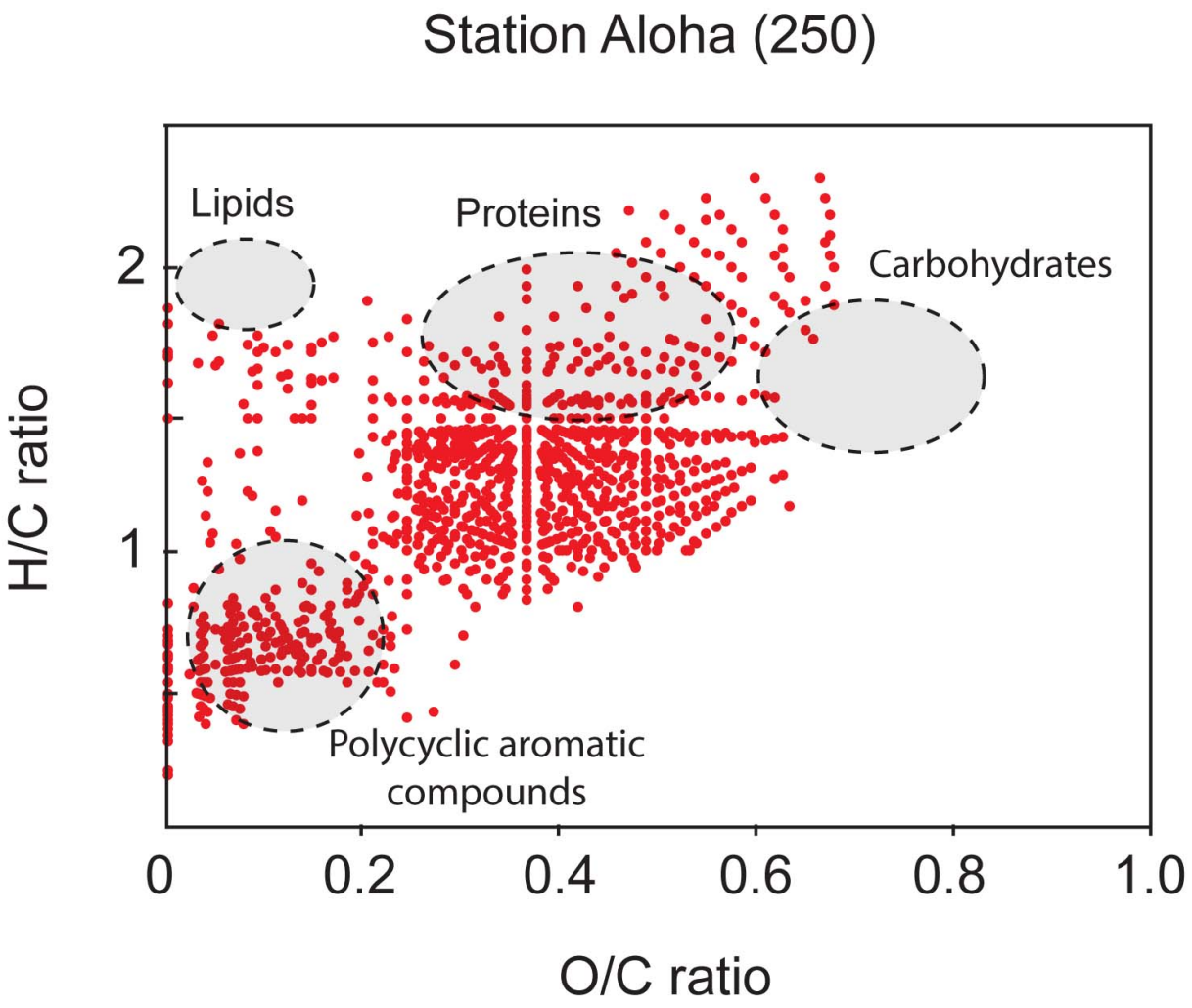
Station Aloha (250)
Lipids
Proteins
Carbohydrates
Polycyclic aromatic compounds
H/C ratio
O/C ratio
2
1
0
0.2
0.4
0.6
0.8
1.0

Figure 12

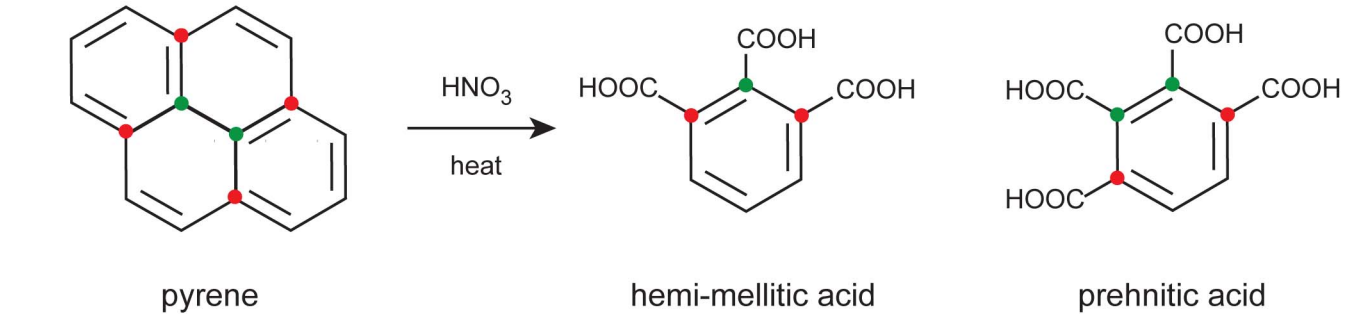
HNO3
heat
COOH
HOOC
COOH
COOH
HOOC
COOH
HOOC
pyrene
hemi-mellitic acid
prehnitic acid

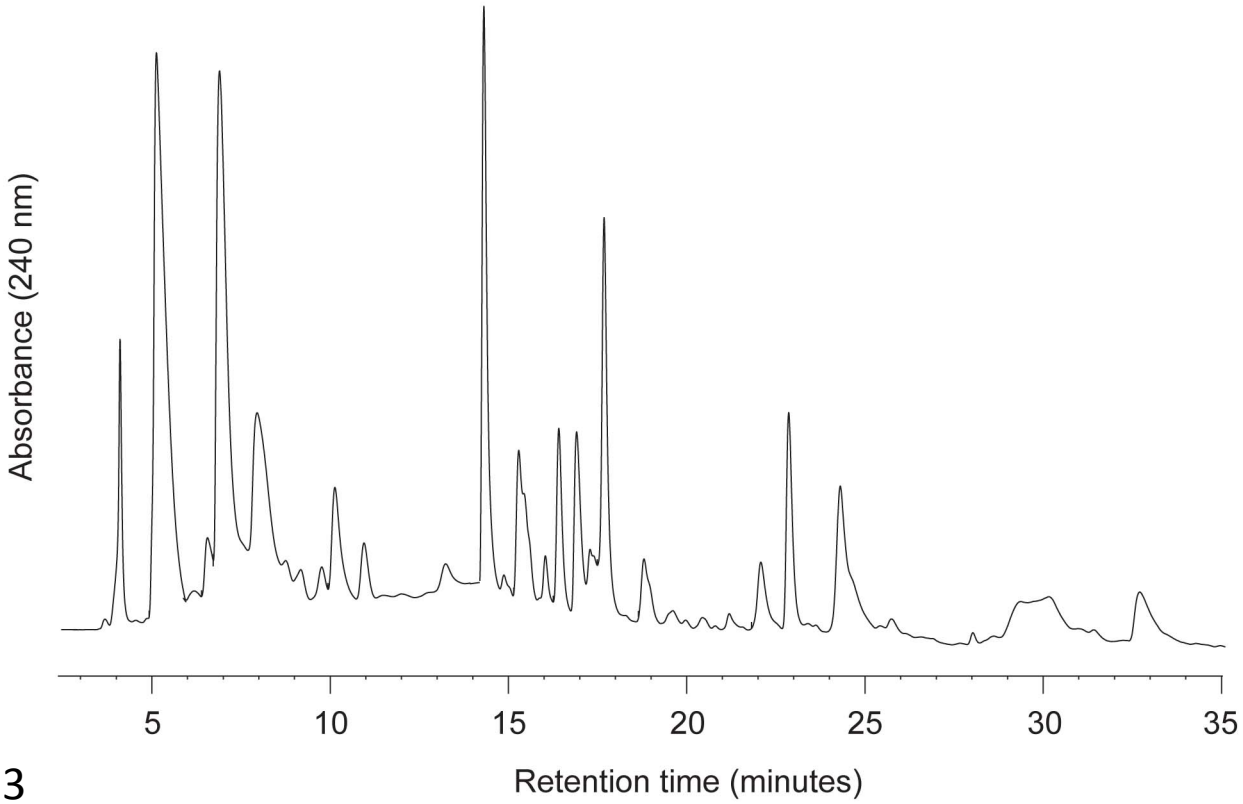
Absorbance (240 nm)
5
10
15
20
25
30
35
Retention time (minutes)

Figure 13

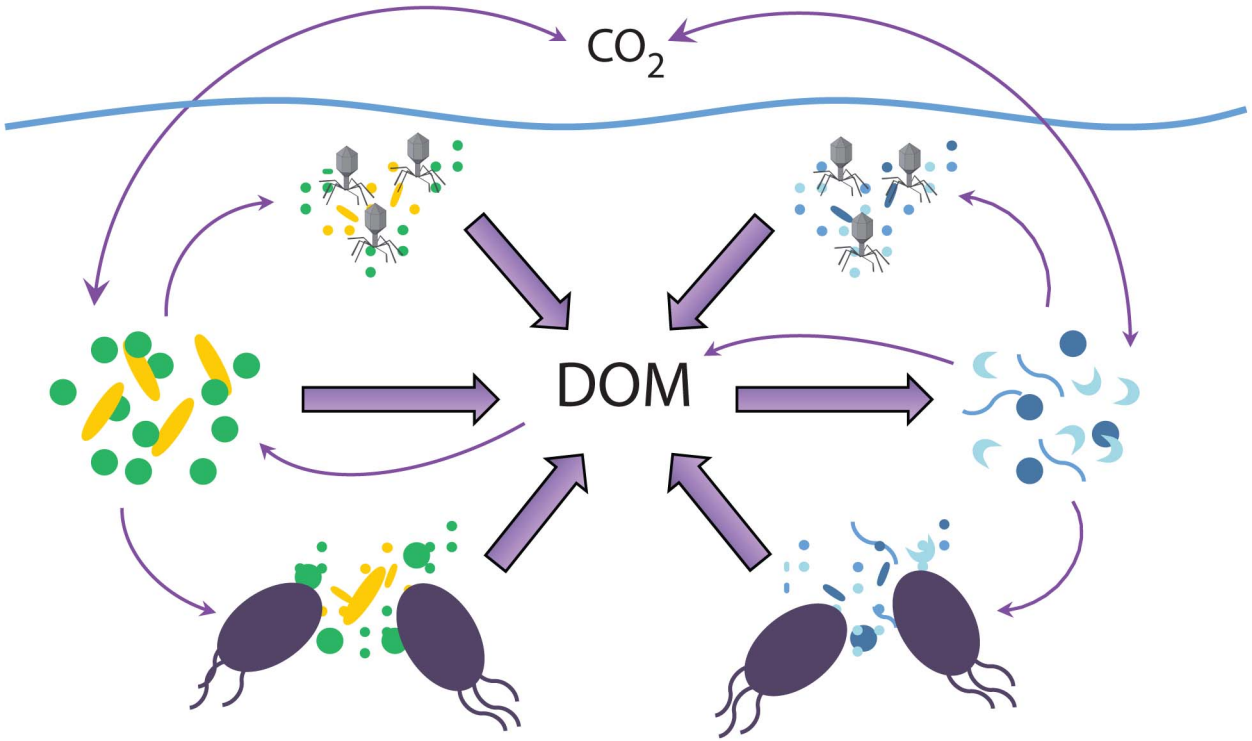

Figure 14

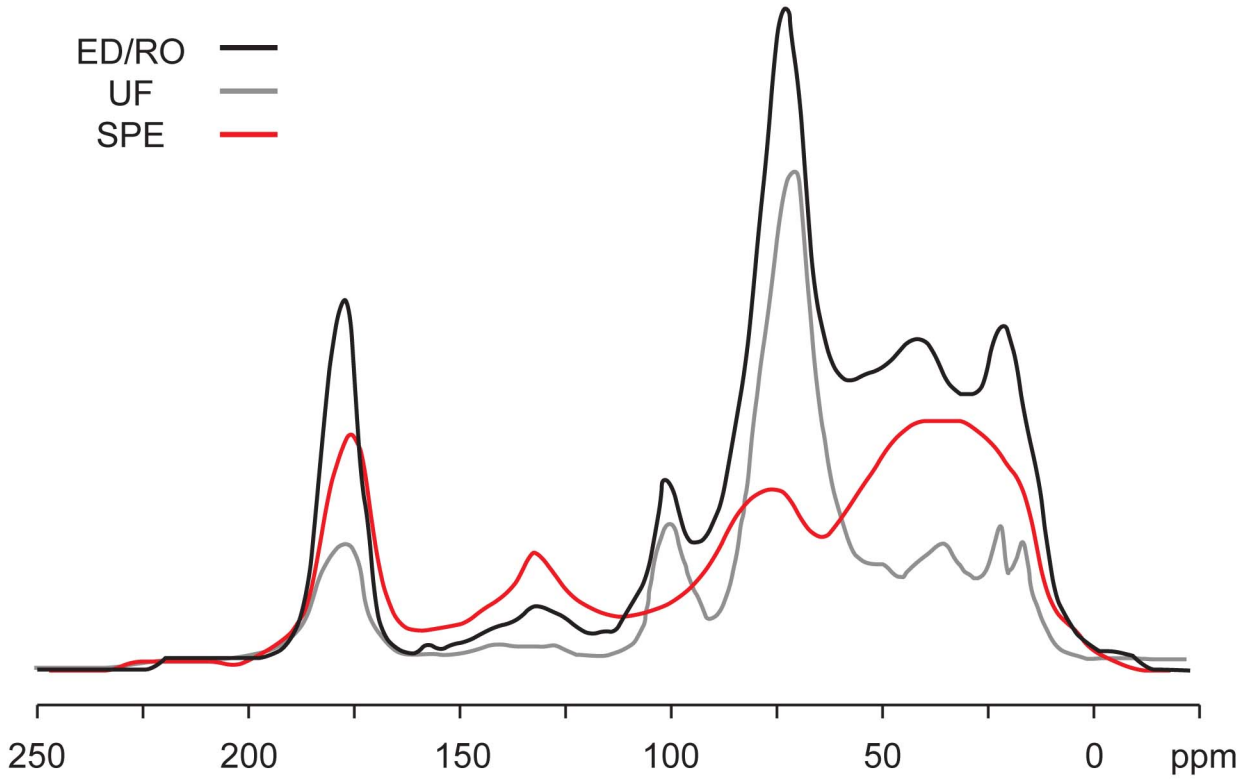

Figure 15

2.6 References

Abdulla H. A. N., Minor E. C. and Hatcher P. G. (2010a) Using two-dimensional correlations of ^{13}C NMR and FTIR to investigate changes in the chemical composition of dissolved organic matter along an estuarine transect. *Environ. Sci. Technol.* **44**, 8044–8049.

Abdulla H. A. N., Minor E. C., Dias R. F. and Hatcher P. G. (2010b) Changes in the compound classes of dissolved organic matter along an estuarine transect: A study using FTIR and ^{13}C NMR. *Geochim. Cosmochim. Acta* **74**, 3815–3838.

Abdulla H. A. N., Sleighter R. L. and Hatcher P. G. (2013) Two dimensional correlation analysis of fourier transform ion cyclotron resonance mass spectra of dissolved organic matter: A new graphical analysis of trends. *Anal. Chem.* **85**, 3895–3902.

Aluwihare L. I. and Meador T. (2008) *Chemical Composition of Marine Dissolved Organic Nitrogen*. In: Nitrogen in the Marine Environment (Eds. D. G. Capone, D. A. Bronk, M. Mulholland, and E. Carpenter). Kluwer Press.

Aluwihare L. I. and Repeta D. J. (1999) A comparison of the chemical characteristics of oceanic and extracellualr DOM produced by marine algae. **186**, 105–117.

Aluwihare L. I., Repeta D. J., Pantoja S. and Johnson C. G. (2005) Two chemically distinct pools of organic nitrogen accumulate in the ocean. *Science* **308**, 1007–10.

Aluwihare L., Repeta D. and Chen R. (1997) A major biopolymeric component to dissolved organic carbon in surface sea water. *Nature* **387**, 166–169.

Aluwihare L., Repeta D. and Chen R. (2002) Chemical composition and cycling of dissolved organic matter in the Mid-Atlantic Bight. *Deep Sea Res. Part II Top. Stud. Oceanogr.* **49**, 4421–4437.

Amin S. A, Parker M. S. and Armbrust E. V. (2012) Interactions between diatoms and bacteria. *Microbiol. Mol. Biol. Rev.* **76**, 667–84.

Amon R. M. W. and Benner R. (2003) Combined neutral sugars as indicators of the diagenetic state of dissolved organic matter in the Arctic Ocean. *Deep Sea Res. Part I Oceanogr. Res. Pap.* **50**, 151–169.

Amon R. M. W., Fitznar H. and Benner R. (2001) Linkages among the bioreactivity, chemical composition , and diagenetic state of marine dissolved organic matter. *Limnol. Oceanogr.* **46**, 287–297.

Arnosti C. (2011) Microbial Extracellular Enzymes and the Marine Carbon Cycle. *Ann. Rev. Mar. Sci.* **3**, 401–425.

1670 Arnosti C., Steen A. D., Ziervogel K., Ghobrial S. and Jeffrey W. H. (2011) Latitudinal
1671 gradients in degradation of marine dissolved organic carbon. *PLoS One* **6**, e28900.

1672 De Baar H. J. W., Boyd P. W., Coale K. H. and Landry M. R. (2005) Synthesis of iron
1673 fertilization experiments: From the Iron Age in the Age of Enlightenment. *J.*
1674 *Geophys. Res* **110**, 1–24.

1675 Barton A. D., Dutkiewicz S., Flierl G., Bragg J. and Follows M. J. (2010) Patterns of
1676 diversity in marine phytoplankton. *Science.* **327**, 1509–1511.

1677 Bauer J. E. and Bianchi T. S. (2011) *Dissolved organic carbon cycling and*
1678 *transformation*. In: Treatise on Estuarine and Coastal Science. (Eds. E. Wolanski
1679 and D. S. McLusky), Academic Press.

1680 Benner R. and Kaiser K. (2003) Abundance of amino sugars and peptidoglycan in marine
1681 particulate and dissolved organic matter. *Limnol. Oceanogr.* **48**, 118–128.

1682 Benner R., Pakulski J. D., McCarthy M., Hedges J. I. and Hatcher P. G. (1992) Bulk
1683 chemical characteristics of dissolved organic matter in the ocean. *Science.* **255**,
1684 1561–1564.

1685 Bertrand E. M., Allen A. E., Dupont C. L., Norden-Krichmar T. M., Bai J., Valas R. E.
1686 and Saito M. a (2012) Influence of cobalamin scarcity on diatom molecular
1687 physiology and identification of a cobalamin acquisition protein. *Proc. Natl. Acad.*
1688 *Sci. U. S. A.* **109**, E1762–71.

1689 Bertrand E. M., Saito M. A, Lee P. A, Dunbar R. B., Sedwick P. N. and Ditullio G. R.
1690 (2011) Iron limitation of a springtime bacterial and phytoplankton community in the
1691 ross sea: implications for vitamin B_{12} nutrition. *Front. Microbiol.* **2**, 160.

1692 Biddanda B. and Benner R. (1997) Carbon , nitrogen , and carbohydrate fluxes during the
1693 production of particulate and dissolved organic matter by marine phytoplankton.
1694 *Limnol. Oceanogr.* **42**, 506–518.

1695 Boiteau R., Fitzsimmons J. N., Repeta D. J. and Boyle E. A. (2013) A method for the
1696 characterization of iron ligands in seawater and marine cultures by HPLC-ICP-MS.
1697 *Anal. Chem.* **85**, 4357-4362.

1698 Boon J. J., Klap V. A. and Eglinton T. I. (1998) Molecular characterization of microgram
1699 amounts of oceanic colloidal organic matter by direct temperature-resolved
1700 ammonia chemical ionization mass spectrometry. *Org. Geochem.* **29**, 1051–1061.

1701 Boyd P. W. and Ellwood M. J. (2010) The biogeochemical cycle of iron in the ocean.
1702 *Nat. Geosci.* **3**, 675–682.

1703 Boye M., van den Berg C. M. G., de Jong J., Leach H., Croot P. and de Baar H. J. W.
1704 (2001) Organic complexation of iron in the Southern Ocean. *Deep Sea Res. Part I*
1705 *Oceanogr. Res. Pap.* **48**, 1477–1497.

1706 Bragg J. G., Dutkiewicz S., Jahn O., Follows M. J. and Chisholm S. W. (2010) Modeling
1707 selective pressures on phytoplankton in the global ocean. *PLoS One* **5**, e9569.

1708 Burdige D. J. (2007) Preservation of organic matter in marine sediments: controls,
1709 mechanisms, and an imbalance in sediment organic carbon budgets? *Chem. Rev.*
1710 **107**, 467–85.

1711 Calleja M. L., Batista F., Peacock M., Kudela R. and McCarthy M. D. (2013) Changes in
1712 compound specific δ15N amino acid signatures and d/l ratios in marine dissolved
1713 organic matter induced by heterotrophic bacterial reworking. *Mar. Chem.* **149**, 32–
1714 44.

1715 Carlson C. A., Giovannoni S. J., Hansell D. A., Goldberg S. J., Parsons R. and Vergin K.
1716 (2004) Interactions among dissolved organic carbon , microbial processes , and
1717 community structure in the mesopelagic zone of the northwestern Sargasso Sea.
1718 *Limnol. Oceangr*. **49**, 1073–1083.

1719 Carlson C.A., Giovannoni S., Hansell D., Goldberg S., Parsons R., Otero M., Vergin K.
1720 and Wheeler B. (2002) Effect of nutrient amendments on bacterioplankton
1721 production, community structure, and DOC utilization in the northwestern Sargasso
1722 Sea. *Aquat. Microb. Ecol.* **30**, 19–36.

1723 Cava F., Lam H., de Pedro M. a and Waldor M. K. (2011) Emerging knowledge of
1724 regulatory roles of D-amino acids in bacteria. *Cell. Mol. Life Sci.* **68**, 817–31.

1725 Chin W.-C., Orellana M. V. and Verdugo P. (1998) Spontaneous assembly of marine
1726 dissolved organic matter into polymer gels. *Nature* **391**, 568–572.

1727 Corradini C., Cavazza A. and Bignardi C. (2012) High-Performance Anion-Exchange
1728 Chromatography Coupled with Pulsed Electrochemical Detection as a Powerful
1729 Tool to Evaluate Carbohydrates of Food Interest: Principles and Applications. *Int. J.*
1730 *Carbohydr. Chem.* **2012**, 1–13.

1731 Cottrell M. T. and Kirchman D. L. (2000) Natural assemblages of marine proteobacteria
1732 and members of the Cytophaga-Flavobacter cluster consuming low- and high-
1733 molecular-weight dissolved organic matter. *Appl. Environ. Microbiol.* **66**, 1692–7.

1734 Dauwe B., Middelburg J. J., Herman P. M. J. and Heip C. H. R. (1999) Linking
1735 diagenetic alteration of amino acids and bulk organic matter reactivity. *Limnol.*
1736 *Oceanogr.* **44**, 1809–1814.

1737 Davis J., Kaiser K. and Benner R. (2009) Amino acid and amino sugar yields and
1738 compositions as indicators of dissolved organic matter diagenesis. *Org. Geochem.*
1739 **40**, 343–352.

1740 Dittmar T. (2008) The molecular level determination of black carbon in marine dissolved
1741 organic matter. *Org. Geochem.* **39**, 396–407.

1742 Dittmar T., Fitznar H. and Kattner G. (2001) Origin and biogeochemical cycling of
1743 organic nitrogen in the eastern Arctic Ocean as evident from D- and L-amino acids.
1744 *Geochim. Cosmochim. Acta* **65**, 4103–4114.

1745 Dittmar T., Koch B., Hertkorn N. and Kattner G. (2008a) A simple and efficient method
1746 for the solid-phase extraction of dissolved organic matter (SPE-DOM) from
1747 seawater. *Limnol. Ocean. Methods* **6**, 230–235.

1748 Dittmar T., Koch B., Hertkorn N. and Kattner G. (2008b) A simple and efficient method
1749 for the solid-phase extraction of dissolved organic matter (SPE-DOM) from
1750 seawater. *Limnol. Oceanogr. Methods* **6**, 230–235.

1751 Dittmar T. and Koch B. P. (2006) Thermogenic organic matter dissolved in the abyssal
1752 ocean. *Mar. Chem.* **102**, 208–217.

1753 Dittmar T. and Paeng J. (2009) A heat-induced molecular signature in marine dissolved
1754 organic matter. *Nat. Geosci.* **2**, 175–179.

1755 Druffel E. R. M., Griffin S., Bauer J. E., Wolgast D. and Wang X.-C. (1998) Distribution
1756 of particulate organic carbon and radiocarbon in the water column from the upper
1757 slope to the abyssal NE Pacific Ocean. *Deep Sea Res. Part II Top. Stud. Oceanogr.*
1758 **45**, 667–687.

1759 Druffel E. R. M., Williams P. M., Bauer J. E. and Ertel J. R. (1992) Cycling of dissolved
1760 and particulate organic matter in the open ocean. *J. Geophys. Res.* **97**, 15639–15659.

1761 Dutkiewicz S., Follows M. J. and Bragg J. G. (2009) Modeling the coupling of ocean
1762 ecology and biogeochemistry. *Global Biogeochem. Cycles* **23**, 1–15.

1763 Dutkiewicz S., Ward B. A., Monteiro F. and Follows M. J. (2012) Interconnection of
1764 nitrogen fixers and iron in the Pacific Ocean: Theory and numerical simulations.
1765 *Global Biogeochem. Cycles* **26**, GB1012, doi:10.1029/2011GB004039.

1766 Esteves V. I., Otero M. and Duarte A. C. (2009) Comparative characterization of humic
1767 substances from the open ocean, estuarine water and fresh water. *Org. Geochem.* **40**,
1768 942–950.

1769 Flerus R., Lechtenfeld O. J., Koch B. P., McCallister S. L., Schmitt-Kopplin P., Benner
1770 R., Kaiser K. and Kattner G. (2012) A molecular perspective on the ageing of
1771 marine dissolved organic matter. *Biogeosciences* **9**, 1935–1955.

1772 Follows M. J., Dutkiewicz S., Grant S. and Chisholm S. W. (2007) Emergent
1773 biogeography of microbial communities in a model ocean. *Science* **315**, 1843–1846.

1774 Fry B., Hopkinson C. S., Nolin A., Norrman B. and Li U. (1996) Long-term
1775 decomposition of DOC from experimental diatom blooms. *Limnol. Oceanogr.* **41**,
1776 1344–1347.

1777 Fuhrman J. (1987) Close coupling between release and uptake of dissolved free amino
1778 acids in seawater studied by an isotope dilution approach. *Mar. Ecol. Prog. Ser.* **37**,
1779 45–52.

1780 Gagosian R. B. and Steurmer D. H. (1977) The cycling of biogenic compounds and their
1781 dia- genetically transformed products in seawater. *Mar. Chem.* **5**, 605–632.

1782 Gledhill M. and van den Berg C. M. G. (1994) Determination of complexation of iron
1783 (III) with natural organic complexing ligands in seawater using cathodic stripping
1784 voltammetry. *Mar. Chem.* **47**, 41–54.

1785 Gledhill M. and Buck K. N. (2012) The organic complexation of iron in the marine
1786 environment: a review. *Front. Microbiol.* **3**, 1–17.

1787 Gogou A. and Repeta D. J. (2010) Particulate-dissolved transformations as a sink for
1788 semi-labile dissolved organic matter: Chemical characterization of high molecular
1789 weight dissolved and surface-active organic matter in seawater and in diatom
1790 cultures. *Mar. Chem.* **121**, 215–223.

1791 Goldberg S. J., Carlson C. A., Bock B., Nelson N. B. and Siegel D. a. (2010) Meridional
1792 variability in dissolved organic matter stocks and diagenetic state within the
1793 euphotic and mesopelagic zone of the North Atlantic subtropical gyre. *Mar. Chem.*
1794 **119**, 9–21.

1795 Goldberg S. J., Carlson C. A., Hansell D. A., Nelson N. B. and Siegel D. A. (2009)
1796 Temporal dynamics of dissolved combined neutral sugars and the quality of
1797 dissolved organic matter in the Northwestern Sargasso Sea. *Deep Sea Res. Part I*
1798 *Oceanogr. Res. Pap.* **56**, 672–685.

1799 Gonsior M., Peake B. M., Cooper W. T., Podgorski D. C., D'Andrilli J., Dittmar T. and
1800 Cooper W. J. (2011) Characterization of dissolved organic matter across the
1801 Subtropical Convergence off the South Island, New Zealand. *Mar. Chem.* **123**, 99–
1802 110.

1803 Green S. A. and Blough N. V. (1994) Optical absorption and fluorescence properties of
1804 chromophoric dissolved organic matter in natural waters. *Limnol. Oceanogr.* **39**,
1805 1903–1916.

1806 Gurtler B. K., Vetter T. A., Perdue E. M., Ingall E., Koprivnjak J.-F. and Pfromm P. H.
1807 (2008) Combining reverse osmosis and pulsed electrical current electrodialysis for
1808 improved recovery of dissolved organic matter from seawater. *J. Memb. Sci.* **323**,
1809 328–336.

1810 Hansell D. A. (2012) Recalcitrant Dissolved Organic Carbon Fractions. *Ann. Rev. Mar.*
1811 *Sci.*, 1–25.

1812 Hansell D. A. and Carlson C. A. (2013) Localized refractory dissolved organic sinks in
1813 the deep ocean. *Global Biogeochem. Cycles* **27**, 705-710.
1814 doi:10.1002/GBC.20067,2013.

1815 Hansell D. A., Carlson C. A., Repeta D. J. and Schlitzer R. (2009) Dissolved Organic
1816 Matter in the Ocean. *Oceanography* **22**, 202–211.

1817 Hansell D. A., Carlson C. A. and Schlitzer R. (2012) Net removal of major marine
1818 dissolved organic carbon fractions in the subsurface ocean. *Global Biogeochem.*
1819 *Cycles* **26**, GB1016, doi:1029/2011 GB004069.

1820 Hedges J. I., Hatcher P. G., Ertel J. R. and Meyers-schulte K. J. (1988) A comparison of
1821 dissolved humic substances from seawater with Amazon River counterparts by 13C-
1822 NMR spectrometry. *Geochim. Cosmochim. Acta* **56**, 1753–1757.

1823 Helliwell K. E., Wheeler G. L., Leptos K. C., Goldstein R. E. and Smith A. G. (2011)
1824 Insights into the evolution of vitamin B12 auxotrophy from sequenced algal
1825 genomes. *Mol. Biol. Evol.* **28**, 2921–33.

1826 Helms J. R., Mao J., Chen H., Perdue E. M., Green N., Hatcher P. G., Mopper K. and
1827 Stubbins A. (2013) Spectroscopic characterization of oceanic dissolved organic
1828 matter isolated by reverse osmosis coupled with electrodialysis : Implications for
1829 oceanic carbon cycling.

1830 Hertkorn N., Benner R., Frommberger M., Schmittkopplin P., Witt M., Kaiser K.,
1831 Kettrup a and Hedges J. (2006) Characterization of a major refractory component of
1832 marine dissolved organic matter. *Geochim. Cosmochim. Acta* **70**, 2990–3010.

1833 Hertkorn N., Harir M., Koch B. P., Michalke B., Grill P. and Schmitt-Kopplin P. (2012)
1834 High field NMR spectroscopy and FTICR mass spectrometry: powerful discovery
1835 tools for the molecular level characterization of marine dissolved organic matter
1836 from the South Atlantic Ocean. *Biogeosciences Discuss.* **9**, 745–833.

1837 Hubberten U., Lara R. . and Kattner G. (1994) Amino acid composition of seawater and
1838 dissolved humic substances in the Greenland Sea. *Mar. Chem.* **45**, 121–128.

1839 Hubberten U., Laral R. J. and Kattnerl G. (1995) Refractory organic compounds in polar
1840 waters : Relationship between humic substances and amino acids in the Arctic and
1841 Antarctic. *J. Mar. Res.*, 137–149.

1842 Jiao N., Herndl G. J., Hansell D. A, Benner R., Kattner G., Wilhelm S. W., Kirchman D.
1843 L., Weinbauer M. G., Luo T., Chen F. and Azam F. (2010) Microbial production of
1844 recalcitrant dissolved organic matter: long-term carbon storage in the global ocean.
1845 *Nat. Rev. Microbiol.* **8**, 593–9.

1846 Jickells T. D., An Z. S., Andersen K. K., Baker A. R., Bergametti G., Brooks N., Cao J.
1847 J., Boyd P. W., Duce R. A., Hunter K. A., Kawahata H., Kubilay N., LaRoche J.,
1848 Liss P. S., Mahowald N., Prospero J. M., Ridgwell A. J., Tegen I. and Torres R.
1849 (2005) Global iron connections between desert dust, ocean biogeochemistry, and
1850 climate. *Science* **308**, 67.

1851 Jones V., Ruddell C. J., Wainwright G., Rees H. H., Jaffé R. and Wolff G. A (2004) One-
1852 dimensional and two-dimensional polyacrylamide gel electrophoresis: a tool for
1853 protein characterisation in aquatic samples. *Mar. Chem.* **85**, 63–73.

1854 Jurado E., Dachs J., Duarte C. M. and Simó R. (2008) Atmospheric deposition of organic
1855 and black carbon to the global oceans. *Atmos. Environ.* **42**, 7931–7939.

1856 Kaiser K. and Benner R. (2009) Biochemical composition and size distribution of organic
1857 matter at the Pacific and Atlantic time-series stations. *Mar. Chem.* **113**, 63–77.

1858 Kaiser K. and Benner R. (2000) Determination of Amino Sugars in Environmental
1859 Samples with High Salt Content by Chromatography and Pulsed Amperometric
1860 Detection. **72**, 2566–2572.

1861 Kaiser K. and Benner R. (2008) Major bacterial contribution to the ocean reservoir of
1862 detrital organic carbon and nitrogen. *Limnol. Oceanogr.* **53**, 99–112.

1863 Kawasaki N. and Benner R. (2006) Bacterial release of dissolved organic matter during
1864 cell growth and decline: Molecular origin and composition. *Limnol. Oceanogr.* **51**,
1865 2170–2180.

1866 Kido Soule M. C., Longnecker K., Giovannoni S. J. and Kujawinski E. B. (2010) Impact
1867 of instrument and experiment parameters on reproducibility of ultrahigh resolution
1868 ESI FT-ICR mass spectra of natural organic matter. *Org. Geochem.* **41**, 725–733.

1869 Kieber R. J., Zhou X. and Mopper K. (1990) Formation of Carbonyl Compounds from
1870 UV-Induced Photodegradation of Humic Substances in Natural Waters : Fate of
1871 Riverine Carbon in the Sea. *Limnol. Oceanogr.* **35**, 1503–1515.

1872 Koch B. P., Dittmar T., Witt M. and Kattner G. (2007) Fundamentals of molecular
1873 formula assignment to ultrahigh resolution mass data of natural organic matter.
1874 *Anal. Chem.* **79**, 1758–63.

1875 Koch B. P., Witt M., Engbrodt R., Dittmar T. and Kattner G. (2005) Molecular formulae
1876 of marine and terrigenous dissolved organic matter detected by electrospray
1877 ionization Fourier transform ion cyclotron resonance mass spectrometry. *Geochim.*
1878 *Cosmochim. Acta* **69**, 3299–3308.

1879 Koprivnjak J.-F., Pfromm P. H., Ingall E., Vetter T. a., Schmitt-Kopplin P., Hertkorn N.,
1880 Frommberger M., Knicker H. and Perdue E. M. (2009) Chemical and spectroscopic
1881 characterization of marine dissolved organic matter isolated using coupled reverse
1882 osmosis–electrodialysis. *Geochim. Cosmochim. Acta* **73**, 4215–4231.

1883 Kujawinski E. B. and Behn M. D. (2006) Automated analysis of electrospray ionization
1884 fourier transform ion cyclotron resonance mass spectra of natural organic matter.
1885 *Anal. Chem.* **78**, 4363–73.

1886 Kujawinski E. B., Longnecker K., Blough N. V., Vecchio R. Del, Finlay L., Kitner J. B.
1887 and Giovannoni S. J. (2009) Identification of possible source markers in marine
1888 dissolved organic matter using ultrahigh resolution mass spectrometry. *Geochim.*
1889 *Cosmochim. Acta* **73**, 4384–4399.

1890 Lam B. and Simpson A. J. (2008) Direct (1)H NMR spectroscopy of dissolved organic
1891 matter in natural waters. *Analyst* **133**, 263–9.

1892 Lang S. Q., Butterfield D. a., Lilley M. D., Paul Johnson H. and Hedges J. I. (2006)
1893 Dissolved organic carbon in ridge-axis and ridge-flank hydrothermal systems.
1894 *Geochim. Cosmochim. Acta* **70**, 3830–3842.

1895 Lee C. and Bada J. L. (1975) Amino acids in Equatorial Pacific Ocean water. *Earth*
1896 *Planet. Sci. Lett.* **26**, 61–68.

1897 Lee C. and Bada J. L. (1977) Dissolved amino acids in the equatorial Pacific , the
1898 Sargasso Sea , and Biscayne Bay. *Limnol. Oceanogr.* **22**, 502–510.

1899 Lee C., Wakeham S. G. and Hedges J. I. (2000) Composition and flux of particulate
1900 amino acids and chloropigments in equatorial Pacific seawater and sediments. **47**,
1901 1535–1568.

1902 Lin H.-T., Cowen J. P., Olson E. J., Amend J. P. and Lilley M. D. (2012) Inorganic
1903 chemistry, gas compositions and dissolved organic carbon in fluids from sedimented
1904 young basaltic crust on the Juan de Fuca Ridge flanks. *Geochim. Cosmochim. Acta*
1905 **85**, 213–227.

Lindroth P. and Mopper K. (1979) High performance liquid chromatographic determination of subpicomole amounts of amino acids by precolumn fluorescence derivatization with o-phthaldialdehyde. *Anal. Chem.* **51**, 1667–1674.

Macrellis H. M., Trick C. G., Rue E. L., Smith G. and Bruland K. W. (2001) Collection and detection of natural iron-binding ligands from seawater. *Mar. Chem.* **76**, 175–187.

Martin J. H. and Fitzwater S. E. (1988) Iron deficiency limits phytoplankton growth in the north-east Pacific subarctic. *Nature* **371**, 1223-129.

Martin J. H., Gordon R. M. and Fitzwater S. E. (1991) The case for iron. *Limnol. Oceanogr.* **36**, 1793–1802.

Masiello C. A. and Druffel E. R. M. (1998) Black Carbon in Deep-Sea Sediments. *Science* **280**, 1911–1913.

Mawji E., Gledhill M., Milton J. A., Zubkov M. V, Thompson A., Wolff G. A. and Achterberg E. P. (2011) Production of siderophore type chelates in Atlantic Ocean waters enriched with different carbon and nitrogen sources. *Mar. Chem.* **124**, 90–99.

Mawji E., Gledhill M., Worsfold P. J. and Achterberg E. P. (2008) Collision-induced dissociation of three groups of hydroxamate siderophores : ferrioxamines , ferrichromes and coprogens / fusigens. *Rapid Commun. Mass Spectrom.*, 2195–2202.

McCarren J., Becker J. W., Repeta D. J., Shi Y., Young C. R., Malmstrom R. R., Chisholm S. W. and DeLong E. F. (2010) Microbial community transcriptomes reveal microbes and metabolic pathways associated with dissolved organic matter turnover in the sea. *Proc. Natl. Acad. Sci. U. S. A.* **107**, 16420–7.

McCarthy M. D., Beaupré S. R., Walker B. D., Voparil I., Guilderson T. P. and Druffel E. R. M. (2010) Chemosynthetic origin of 14C-depleted dissolved organic matter in a ridge-flank hydrothermal system. *Nat. Geosci.* **4**, 32–36.

McCarthy M. D., Pratum T., Hedges J. I. and Benner R. (1997) Chemical composition of dissolved organic nitrogen in the ocean. *Nature* **390**, 150–154.

McCarthy M., Hedges J. and Benner R. (1998) Major bacterial contribution to marine dissolved organic nitrogen. *Science* **281**, 231–4.

McCarthy M., Hedges J. and Benner R. (1996) Major biochemical composition of dissolved high molecular weight organic matter in seawater. *Mar. Chem.* **55**, 281–297.

1939 McNichol A. P. and Aluwihare L. I. (2007) The power of radiocarbon in biogeochemical
1940 studies of the marine carbon cycle: insights from studies of dissolved and particulate
1941 organic carbon (DOC and POC). *Chem. Rev.* **107**, 443–66.

1942 Meon B. and Kirchman D. L. (2001) Dynamics and molecular composition of dissolved
1943 organic material during experimental phytoplankton blooms. *Mar. Chem.* **75**, 185–
1944 199.

1945 Miethke M. (2013) Molecular strategies of microbial iron assimilation: from high-affinity
1946 complexes to cofactor assembly systems. *Metallomics* **5**, 15–28.

1947 Minor E. C., Boon J. J., Harvey H. R. and Mannino A. (2001) Estuarine organic matter
1948 composition as probed by direct temperature-resolved mass spectrometry and
1949 traditional geochemical techniques. *Geochim. Cosmochim. Acta* **65**, 2819–2834.

1950 Mopper K. and Lindroth P. (1982) Diel and depth variations in dissolved free amino
1951 acids and ammonium in the Baltic Sea determined by shipboard HPLC analysis.
1952 *Limnol. Oceanogr.* **27**, 336–347.

1953 Mopper K. and Stahovec W. L. (1986) Sources and sinks of low molecular weight
1954 organic carbonyl compounds in seawater. *Mar. Chem.* **19**, 305–321.

1955 Mopper K., Stubbins A., Ritchie J. D., Bialk H. M. and Hatcher P. G. (2007) Advanced
1956 instrumental approaches for characterization of marine dissolved organic matter:
1957 extraction techniques, mass spectrometry, and nuclear magnetic resonance
1958 spectroscopy. *Chem. Rev.* **107**, 419–42.

1959 Mopper K., Zhou X., Kieber R. J., Kieber D. J., Sikorski R. J. and Jones R. D. (1991)
1960 Photochemical degradation of dissolved organic carbon and its impact on the ocean
1961 carbon cycle. *Nature* **353**, 60–62.

1962 Nagata T. (2003) Microbial degradation of peptidoglycan in seawater. *Limnol. Oceanogr.*
1963 **48**, 745–754.

1964 Ogawa H., Amagai Y., Koike I., Kaiser K. and Benner R. (2001) Production of refractory
1965 dissolved organic matter by bacteria. *Science* **292**, 917–20.

1966 Orellana M. V, Matrai P. A., Leck C., Rauschenberg C. D. and Lee A. M. (2011) Marine
1967 microgels as a source of cloud condensation nuclei in the high Arctic. *Proc. Natl.*
1968 *Acad. Sci.* **108**, 13612–13617.

1969 Orellana M. V. and Hansell D. a. (2012) Ribulose-1,5-bisphosphate
1970 carboxylase/oxygenase (RubisCO): A long lived protein in the deep ocean. *Limnol.*
1971 *Oceanogr.* **57**, 826–834.

1972 Orellana M. V., Lessard E. J., Dycus E., Chin W.-C., Foy M. S. and Verdugo P. (2003)
1973 Tracing the source and fate of biopolymers in seawater: application of an
1974 immunological technique. *Mar. Chem.* **83**, 89–99.

1975 Orellana M. V., Petersen T. W., Diercks A. H., Donohoe S., Verdugo P. and van den
1976 Engh G. (2007) Marine microgels: Optical and proteomic fingerprints. *Mar. Chem.*
1977 **105**, 229–239.

1978 Panagiotopoulos C., Repeta D. J. and Johnson C. G. (2007) Characterization of methyl
1979 sugars, 3-deoxysugars and methyl deoxysugars in marine high molecular weight
1980 dissolved organic matter. *Org. Geochem.* **38**, 884–896.

1981 Panagiotopoulos C., Repeta D. J., Mathieu L., Rontani J.-F. and Sempéré R. (2013)
1982 Molecular level characterization of methyl sugars in marine high molecular weight
1983 dissolved organic matter. *Mar. Chem.* **154**, 34–45.

1984 Panagiotopoulos C. and Sempéré R. (2005) Analytical methods for the determination of
1985 sugars in marine samples : A historical perspective and future directions. *Limnol.*
1986 *Oceanogr. Methods*, 419–454.

1987 Powell M. J., Sutton J. N., Del Castillo C. E. and Timperman A. T. (2005) Marine
1988 proteomics: generation of sequence tags for dissolved proteins in seawater using
1989 tandem mass spectrometry. *Mar. Chem.* **95**, 183–198.

1990 Powell M. J. and Timperman A. T. (2005) Quantitative analysis of protein recovery from
1991 dilute, large volume samples by tangential flow ultrafiltration. *J. Memb. Sci.* **252**,
1992 227–236.

1993 Quan T. M. and Repeta D. J. (2007) Periodate oxidation of marine high molecular weight
1994 dissolved organic matter: Evidence for a major contribution from 6-deoxy- and
1995 methyl sugars. *Mar. Chem.* **105**, 183–193.

1996 Repeta D. J. and Aluwihare L. I. (2006) Radiocarbon analysis of neutral sugars in high-
1997 molecular-weight dissolved organic carbon: Implications for organic carbon cycling.
1998 *Limnol. Oceanogr.* **51**, 1045–1053.

1999 Rich J. H., Ducklow H. W. and Kirchman D. L. (1996) Concentrations and uptake of
2000 neutral monosaccharides along 140 o W in the equatorial Pacific : Contribution of
2001 glucose to heterotrophic bacterial activity and the DOM flux. *Limnol. Oceanogr.* **41**,
2002 595–604.

2003 Rue E. L. and Bruland K. W. (1997) The role of organic complexation on ambient iron
2004 chemistry in the equatorial Pacific Ocean and the response of a mesoscale iron
2005 addition experiment. *Limnol. Oceanogr.* **42**, 901–910.

2006 Sakugawa H. and Handa N. (1985) Isolation and chemical characterization of dissolved
2007 and particulate polysaccharides in Mikawa Bay. *Geochim. Cosmochim. Acta* **49**,
2008 1185–1193.

2009 Sannigrahi P., Ingall E. D. and Benner R. (2005) Cycling of dissolved and particulate
2010 organic matter at station Aloha: Insights from 13C NMR spectroscopy coupled with
2011 elemental, isotopic and molecular analyses. *Deep Sea Res. Part I Oceanogr. Res.*
2012 *Pap.* **52**, 1429–1444.

2013 Sañudo-Wilhelmy S. a, Cutter L. S., Durazo R., Smail E. a, Gómez-Consarnau L., Webb
2014 E. a, Prokopenko M. G., Berelson W. M. and Karl D. M. (2012) Multiple B-vitamin
2015 depletion in large areas of the coastal ocean. *Proc. Natl. Acad. Sci. U. S. A.* **109**,
2016 14041–5.

2017 Sarmento H. and Gasol J. M. (2012) Use of phytoplankton-derived dissolved organic
2018 carbon by different types of bacterioplankton. *Environ. Microbiol.* **14**, 2348–60.

2019 Schmidt A., Karas M. and Dülcks T. (2003) Effect of different solution flow rates on
2020 analyte ion signals in nano-ESI MS, or: when does ESI turn into nano-ESI? *J. Am.*
2021 *Soc. Mass Spectrom.* **14**, 492–500.

2022 Sher D., Thompson J. W., Kashtan N., Croal L. and Chisholm S. W. (2011) Response of
2023 Prochlorococcus ecotypes to co-culture with diverse marine bacteria. *ISME J.* **5**,
2024 1125–1132.

2025 Simjouw J.-P., Minor E. C. and Mopper K. (2005) Isolation and characterization of
2026 estuarine dissolved organic matter: Comparison of ultrafiltration and C18 solid-
2027 phase extraction techniques. *Mar. Chem.* **96**, 219–235.

2028 Skoog A. and Benner R. (1997) Aldoses in various size fractions of marine organic
2029 matter : Implications for carbon cycling. *Limnol. Oceanogr.* **42**, 1803–1813.

2030 Suzuki S., Kogure K. and Tanoue E. (1997) Immunochemical detection of dissolved
2031 proteins and their source bacteria in marine environments. *Mar. Ecol. Prog. Ser.*
2032 **158**, 1–9.

2033 Tada K., Tada M. and Maita Y. (1998) Dissolved Free Amino Acids in Coastal Seawater
2034 Using a Modified Fluorometric Method. *J. Oceanogr.* **54**, 313–321.

2035 Tang Y. Z., Koch F. and Gobler C. J. (2010) Most harmful algal bloom species are
2036 vitamin B1 and B12 auxotrophs. *Proc. Natl. Acad. Sci. U. S. A.* **107**, 20756–61.

2037 Tanoue E. (1995) Detection of dissolved protein molecules in oceanic waters. *Mar.*
2038 *Chem.* **51**, 239–252.

2039 Tanoue E., Masao I. and Takahashi M. (1996) Discrete dissolved and particulate proteins
2040 in oceanic waters. *Limnol. Oceanogr.* **41**, 1334–1343.

2041 Tanoue E., Nishiyama S., Kamo M. and Tsugita A. (1995) Bacterial membranes: possible
2042 source of a major dissolved protein in seawater. *Geochim. Cosmochim. Acta* **59**,
2043 2643–2648.

2044 Velasquez I., Nunn B. L., Ibisanmi E., Goodlett D. R., Hunter K. A. and Sander S. G.
2045 (2011) Detection of hydroxamate siderophores in coastal and Sub-Antarctic waters
2046 off the South Eastern Coast of New Zealand. *Mar. Chem.* **126**, 97–107.

2047 Verdugo P. (2012) Marine Microgels. *Ann. Rev. Mar. Sci.* **4**, 375–400.

2048 Vetter T., Perdue E., Ingall E., Koprivnjak J. and Pfromm P. (2007) Combining reverse
2049 osmosis and electrodialysis for more complete recovery of dissolved organic matter
2050 from seawater. *Sep. Purif. Technol.* **56**, 383–387.

2051 Vraspir J. M. and Butler A. (2009) Chemistry of Marine Ligands and Siderophores. *Ann.*
2052 *Rev. Mar. Sci.* **1**, 43–63.

2053 Walker B. D., Beaupré S. R., Guilderson T. P., Druffel E. R. M. and McCarthy M. D.
2054 (2011) Large-volume ultrafiltration for the study of radiocarbon signatures and size
2055 vs. age relationships in marine dissolved organic matter. *Geochim. Cosmochim. Acta*
2056 **75**, 5187–5202.

2057 Weishaar J. L., Aiken G. R., Bergamaschi B. a, Fram M. S., Fujii R. and Mopper K.
2058 (2003) Evaluation of specific ultraviolet absorbance as an indicator of the chemical
2059 composition and reactivity of dissolved organic carbon. *Environ. Sci. Technol.* **37**,
2060 4702–8.

2061 Williams P. M. and Druffel E. R. M. (1987) Radiocarbon in dissolved organic matter in
2062 the central North Pacific Ocean. *Nature* **330**, 246–248.

2063 Yamada N., Suzuki S. and Tanoue E. (2000) Detection of Vibrio (Listonella)
2064 anguillarum Porin Homologue Proteins and Their Source Bacteria from Coastal
2065 Seawater. *J. Ocean.* **56**, 583–590.

2066 Yamada N. and Tanoue E. (2003) Detection and partial characterization of dissolved
2067 glycoproteins in oceanic waters. *Limnol. Oceanogr.* **48**, 1037–1048.

2068 Yamashita Y. and Tanoue E. (2004) Chemical characteristics of amino acid-containing
2069 dissolved organic matter in seawater. *Org. Geochem.* **35**, 679–692.

2070 Yamashita Y. and Tanoue E. (2003a) Chemical characterization of protein-like
2071 fluorophores in DOM in relation to aromatic amino acids. *Mar. Chem.* **82**, 255–271.

2072 Yamashita Y. and Tanoue E. (2003b) Distribution and alteration of amino acids in bulk
2073 DOM along a transect from bay to oceanic waters. *Mar. Chem.* **82**, 145–160.

2074 Ziolkowski L. A. and Druffel E. R. M. (2010) Aged black carbon identified in marine
2075 dissolved organic carbon. *Geophys. Res. Lett.* **37**, 4–7.

2076 Zubarev R. A and Makarov A. (2013) Orbitrap mass spectrometry. *Anal. Chem.* **85**,
2077 5288–96.

2078